JOURNAL OF THE OPTICAL SOCIETY OF AMERICA VOLUME 52, NUMBER 10 OCTOBER 1962

Reconstructed Wavefronts and Communication Theory*

EMMETT N. LEITH AND JURIS UPATNIEKS
The Institute of Science and Technology, The University of Michigan, Ann Arbor, Michigan

(Received October 16, 1961)

With Regards
Emmett
Leith

A two-step imaging process discovered by Gabor involves photographing the Fresnel diffraction pattern of an object and using this recorded pattern, called a hologram, to construct an image of this object. Here, the process is described from a communication-theory viewpoint. It is shown that construction of the hologram constitutes a sequence of three well-known operations: a modulation, a frequency dispersion, and a square-law detection. In the reconstruction process, the inverse-frequency-dispersion operation is carried out. The process as normally carried out results in a reconstruction in which the signal-to-noise ratio is unity. Techniques which correct this shortcoming are described and experimentally tested. Generalized holograms are discussed, in which the hologram is other than a Fresnel diffraction pattern.

1. INTRODUCTION

A TWO-STEP imaging process discovered by Gabor[1] involves the photography of the Fresnel diffraction pattern of an object and the use of the recorded pattern to construct an image of the original object. The recorded diffraction pattern, called a hologram, bears little resemblance to the object, but contains most of the information required to reconstruct the object. The process is described here in terms of communication theory, and such a description shows the similarity of the process to those arising in communication engineering.

The hologram is produced by recording the Fresnel diffraction pattern on a photographic plate. The light wave impinging on the plate has a complex amplitude, which the photographic process records only the amplitude; the phase portion is discarded. Thus, half of the information content of the wave is lost. The consequence is that the reconstruction is imperfect, due principally to the presence of a twin or conjugate image, identical to the reconstructed image, but occurring in a different focal plane and thus appearing considerably out of focus. The in-focus image always has this defocussed image as a background. The latter can be regarded as noise, and since the light flux is evenly distributed between the two images, the reconstructed image can be said to have a root-mean-square signal-to-noise-ratio of unity. Several techniques are described here which lead to complete elimination of the twin image by fairly simple means.

The basis of the process is shown in Fig. 1. A collimated beam of monochromatic light derived from a point source impinges on plane P_1, which contains a point scatterer O. A spherical wave, coherent with the incident wave, is generated by the scatter. At plane P_2, a distance z from plane P_1, a Fresnel diffraction pattern is produced by the interference between the background wave and the scattered wave. If the plane P_1 contains an object with a complicated transmittance pattern, then each point of the object acts independently of the others to produce its own pattern at P_2. If the photographic record produced at P_2 is later placed in a beam of collimated monochromatic light, the modulation of the beam by the transparency produces diffracted waves, a component of which is identical to the wavefronts incident on P_2 when the hologram was recorded. This component produces a virtual image of the original object at a distance z on the source side of the hologram. A second component of the diffracted waves resembles the original wavefronts except for having an opposite curvature. This component produces a real image of the original object. The two reconstructed images appear as in Fig. 2.

The process can be discussed within the framework of communication theory and it is advantageous to do so. The process has three essential parts: (1) the defocusing or spatial-frequency dispersion of the image; (2) the hologram recording process, which can be likened to a square-law or nonlinear detection; (3) the focusing, or compression, which occurs in the reconstruction.

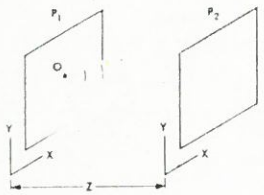

FIG. 1. Construction of the hologram.

2. DISPERSION PROCESS

Let a transparency having amplitude transmittance $s=s_b+s_r$ be placed at plane P_1 (Fig. 1). The transparency has an average transmittance s_b, and this bias, or zero-frequency term is written separately from the remainder s_r for reasons which will become evident. A

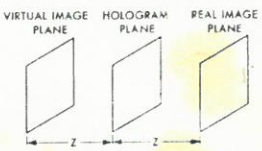

FIG. 2. Hologram and reconstructed images.

*This work was conducted by Project Michigan under a Department of the Army Contract, administered by the U. S. Army Signal Corps. It was presented at the October 1961, Los Angeles meeting of the Optical Society of America [J. Opt. Soc. Am. 51, 1469 (1961)].

[1] D. Gabor, Nature **161**, 777 (1948); Proc. Roy. Soc. (London) A197, 454 (1949).

monochromatic plane wave $e^{i\omega t}$ illuminates the plane P_1 and is modulated by the transparency, resulting in the light amplitude distribution

$$se^{i\omega t}=[s_b+s_r(x,y)]e^{i\omega t}. \quad (1)$$

This is similar to the expression $[1+ms(t)]e^{i\omega t}$ for an amplitude-modulated signal, in which $e^{i\omega t}$ is the carrier and $ms(t)e^{i\omega t}$ supplies the sidebands. Comparison of Eq. (1) with the latter expression shows the analogy of the bias term $s_be^{i\omega t}$ to a carrier. The significant difference between the present case and the usual modulation problem is that in the latter, both the carrier wave and the sidebands are functions of time, while here, the sidebands are in part a function of spatial variables. This difference, while important, in no way inhibits the analysis and does not alter it in any fundamental way.

At plane P_2, an "out of focus" image or Fresnel diffraction pattern of the transparency is formed. The structure of this image can be calculated using the Fresnel–Kirchhoff diffraction integral, which for this application becomes

$$\chi(x,y)=i(\lambda z)^{-1}\int\int[s_b+s_r(\alpha,\beta)]$$
$$\times\exp\{-i2\pi\lambda^{-1}[z^2+(x-\alpha)^2+(y-\beta)^2]^{\frac{1}{2}}\}d\alpha d\beta, \quad (2)$$

where (α,β) are the coordinates of a point in the P_1 plane. The obliquity factor has been dropped, since only small scattering angles are considered. At this point we make another small-angle approximation which will be used throughout the remainder of the paper:

$$[z^2+(x-\alpha)^2+(y-\beta)^2]^{\frac{1}{2}}\approx z+\tfrac{1}{2}(x-\alpha)^2z^{-1}+\tfrac{1}{2}(y-\beta)^2z^{-1}.$$

Equation (2) becomes

$$\chi(x,y)=i(\lambda z)^{-1}\int\int[s_b+s_r(\alpha,\beta)]$$
$$\times\exp\{-ik[(x-\alpha)^2+(y-\beta)^2]\}d\alpha d\beta, \quad (3)$$

where $k=\pi/(\lambda z)$. Also, a constant phase factor $e^{-2\pi iz/\lambda}$ has been dropped, since a constant phase delay is of no consequence. Equation (3) is a convolution of the signal with an impulse function $i(\lambda z)^{-1}\exp[-ik(x^2+y^2)]$, which we will henceforth designate as $f(x,y)$.

The portion of the radiation corresponding to s_b is essentially a plane wave which propagates unaltered, except for diffraction around the edges of the aperture at P_1. If this diffraction is negligible, Eq. (3) becomes

$$\chi(x,y)=s_b+i(\lambda z)^{-1}\int\int s_r(\alpha,\beta)$$
$$\times\exp\{-ik[(x-\alpha)^2+(y-\beta)^2]\}d\alpha d\beta \quad (4)$$
$$=s_b+s_r(x,y)*f(x,y),$$

where the $*$ denotes the convolution operation.

Using the property that a convolution of two function corresponds to the multiplication of their transforms, and noting that

$$i(\lambda z)^{-1}\exp[-ik(x^2+y^2)] \quad \text{and} \quad \exp[i(4k)^{-1}(\xi^2+\eta^2)]$$

form a Fourier transform pair, Eq. (4) can be written

$$\chi(x,y)=s_b+\mathfrak{F}\{S_r(\xi,\eta)\exp[i(4k)^{-1}(\xi^2+\eta^2)]\} \quad (5)$$
$$=s_b+\mathfrak{F}[S_r(\xi,\eta)F(\xi,\eta)],$$

where ξ and η are the spatial frequency variables corresponding to x and y, respectively, $\mathfrak{F}$ denotes the Fourier transform operation, and $S_r(\xi,\eta)$ and $F(\xi,\eta)$ are, respectively, the Fourier transforms of $s_r(x,y)$ and $f(x,y)$. The defocusing process is seen to constitute a multiplication of the signal spectrum by the phase factor.

$$F(\xi,\eta)=\exp[i(4k)^{-1}(\xi^2+\eta^2)].$$

Both the original and defocused signals have the same Wiener spectrum, but the frequency components of the latter have been phase-shifted relative to those of the original signal. The agency producing this dispersion is simply free space, which behaves as an all-pass linear filter with a dispersion factor

$$d\phi/d\xi=(\lambda z/2\pi)\xi \quad d\phi/d\eta=(\lambda z/2\pi)\eta, \quad (7)$$

where $\phi=(4k)^{-1}(\xi^2+\eta^2)$.

It is often instructive to assume a simple form for a signal. Two such forms are commonly used: the simple sinusoid and the impulse. Each form, in its own way, is helpful in supplying physical insight. Suppose s_r to be $\sigma\cos Ax$, where $A/(2\pi)$ is a spatial frequency. Equation (1) becomes

$$se^{i\omega t}=s_be^{i\omega t}+\tfrac{1}{2}\sigma e^{i(\omega t+Ax)}+\tfrac{1}{2}\sigma e^{i(\omega t-Ax)}. \quad (8)$$

The second and third terms are the upper and lower sidebands of the modulated signal. The physical significance of the dispersion is readily seen from Fig. 3. The zero-frequency components s_b proceeds from P_1 to P_2 as a plane wave oriented normal to the optical system axis. However, the frequency component $\frac{1}{2}\sigma e^{iAx}$ produces a plane wave which makes an angle θ with the optical-system axis, and when it arrives at P_2 it has undergone the phase delay $\exp[-i2\pi z(\lambda\cos\theta)^{-1}]$ since $z/\cos\theta$ is the distance the wave travels in passing from P_1 to P_2. This can be written $\exp[-i2\pi z\lambda^{-1}(1+\frac{1}{2}\theta^2)]$ since $(\cos\theta)^{-1}\approx 1+\frac{1}{2}\theta^2$ for small angles. Dropping the constant phase term $\exp(-i2\pi z/\lambda)$ and using the relation $\theta=\lambda A/(2\pi)$ [that is, a grating of period $2\pi/A$ diffracts light at an angle $\lambda A/(2\pi)$], the phase factor

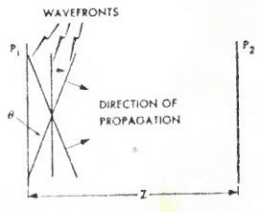

FIG. 3. Meaning of dispersion.

becomes $\exp(-i\frac{1}{4}A^2\lambda/\pi)$. In addition, the wave is physically displaced a distance

$$-z\sin\theta\approx -z\theta=-A\lambda z/(2\pi).$$

The signal component e^{iAx} thus becomes

$$\exp[iA(x+\tfrac{1}{2}A\lambda z/\pi)]\exp(-i\tfrac{1}{4}A^2\lambda z/\pi)=\exp i(Ax+\phi_A),$$

where $\phi_A=\frac{1}{4}A^2\lambda z/\pi$. The l sideband or negative frequency is diffracted at an angle $-\theta$ and a similar analysis applies. Therefore, given the signal $s_b+\sigma\cos Ax$ at plane P_1, the light amplitude at plane P_2 is

$$\chi_A e^{i\omega t}=s_b e^{i\omega t}+\tfrac{1}{2}\sigma e^{i(\omega t+Ax+\phi_A)}+\tfrac{1}{2}\sigma e^{i(\omega t-Ax+\phi_A)}. \quad (9)$$

Alternatively, this result can be obtained by inspection from Eq. (5) or by evaluation of Eq. (4).

3. RECORDING THE HOLOGRAM

The dispersed signal $s*f$ is in general a complex quantity, but the photographic process which records the signal is insensitive to phase and therefore records only the absolute value of the amplitude. Let us suppose that the photographic emulsion has a linear transmittance-exposure characteristic; that is, a linear relation exists between the intensity of the incident light and the resultant transmittance of the developed negative. The transmittance-exposure curve, of course, has a negative slope; this means only that the signal upon being recorded will undergo a 180° phase shift and a possible alteration of the bias level. Neither factor is of any significance and both will be disregarded.

The recorded hologram represents the function

$$\chi\chi^*=[(s_b+s_r)*f][(s_b+s_r)*f]^*, \quad (10)$$

where, as before, the asterisk * denotes a convolution, and the superscript asterisk * denotes the complex conjugate. This equation is readily written

$$\chi\chi^*=s_b^2+s_b(s_r*f)+s_b(s_r*f)^*+|s_r*f|^2 \quad (11)$$

since $s_b*f=s_b$, as indicated in Eq. (4). It is seen that the first two terms are, to within a constant, just the dispersed signal incident at P_2 when the hologram was recorded. In addition, the recording process has produced two new terms. First, there is $s_b(s_r*f)^*$, which is the complex conjugate of the dispersed signal; this term gives rise to the real image part of the reconstruction. Also, there is the distortion term $|s_r*f|^2$, resulting from the nonlinear nature of the recording or demodulation process, which is essentially a square-law detection and produces intermodulation products. If the object is of low contrast, s_b will be much larger than s_r and the distortion term will be small. Intermodulation terms arising in square-law detection devices can be removed, however, and the removal can be carried out in this instance also; the procedure for so doing is described in a later section.

The sinusoidal signal of Eq. (9) when recorded becomes

$$\begin{aligned}\chi_A\chi_A^*&=s_b^2+\tfrac{1}{2}\sigma^2+s_b\sigma\cos(Ax+\phi_A)\\&\quad+s_b\sigma\cos(Ax-\phi_A)+\tfrac{1}{2}\sigma^2\cos 2Ax\\&=s_b^2+\tfrac{1}{2}\sigma^2+2s_b\sigma\cos Ax\cos\phi_A+\tfrac{1}{2}\sigma^2\cos 2Ax. \quad (12)\end{aligned}$$

It is seen that the amplitude of the sinusoidal component $\cos Ax$ is uncertain because of the factor $\cos\phi_A$; this is one way of regarding the incompleteness of the recording process, which discards the phase portion of the modulated light wave. The distortion term is manifested here as an additional bias term $\frac{1}{2}\sigma^2$ and as a double-frequency term $\frac{1}{2}\sigma^2\cos 2Ax$.

4. RECONSTRUCTION PROCESS

The reconstruction is carried out by illuminating the hologram with coherent light. Although the reconstructed image can be brought to a focus using a variety of optical systems, two stand out as being most illustrative of the process. The first is shown in Fig. 4. In the dispersion process, an object plane P_1 is imaged at the plane P_3, and the hologram is recorded at some plane P_2 between P_1 and P_3. When the hologram is produced, the original object is removed and the hologram is reinserted at P_2. The wavefronts generated at P_2 are replicas of those that had impinged at P_2 when the hologram was made, and these wavefronts continue to P_3 and form an image, just as the original waves would have done if they had not been interrupted at P_2. This viewpoint emphasizes the reconstruction process as a delayed continuation of the original process which produced the hologram; the two together are equivalent to an ordinary one-step imaging process. Obviously, this view calls for use of the virtual image of the hologram, although a readjustment of the lens system would also permit use of the real image.

The view we wish to develop here regards the reconstruction process as the inverse of the hologram-producing process. Let us now place the developed hologram not at its original position P_2 (Fig. 4), but at P_1, in the place formerly occupied by the object. The space between P_1 and P_2 was seen from expression (6) to act as a dispersive filter, introducing the phase factor $F(\xi,\eta)$. With the dispersed signal of Eq. (11) placed at P_1, this space again introduces the dispersion factor $F(\xi,\eta)$. Let us consider only the real-image term of Eq. (11), which is $s_b(s_r*f)^*$. This term, when operated on by the dispersive filter, becomes $s_b(s_r*f)^**f$, which can be written in terms of its Fourier transform as

$$s_b(s_r*f)^**f=\mathfrak{F}[s_b S_r^*(-\xi,-\eta)F^*(-\xi,-\eta)F(\xi,\eta)], \quad (13)$$

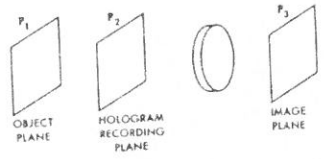

FIG. 4. Optics for wavefront reconstruction.

where as before, S_r and F are the Fourier transforms of s_r and f. Here, we have used the property that if $f(x,y)$ and $F(\xi,\eta)$ form a Fourier transform pair, then $f^*(x,y)$ and $F^*(-\xi,-\eta)$ likewise form a Fourier transform pair. Because F is a symmetrical function and has a magnitude of unity, Eq. (13) reduces to $s_b S_r^*(-\xi,-\eta)$ and its transform is $s_b s_r^*(x,y)=s_b s_r(x,y)$, since s_r is assumed to be a real function. This term, along with the bias term s_b^2 [Eq. (11)], constitutes the reconstructed image, and is formed at plane P_2. This manner of reconstruction, in which the same optical path is used both for the dispersion and the reconstruction, is possible because of two factors: (1) the existence of the conjugate term $(s_r*f)^*$, which is produced from the recording process, and (2), the symmetry of the function $F(\xi,\eta)$.

5. GENERALIZED HOLOGRAMS

A somewhat modified optical system for hologram construction is shown in Fig. 5, and leads to what we will call generalized holograms. The object transparency is placed at P_1 and is imaged at P_3. Plane P_2 is the back focal plane of lens L_1 and therefore displays the Fourier transform of the object at P_1. Let x,y and α,β be the coordinates of the planes P_1 and P_2, respectively. If lens L_1 has a focal length F_1, the light amplitude at P_2 is[2]

$$a(\alpha,\beta)=i(\lambda F_1)^{-1}\int\int s(x,y)$$

$$\times\exp[i2\pi(\lambda F_1)^{-1}(x\alpha+y\beta)]dxdy. \quad (14)$$

This is a Fourier transform relation and can be put in more familiar form by the substitution $\xi=-2\pi\alpha(\lambda F_1)^{-1}$ and $\eta=-2\pi\beta(\lambda F_1)^{-1}$.

Suppose a lens of focal length F_2 to be placed at P_2. To a first approximation, the lens introduces the phase or dispersion function $\exp[i\pi(\alpha^2+\beta^2)(\lambda F_2)^{-1}]$. The light emerging from P_2 has the form

$$S(\xi,\eta)\exp[-i\lambda F_1^2(\xi^2+\eta^2)(4\pi F_2)^{-1}], \quad (15)$$

where $S(\xi,\eta)$ is the Fourier spectrum of $s(x,y)$, and the exponential factor is the phase retardation introduced by the lens. Here, we may say that it is the lens at P_2 which has produced the dispersion. This viewpoint, while entirely reasonable, is really quite arbitrary, for it may be pointed out that the lens at P_2 has resulted in the image at P_3 being moved to a new plane P_4, and the dispersive properties of the system can therefore equally well be attributed to the space between P_3 and P_4.

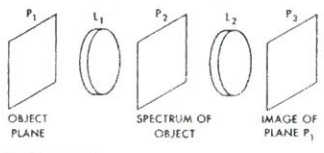

FIG. 5. System for producing generalized holograms.

[2] L. J. Cutrona, E. N. Leith, C. J. Palermo, L. J. Porcello, Trans. IRE **IT-6**, 386 (1960).

However, the present optical system and the viewpoint adopted in describing it have great power when applied to more general types of holograms. For with the optical system of Fig. 5, phase functions can conveniently be placed in P_2 which are other than those produced by a spherical lens. For example, a cylindrical lens can be used, which will produce holograms having dispersion in one dimension only. Also, lenses with severe aberrations can be used, which of themselves are incapable of producing a satisfactory image. The hologram produced by such a process will be incapable of yielding satisfactory reconstructions except when the reconstruction is made in the same manner as the hologram was made, using the imperfect lens to produce the inverse dispersion. Here, the aberrations of the lens, regardless of their form and severity, will be completely compensated in the reconstruction process, provided the thin-lens approximation holds, and provided the lens aberrations have axial symmetry. The dispersive element need not be a lens at all, but can be an arbitrary phase function. One possible form is a half-wave phase plate, in which the phase is reversed in some sections and not in others. If the phase function has the property $F(\xi,\eta)=F^*(-\xi,-\eta)$, the light distribution at the hologram recording plane will be real and in the reconstruction there will be no interference from a twin image.

6. ELIMINATION OF THE EXTRANEOUS TERMS

In this section, techniques for removing the extraneous terms are discussed. It will be recalled that the principal extraneous term, the twin image, is produced as a consequence of recording only the amplitude modulus of a complex signal. Recording the entire complex function is the obvious, but hardly practicable solution. However, other procedures are available, some of which are considered here.[3] First, a dispersion process can be employed in which the signal (a real quantity) remains a real quantity after dispersion, and therefore can be recorded photographically without loss of any components. A second approach is based on the principle that a complex signal of bandwidth W can be represented by a real signal of bandwidth $2W$, in which the real signal is derived from the complex one by placing the signal on a carrier and using only the real part.[4]

The first method was suggested in the previous section. The requirement that the dispersed signal be a real quantity was seen to impose the condition on the dispersive filter that $F(\xi,\eta)=F^*(-\xi,-\eta)$. The transfer function associated with free space does not satisfy this condition (which accounts, of course, for the presence

[3] A discussion of various similar techniques for eliminating the twin image is given by Lohmann, Optica Acta (Paris) 3, 97 (1956). These are likewise developed by use of a communication theory approach.

[4] See reference 2, p. 391.

of the twin image). Therefore, this method requires the use of the generalized hologram technique described in Sec. 5.

The second approach, conversion of a complex signal into a real one of twice the bandwidth, is carried out in the following way. Let us introduce the complex function $\zeta(x,y)=\gamma(x,y)e^{i\varphi(x,y)}$ of spatial frequency bandwidth W, centered about zero frequency; ζ thus has spatial frequency components $\xi/2\pi$ and $\eta/2\pi$ extending from $-\frac{1}{2}W$ to $\frac{1}{2}W$. Let ζ be multiplied by the carrier frequency $e^{i\xi_c x}$, where $\xi_c \geq W/2$. The real part of the resulting function is $\gamma(x,y)\cos[\xi_c x+\varphi(x,y)]$. This can be written as $\frac{1}{2}\gamma e^{i(\xi_c x+\varphi)}+\frac{1}{2}\gamma e^{-i(\xi_c x+\varphi)}$. The first term is the original complex signal, with spectrum shifted by ξ_c. Thus, its spectrum consists only of positive ξ-frequencies and is confined to the half plane $\xi \geq 0$. The conjugate term, however, consists only of negative ξ frequencies. Therefore, the two terms can be separated by spatial filtering, and the original complex signal is thus recoverable. One may note that the bandwidth of the real signal is indeed twice that of the original complex signal, since each of the two exponential components has the original bandwidth W.

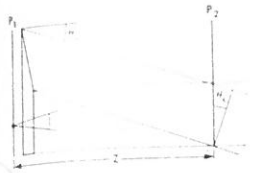

FIG. 6. Wedge for two-beam hologram construction.

An optical technique for placing the dispersed signal on a carrier is shown in Fig. 6. A wedge deflects a portion of a collimated beam of light through the angle θ_c, and the two beams are brought into coincidence at plane P_2, at a distance z from the plane of the wedge. The object is placed at plane P_1, but occupies only the lower portion of the plane, where the light is unrefracted. The hologram is made at plane P_2.

The light distribution at P_2 is identical with that described in Sec. 2, except that an additional term $s_c e^{i\xi_c x}$ has been added as a consequence of the prism. The carrier ξ_c is related to the refraction angle by $\xi_c=2\pi\theta_c/\lambda$. The dispersed signal is

$$\chi = s_c e^{i\xi_c x}+s_b+s_r*f \tag{16}$$

and the recorded signal is

$$\chi\chi^* = s_c^2+s_b^2+2s_b s_c\cos\xi_c x+s_b[s_r*f+(s_r*f)^*] +s_c[(s_r*f)e^{-i\xi_c x}+(s_r*f)^*e^{i\xi_c x}]+|s_r*f|^2. \tag{17}$$

The spectrum of $\chi\chi^*$ is shown in Fig. 7. The first two terms constitute a dc or bias term and the third is a constant spatial frequency. The first set of bracketed terms is the dispersed signal and its complex conjugate; these are of no interest, since they have overlapping spectra and produce the same inseparable twin images encountered before. The second set of bracketed terms

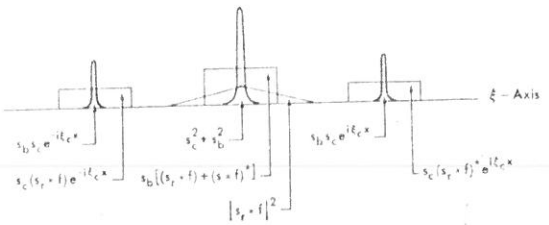

FIG. 7. Spectrum of hologram.

represents the dispersed signal and its conjugate, each on a carrier. Since one is on a positive carrier and the other is on a negative carrier, they can be separated by spatial filtering. If s_r*f has bandwidth W (again, measured from $\xi=-\frac{1}{2}W$ to $\xi=\frac{1}{2}W$), then the requirement on ξ_c that these two terms have nonoverlapping spatial frequency spectra is that $\xi_c \geq \frac{1}{2}W$. The more stringent criterion $\xi_c \geq W$ ensures that the spectra of these terms will not overlap the spectra of s_r*f and $(s_r*f)^*$. Finally, the term in absolute value signs is the distortion term encountered previously, resulting from the nonlinear nature of the detection or recording process. This term consists of intermodulation products and has frequency components as great as $\pm W$. Therefore, in order that these extraneous frequencies fall outside the frequency band of the signal of interest, we require that $\xi_c \geq \frac{3}{2}W$, or, put otherwise, the signal after modulation onto the carrier ξ_c should not span more than one octave. These requirements are readily perceived from examination of Fig. 7.

The question may occur to the reader as to the necessity of the s_b term in making the hologram. This term should be retained because it represents the dc or bias level of the object transparency and is therefore a part of the object and must be used in the reconstruction. It gives rise to the term $2s_c s_b\cos\xi_c x$ on the hologram, and this term supplies the bias level to the reconstructed image.

The reconstruction can be made using the optical system of Fig. 5. The hologram is placed in plane P_1, the spectrum is displayed at P_2, and the reconstructed image appears at P_3. For reconstruction, only two of the spectral terms are used. These can be either the combination

$$s_b s_c e^{i\xi_c x}+s_c(s_r*f)^*e^{i\xi_c x} \tag{18}$$

or

$$s_b s_c e^{-i\xi_c x}+s_c(s_r*f)e^{-i\xi_c x}, \tag{19}$$

where the term $s_b s_c\cos\xi_c x$ of Eq. (17) has been divided into its constituent exponential parts. Expression (19) represents the real image and expression (18) represents the virtual image. The appropriate terms are selected at P_2 by spatial filtering which consists of blocking out all spectral terms but the two desired ones. To reconstruct, for example, using the real-image term, one allows only the two real-image terms to be passed by the slit at P_2. In passing through the optical system.

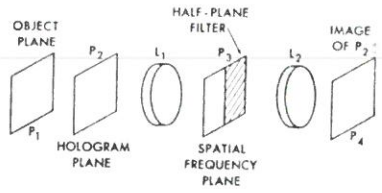

FIG. 8. Optical system for single-sideband holograms.

the dispersed signal is convolved with the function f, and a properly reconstructed image appears at plane P_3.

Another way to produce a carrier-frequency hologram is to use an interferometer; a Mach-Zehnder type would be especially suitable. The object transparency would be placed in one leg and the carrier would be introduced by means of the light in the second leg. The result would be substantially as described above.

A single-sideband technique described by Lohmann[5] achieves the separation of real and virtual images without the use of the carrier term. This is accomplished as follows, using the optical system of Fig. 8. The object is placed at P_1 and a dispersed image is formed at plane P_2; however, instead of making the hologram at this plane, let the lens system L_1, L_2 image the P_2 plane at P_4, and let the hologram be made at P_4. Plane P_3 is the back focal plane of lens L_1 and therefore displays the Fourier transform of the signal. A stop, consisting of a half-plane is placed at P_3 and removes half of the spectrum thereby converting the image to a single-sideband signal. The plane extends almost but not quite to the optical system axis since we do not want to alter the bias term which is displayed as a point image on the optical system axis. Suppose the negative frequencies are eliminated. The dispersed signal at P_4 is

$$\chi = s_b + (s_r * f * g) \tag{20}$$

where g is the impulse response of the half-plane filter[6] and is given by

$$g = \tfrac{1}{2}\delta(x) + i/(\pi x), \tag{21}$$

where $\delta(x)$ is the Dirac delta function. The recorded hologram is

$$\chi\chi^* = s_b^2 + s_b(s_r * f * g) + s_b(s_r * f * g)^* + |s_r * f * g|^2. \tag{22}$$

The hologram is inserted at P_1, in place of the original object, and the half-plane filter is now shifted so as to remove the positive ξ frequencies. The analysis is completed by convolving $\chi\chi^*$ with f and with the impulse response of the shifted half-plane filter. The pro can be simplified by consideration of the spectr $\chi\chi^*$. The term $s_b(s_r * f * g)$ contains only positive quencies, hence is entirely removed by the half filter. The conjugate term has only negative freque hence is unaffected by the half-plane filter. Eq (22) thus becomes

$$(\chi\chi^*) * f = s_b^2 * f + s_b(s_r * f * g)^* * f + |s_r * f * g|^2 * f * g^*.$$

As before, we have $s_b^2 * f = s_b^2$. The term $s_b(s_r * f *$ can be reduced to $s_b(s_r * g^*)$ in the following way. frequency domain representation of this expressi $s_b S_r^*(-\xi, -\eta)F^*(-\xi, -\eta)G^*(-\xi)F(\xi,\eta)$. Now, w from Eq. (6) that $F^*(-\xi, -\eta)F(\xi,\eta) = 1$. Also is assumed to be real, which implies the rela $S_r^*(-\xi, -\eta) = S_r(\xi,\eta)$. The above expression thu duces to $s_b S_r(\xi,\eta)G^*(-\xi)$, which has the inverse Fou transform $s_b(s_r * g^*)$. Equation (23) becomes, after u Eq. (21),

$$(\chi\chi^*) * f = s_b^2 + \tfrac{1}{2}s_b s_r - \tfrac{1}{2}s_b s_r * i/(\pi x) + |s_r * f * g|^2 * f * g^*. \quad (23)$$

The term $\frac{1}{2}s_b s_r$, along with the bias term s_b^2, is just reconstructed image, with reduced contrast. The te $\frac{1}{2}s_b s_r * i/(\pi x)$ is a new extraneous term, produced fr the initial half-plane filtering operation and replaci the twin image as the principal "noise" term. The di tortion caused by this term is considerably differe from that caused by the twin image. The effect of th term on a pulse-like object (for example, a line of no negligible width) is to produce a positive peak at on edge of the line, a negative peak at the other, and decaying response on each side of the line.

There is, however, a partially-saving grace. Th extraneous term is in phase-quadrature with the bia term s_b, and therefore represents a "phase" image which largely disappears in recording the image, pro vided the bias term is large in comparison with the extraneous term. Unfortunately, this condition is not satisfied except for low-contrast images. In summary, it can be said that the half-plane filtering process is a partial, though incomplete solution to the problem of eliminating the twin image.

The effect of the reconstruction process on the distortion term $|s_r * f * g|^2$ is not easily analyzed and will not be discussed here.

7. ZONE-PLATE DESCRIPTION OF THE CARRIER-FREQUENCY METHOD

An interesting interpretation of the carrier-frequency method of eliminating the twin image is obtained when we consider a point scatterer or impulse as the object. The hologram of a point scatterer is a structure similar to a Fresnel zone-plate. Suppose, however, that the carrier-frequency method of hologram construction is used. The usable component of the recorded hologram signal will resemble an asymmetrical zone plate. If ξ_c is

[5] See reference 3.

[6] The impulse response of the half-plane filter is derived from Hilbert transform relations. For a discussion of Hilbert transforms, see, for example, W. Brown, *Analysis of Linear Time-Invariant Systems* (McGraw-Hill Book Company, Inc., New York, 1962). As given by Brown, the Hilbert transform of a function $s(t)$ is represented in the frequency domain by a filter which phase-shifts the positive frequencies by π, and in the time domain by the convolution integral

$$1/\pi \int_{-\infty}^{\infty} s(\tau)(t-\tau)^{-1} d\tau.$$

sufficiently large, that is, larger than the spatial frequencies produced by the scatterer, then the asymmetrical zone plate will be a one-sided one, as shown in Fig. 9(b). The optical axis, or center of the concentric zones, lies outside the boundaries of the produced portion of the zone plate.

The basis for separation of the real and virtual reconstructed images is seen from consideration of the image-forming properties of a zone plate. This, when illuminated with collimated coherent light, produces a real and a virtual image, as shown in Fig. 9(a). The real image is seen against the background of the out-of-focus virtual image, and the virtual image, if brought to a real focus, would be seen against the background of the out-of-focus real image. If, however, the asymmetrical or offset zone plate is produced, the real and virtual images are separated, as shown in Fig. 9(b). Both images form on the optical axis of the zone plate, and the light from the virtual image is seen to be radiated in a direction such that it does not contain the real image within its beam. A similar situation occurs when the virtual image is brought to a focus.

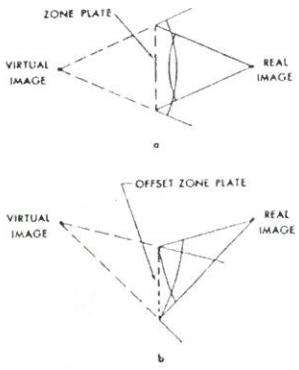

FIG. 9. Zone-plate imaging properties.

If the dispersed signal consists of a number of overlapping but displaced zone plates, then the real image of one zone plate can still encounter interference from the virtual image of another zone plate. However, this possibility is removed by frequency filtering the hologram before the plane of the reconstructed image. The hologram is placed at plane P_1 (Fig. 5). At the frequency plane P_2, the virtual-image light forms on one side of the central image and the light from the real images form on the other side. This occurs because the virtual image contains only negative frequencies and the real image contains only positive frequencies. The half-plane slit removes the virtual-image light without affecting the light from the real image.

8. EXPERIMENTAL RESULTS

The half-plane filtering and carrier-frequency techniques were experimentally verified and the results are shown in Figs. 10 and 12.

For the half-plane filtering technique, the optical system used was that of Fig. 6, and a cylindrical lens was placed at P_2, resulting in holograms having dispersion in one dimension only. This enabled the illumination to be supplied from a line source rather than a point source, and resulted in holograms essentially free from the noise produced by dust particles, etc., such as unavoidably lodge on the air–glass surfaces of the optical-system lenses. Such effects occur in optical systems illuminated by point sources, where all scatterparticles, even if not located in the object plane, produce Fresnel diffraction patterns which degrade results. Having the illumination incoherent in one dimension alleviates these problems.

Figure 10(a) shows the object used for making the hologram. Figure 10(b) shows the resulting hologram when double sideband operation was used. Note that vertical lines remain undispersed, but horizontal lines are quite dispersed. Figure 10(c) shows the reconstructed image. The out-of-focus twin image produces a strong background. Figure 10(d) shows a single sideband hologram, and the image reconstructed from it is shown in Fig. 10(e). The background from the twin

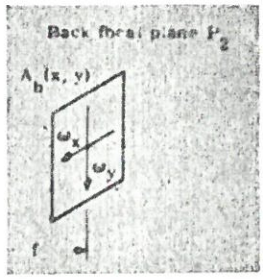

(a)

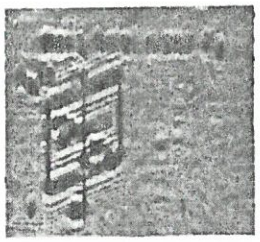

(b)

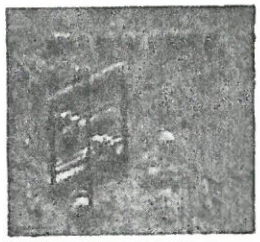

(c)

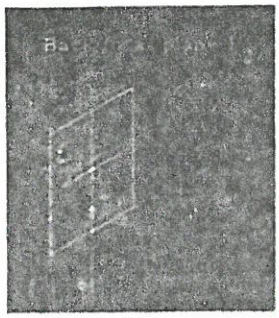

(d)

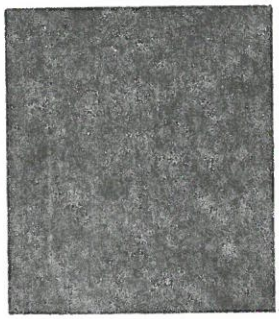

(e)

FIG. 10. Results of half-plane filtering: (a) original object, (b) double sideband hologram, (c) reconstruction from (b), (d) single sideband hologram, (e) reconstruction from (d).

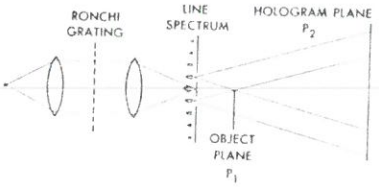

FIG. 11. Modified carrier-frequency system.

image is absent. However, the reconstructed image shows the imperfections anticipated in Sec. 6.

The carrier-frequency method of producing holograms was carried out in the manner illustrated in Fig. 11, which differs from the wedge technique shown in Fig. 5. This alternative method was chosen because gratings were readily available. The results should be the same in either case. Here, the two-beam interference pattern was produced by using a Ronchi grating, selecting two lines from the diffraction pattern, and making the hologram at a plane where the beams overlap (plane P_2). The object is placed at plane P_1, which is the plane where the two beams just begin to merge.

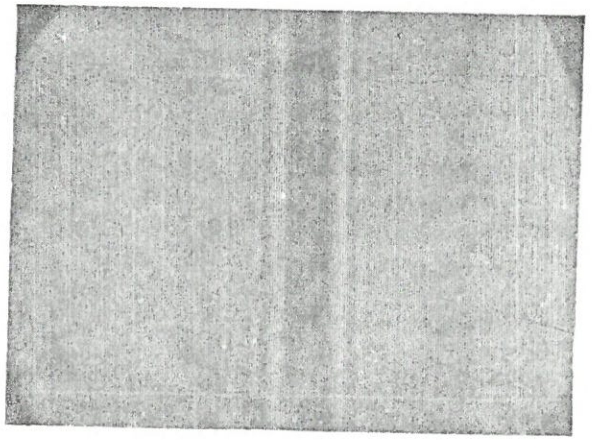

(a)

(b)

FIG. 12. Carrier-frequency hologram and reconstruction: (a) hologram of a straight wire, (b) reconstruction.

The experimental results are shown in Fig. 12. Figure 12(a) shows the hologram produced by a straight wire. The fine line structure arises from the term $2s_r s_b \cos\xi z$ of Eq. (18). The carrier-modulated zone plate term is not discernible to the observer, since it is masked by the other terms of Eq. (18). It is nevertheless present, and led to the reconstruction shown in Fig. 12(b), which shows both the reconstructed image and the twin image. They are seen to be widely separated. The central image and its inseparable real and virtual reconstructed images have been blocked by use of a stop.

LIST OF SYMBOLS, WITH DEFINITIONS

a	light amplitude distribution.
A	radian spatial-frequency of a sinusoidal signal.
f	impulse response of a filter.
F	transfer function of a filter; Fourier transform of f.
F_1	focal length of a lens.
F_2	focal length of a lens used as a dispersive filter.
g	impulse response of half-plane filter.
G	transfer function of half-plane filter, Fourier transform of g.
k	$k=\pi/(\lambda z)$.
m	modulation index of an amplitude-modulated temporal signal.
s	signal.
s_b	bias level of signal.
s_r	remainder of signal.
S	Fourier transform of s.
S_r	Fourier transform of s_r.
W	bandwidth of signal s.
x, y	coordinates
z	a distance measured along the optical-system axis.
α,β	dummy variables, used as variables of integration.
γ	magnitude of a complex function.
δ	Dirac delta function.
ζ	a complex function.
θ	angle of diffraction produced by the signal $\exp(-iAx)$.
θ_c	angle of diffraction produced by an optical wedge.
λ	wavelength of light.
ξ, η	spatial radian frequencies corresponding to x, y, respectively.
ξ_c	spatial-carrier frequency.
σ	amplitude of a sinusoidal signal.
φ	phase portion of a complex function.
ϕ	phase portion of transfer function F.
ϕ_A	phase modification of dispersed sinusoidal signal.
χ	dispersed signal, or $\chi=s^*f$.
χ_A	dispersed sinusoidal signal.
ω	radian frequency of a monochromatic light beam.
$\mathfrak{F}$	(script F) symbol for Fourier transformation.

SOVIET PHYSICS – DOKLADY VOL. 7, NO. 6 DECEMBER, 1962

PHYSICS

PHOTOGRAPHIC RECONSTRUCTION OF THE OPTICAL PROPERTIES OF AN OBJECT IN ITS OWN SCATTERED RADIATION FIELD

Yu. N. Denisyuk

(Presented by Academician V. P. Linnik, February 19, 1962)
Translated from Doklady Akademii Nauk SSSR, Vol. 144, No. 6, pp. 1275-1278, June, 1962
Original article submitted February 4, 1962

To Mr. Wesley Edwards the best wish wishes Denisyuk 4.08.81.

The following discussion pertains to a phenomenon discovered by the author, wherein the reflecting properties of an object are manifested with extraordinary fidelity.

We have an arbitrary object O, on which radiation from a source S is allowed to fall (see Fig. 1). In the case of Rayleigh scattering the radiation reflected by the object will combine with the radiation emanating from the source, thereby forming a stationary standing wave pattern. In Fig. 1 the loci d_1, d_2, d_3 respresent the antinodal surfaces of these waves. We assume, further, that in the space surrounding the object there is a definite volume V filled with a photosensitive emulsion (such as a Lippman emulsion). After an appropriate exposure and chemical processing, a photographic deposit will be formed in the volume, its density exactly simulating the intensity pattern in the standing wave.

It turns out that such a spatial structure is a unique kind of optical equivalent of the object. If radiation from the same source that illuminated the object during exposure is allowed to impinge on this structure, it will reflect this radiation in such fashion that the wave field of the reflected radiation will be identical to the wave field of the radiation reflected by the object. The observer h in this case will detect the appearance of a virtual spatial image of the object O' (see Fig. 2).

The reflecting properties of the photographic model of the standing wave pattern extend even into the spectral composition. If the radiation incident on the object in producing the photograph is monochromatic, while the radiation incident on the photographic reconstruction during observation has a continuous spectrum, the photograph will reflect only the monochromatic component to which it was originally exposed.

Let us examine in general terms one version of the theory of this phenomenon. We will confine our discussion to the case when the amplitude a_s of the radiation incident on the object does not depend on the coordinate, and we will write the wave functions for the incident and reflected radiations as follows:

$$\psi_s = a_s e^{ikL_s(r)}, \quad \psi_0 = a_0(r)\, e^{ikL_0(r)},$$

where $k = 2\pi/\lambda$.

The wave function for the total field will be equal to

$$\psi_w = \psi_s + \psi_0.$$

We find the intensity of this field by multiplying ψ_w by ψ_w^*:

$$I_w = a_s^2 + \psi_0\psi_s^* + \psi_s\psi_0^* + a_0^2. \qquad (1)$$

We are assuming that the total wave field in the volume filled with the photosensitive emulsion acted to form a substance whose density q is proportional to I_w. We will call this structure the wave photograph. If the photographic deposit is a nonmagnetic dielectric and if q is small, then the dielectric constant of the wave photograph will have the form

$$\varepsilon = \varepsilon_{f0} + \delta\varepsilon, \qquad (2)$$

where

$$\delta\varepsilon = \varkappa I_w. \qquad (3)$$

Consider the image formation process. Let the same radiation that was incident on the object during the photographic reconstruction now impinge on the

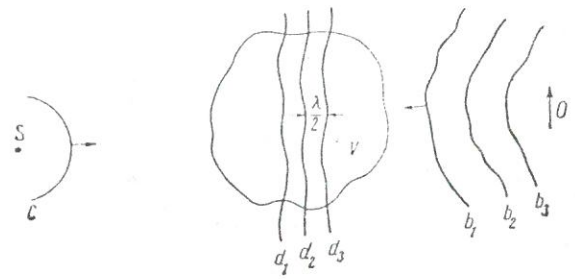

Fig. 1. Diagram showing the formation of the wave image. S is the radiation source, O the object, C the wave surface of the incident radiation; b_1, b_2, b_3 are the wave surfaces of the radiation reflected by the object; d_1, d_2, d_3 are the antinodal surfaces of the standing waves formed as the result of interference between the wave C and the waves b_1, b_2, b_3.

wave photograph. We will consider only the case of a scalar wave field, i.e., one in which ψ obeys the Helmholtz equation

$$\nabla^2 \psi + \varepsilon k^2 \psi_0 = 0. \quad (4)$$

We now make use of the fact that $\delta\varepsilon$ is small in order to determine the wave function of the radiation reflected by the photograph, solving (4) in the first approximation of perturbation theory. For this purpose we write ψ as the sum of the unperturbed function ψ_s, which satisfies Eq. (4) for $\varepsilon = \varepsilon_{f_0}$, and some small perturbation ψ_f evoked by the presence of $\delta\varepsilon$:

$$\psi = \psi_s + \psi_f. \quad (5)$$

It is obvious that ψ_f is the sought-after wave function of the radiation reflected by the wave photograph.

Substituting (5) and (2) into (4) and invoking the equation for the unperturbed problem, we obtain

$$\nabla^2 \psi_f + \varepsilon_{f0} k^2 \psi_f = -\delta\varepsilon k^2 \psi_s. \quad (6)$$

This equation, the right-hand side of which contains the known quantities, is the inhomogeneous Helmholtz equation. For simplicity we will let $\varepsilon_{f_0} = 1$, whereupon

$$\psi_f = \frac{1}{4\pi} \int_V \frac{\delta\varepsilon k^2 \psi_s e^{ikr}}{r} dV, \quad (7)$$

where V is the volume of the wave photograph. Substituting into (7) the value of $\delta\varepsilon$ from (3), into which the value of I_w from (1) has in turn been substituted, and carrying out the indicated transformations, we find

$$\psi_f = \frac{\varkappa k^2}{4\pi} \int_V \frac{(a_s^2 + a_0^2)\psi_s e^{ikr}}{r} dV + \frac{\varkappa k^2}{4\pi} \int_V \frac{\psi_s^2 \psi_0^* e^{ikr}}{r} dV + \frac{\varkappa k^2}{4\pi} a_s^2 \int_V \frac{\psi_0 e^{ikr}}{r} dV. \quad (8)$$

We analyze all the components of this expression below.

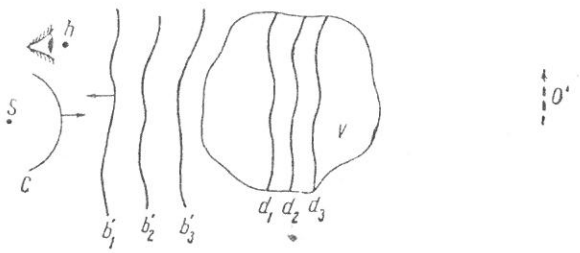

Fig. 2. Production of an image from the wave photograph. d_1, d_2, d_3 are the reflecting "mirror" layers formed at the site of the antinodal surfaces: b_1', b_2', b_3' are the wave surfaces of radiation reflected from the photograph.

It can be shown that if the region in which the function ψ_0 is considered is separated from the object by a distance R which is much greater than the linear dimensions of the object d or the radiation wavelength λ ($R \gg d$, $R \gg \lambda$), the gradients a_0 will be negligibly small in comparison with the gradients of the function ψ_0. With this in mind, it is quickly understood that the first term in (8) describes the interaction of the radiation with a medium that has a constant index of refraction. This case reduces of course to the reflection from the boundary of the volume filled by such a medium.

The second integral of Eq. (8) is also not important, for, as is readily demonstrated, its integrand oscillates and the integral goes to zero everywhere except in the region of the geometric shadow of the object.

Notice the third component of the wave function of the radiation reflected by the wave photograph. It is seen without great difficulty that this component describes radiation issuing from sources which fill the volume and fluctuate in phase with the radiation field reflected from the object. On this basis we identified the wave function corresponding to this component with the wave function of the radiation that, after reflection from the object, passed through the volume of the wave photograph as through a medium with a slight negative index of refraction [the smallness of the negative index of refraction is implied by the fact that the secondary interaction of the radiation emitted by the volume V with the active substance contained in this volume is not included in Eq. (8)].

An observer registering this radiation will see a spatial image of the object of the photograph O' (see Fig. 2), where those details of the object from which the issuing rays traverse a greater thickness of the volume V will show up more clearly than those details whose issuing rays pass through the volume V where the thickness is less.

We also looked into another version of the wave photograph theory, wherein it is shown that upon reflection of radiation from a standing wave surface established by the wave photograph (for example d_2 in Fig. 2), the boundary conditions of radiation reflected from the object are reproduced at this surface.

In view of the unique relation between the boundary conditions and the wave function, it follows that the wave function of radiation reflected from each such surface will coincide with the wave function of radiation reflected from the object. Summing the wave functions corresponding to all the standing wave surfaces, it can be shown that in the radiation reflected from the wave photograph the same rays will be present as in the radiation reflected from the object and that the amplitude of these rays will be proportional to the paths which they covered in the volume V.

Following the same line of reasoning, it can also be shown that the wave photograph will imitate the

radiation even in spectral composition. In order to give a unified explanation for the wave photograph simultaneously reproducing such a wide range of the optical properties of the object, we introduced the concept of the "optical scattering operator," which is interpreted as a certain idealized scattering structure acting on the given radiation in the same manner as the real object. The wave photograph may be regarded as the model of such an operator.

In order to lend support to the postulates of the theory, we set up an experiment, the general layout of which corresponded to the diagram of Figs. 1 and 2. The incident radiation on the object in this case had a wavelength of 5460 A. The standing wave pattern was recorded by means of Lippman photosensitive plates. For the objects we used spherical mirrors of various radii of curvature and the scale of an object-micrometer. The wave photographs of the mirrors were similar in their attributes to concave diffraction gratings and exhibited the same optical strength for $\lambda = 5460$ A as the original mirror. The radiation reflected by the wave photograph of the object-micrometer scale, in accordance with the theory, formed a spatial image of this scale outside the emulsion layer.

The phenomenon discussed represents a generalization of the group of phenomena which form the basis of the Lippman color photographic process [1] and the hologram method of Gabor [2]. It can be used to advantage for the development of optical imagery techniques, creating a complete illusion of reality in the reproduction of objects, as well as in structural analysis (electron structural analysis, x-ray structural analysis, etc.), sonar, radar, ultrasonic flaw detection, and in the preparation of dispersing elements of the diffraction grating type.

LITERATURE CITED

1. G. Lippman, J. de Phys., 3, 97 (1894).
2. D. Gabor, Proc. Roy. Soc. London, A 197, 454 (1949).

ON THE REPRODUCTION OF THE OPTICAL PROPERTIES OF AN OBJECT BY THE WAVE FIELD OF ITS SCATTERED RADIATION

Yu. N. Denisyuk (pp. 522–532)

Received 6 April 1962

In this paper the formation of a unique kind of optical equivalent of a given object is considered. This optical equivalent is formed by the photographic model, created under certain conditions, of the standing wave which results from superposition of the radiation incident on, and the radiation reflected by, the object. It is shown that if radiation from the same source as is used to make the photograph is incident on such a model (called a "wave photograph"), then the wave function of the radiation reflected by each fixed photographic surface of the standing wave coincides with the wave function of the radiation scattered by the object, in some region of space. The wave function of the radiation reflected by the wave photograph as a whole was found by summation of the wave functions of the radiation reflected by the above-mentioned surfaces. It turned out that this wave function is also related to the wave function of the radiation scattered by the object—it describes the radiation which on being scattered by the object, passed through the wave photograph volume just as if it were filled by a medium with a negative absorption index. The observer, detecting the radiation which is reflected by the wave photograph, sees, accordingly, the spatial image of the object; features of the image, rays of which passed through the photograph volume over a long path, will appear clearer than those features, the rays of which passed through a smaller region of the wave photograph volume. The theory is tested. A special case in which the object was a spherical mirror was studied. In accordance with the theory, the wave photographs of such mirrors were equal in optical strength to the optical strength of the original mirror. In its dispersion properties the photographic layer which was obtained resembled a concave diffraction grating.

Analyzing Gabor's hologram method[1] and Lippman's light photography method,[2] one reaches the conclusion[3] that the phenomena underlying these methods are special cases of the more general phenomenon of the representation of the optical properties of the object by the spatial photographic model of the standing wave which is formed from the superposition of the incident radiation and the radiation scattered by the object. Let us suppose that there exists some arbitrary object O, upon which radiation from source S (Fig. 1a) is incident. For Rayleigh scattering, the radiation reflected by the object, superposed on the radiation issuing from the source, forms a stationary standing wave pattern.* The antinodal surfaces of these waves are designated in Fig. 1 by d_1, d_2, etc. Into the space surrounding the object, the volume V, is filled by a light-sensitive Lippman emulsion, is introduced. After appropriate exposure and chemical processing a photographic image is formed in this volume with a density which is a reproduction of the intensity distribution in the standing wave. It appears that such a spatial structure is a unique kind of optical equivalent of the object. If radiation from the same source which illuminated the object during its exposure is incident upon this structure, then it reflects this radiation in such a way that the wave field of the reflected radiation will be identical, up to some fixed degree, to the wave field of the radiation reflected by the object. Thus, the observer h records the appearance of a virtual spatial image of the object O′ (Fig. 1b). The reproducing properties of the photographic model of the standing wave pattern also extend to the area of spectral composition. If the radiation incident on the object during the making of the photograph is monochromatic, and the radiation incident on the photograph during observation has a complex spectrum, then the photograph reflects only the monochromatic component to which it was exposed.

*Here Rayleigh scattering is that leaving wavelength unchanged.

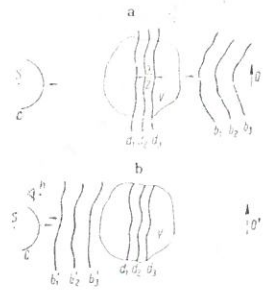

Fig. 1. (a) Schematic diagram showing production of the wave photograph. O—object; c—wave surface of radiation incident on the object; b_1, b_2, b_3—wave surfaces of radiation reflected by object; d_1, d_2, d_3—antinode surfaces of standing wave which is formed as a result of the interference of wave c with waves b_1, b_2, b_3. (b) Schematic diagram showing the formation of image by the wave photograph. d_1, d_2, d_3—The reflecting layers formed at the site of the antinode surfaces; b_1', b_2', b_3'—wave surfaces of radiation reflected by the layers d_1, d_2, d_3; O′—image of the object.

We call this type of photograph a "wave photograph". To produce it, the following conditions must be fulfilled: (a) plane or weakly divergent spherical waves

must be incident on the object; (b) the volume of the wave photograph V must be situated at a large distance from the source of radiation and the object; and (c) the density of the photographic deposit must be small and proportional to the intensity of the standing wave.

Let us consider the theory of the process. In accordance with (a) and (b) we write the wave functions of the incident radiation and the radiation scattered by the object.*

*The phase multiplier $e^{i\varphi}$ is hereafter omitted.

$$\psi_s = a_s e^{ikL_s(r)} \tag{1}$$

$$\psi_0 = a_0(r)\, e^{ikL_0(r)}. \tag{2}$$

Here the functions $L_s(r)$ and $L_0(r)$ satisfy the eikonal equation. The wave function of the field which results from superposition of the incident and the scattered radiation has the following form:

$$\psi_W = a_s e^{ikL_s} + a_0(r)\, e^{ikL_0}. \tag{3}$$

Multiplying ψ_W by ψ_W^* we find the intensity of the standing wave

$$I_W = a_s^2 + a_0^2 + 2a_s a_0 \cos k(L_s - L_0). \tag{4}$$

Setting the argument of (4) equal to a constant, kp, we get the equation of the "isophase" surface. For the special case when $kp = 2\pi n$, where n is integral, this surface coincides with the antinode surface.

$$L_s(r) - L_0(r) = p. \tag{5}$$

Substituting (5) into (4) we find

$$I_W = a_s^2 + a_0^2 + 2a_s a_0 \cos kp. \tag{6}$$

We now assume that the total wave field recorded in volume V is such that the density of the photographic deposit q which has been formed is proportional to I_W

$$q = \varkappa I_W. \tag{7}$$

Let us suppose that this deposit is a nonmagnetic dielectric, for which $\mu = 1$ and $\sigma = 0$. For small values of q, the function $\varepsilon(q)$ can be expanded in a series bounded by the first two terms of the expansion

$$\varepsilon_f = \varepsilon_{f0} + \frac{\partial \varepsilon}{\partial q} q = \varepsilon_{f0} + \gamma q, \tag{8}$$

where ε_{f0} is the dielectric constant of the emulsion prior to exposure. Substituting I_W from (6) into (7) and then substituting the value of q which is obtained, into (8), we find the dielectric constant of the wave photograph

$$\varepsilon_f = \varepsilon_{f0} + \gamma\varkappa(a_0^2 + a_s^2 + 2a_s a_0 \cos kp). \tag{9}$$

In the volume V we select the infinitesimally thin layer found between the isophase surfaces on which the parameter p has the values p and p + dp (Fig. 2a). Having taken the gradient of (5), it is a simple matter to verify that the normal to this layer is directed along the gradient of ε_f and that, consequently, such a layer may be considered as the boundary separating two media with dielectric constants ε and $\varepsilon + d\varepsilon$. Differentiating (9) with respect to p, we define the quantity $d\varepsilon$

$$d\varepsilon = 2\varkappa\gamma k a_s a_0(\rho) \sin kp\, dp. \tag{10}$$

Here, ρ is the radius vector of the surface layer. Substituting (10) into the Fresnel formula and taking into account the fact that ε_f varies only slightly, we find the "amplitude" reflection coefficient of the layer for natural light, which most closely corresponds to the scalar approximation we assumed,

$$d\mu = \zeta a_0(\rho) \sin kp\, dp, \tag{11}$$

where

$$\zeta = \frac{1}{2}\frac{\varkappa\gamma}{\varepsilon} k a_s.$$

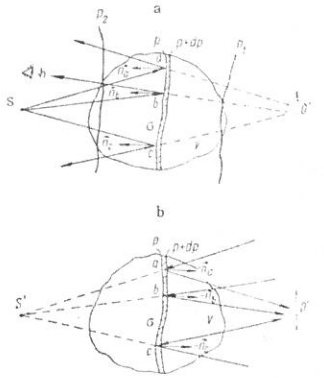

Fig. 2. (a) Radiation from the same source S as illuminates the object during the making of the wave photograph is incident on the isophase surface. Sa, Sb, Sc—the rays incident on the isophase surface; n_a, n_b, and n_c—normals to the isophase surface, O'—virtual image of the object. (b) Radiation which forms a real image of the source S is incident on an isophase surface of the wave photograph. S'—the real image of the source, and O'—real image of the object.

Let us suppose now that the same radiation ψ_s which was incident on the object during the making of the photograph is incident on the wave photograph (Fig. 2a). Taking advantage of the low density of the photographic image we determine the wave function of the radiation reflected from each individual isophase layer, in order to later combine these functions to determine the function of the incident radiation reflected by the entire photograph.*

*An analogous calculation technique is described in ref. 2.

Multiplying the wave function of the incident radiation ψ_s by the reflection coefficient of the layer $d\mu$ we find the value which the wave function $d\psi_f$ of the radiation reflected by this layer assumes at the surface of the layer itself. In other words we find the boundary condition of the Dirichlet problem for the wave function $d\psi_f$

$$d\psi_f(\rho) = d\mu\psi_s. \tag{12}$$

Substituting into (12) the value of $d\mu$ from (11) and ψ_s from (1), and also using the equation of the isophase surface (5), we get

$$d\psi_f(\rho) = \zeta a_s a_0 e^{ikL_0(\rho)} e^{ikp} \sin kp\, dp. \tag{13}$$

It is easy to see that $d\psi_f(\rho)$ differs from the wave function, ψ_0 of (2), of the radiation reflected from the object, only by the constant multiplier

$$\chi = \zeta a_s e^{ikp} \sin kp\, dp \tag{14}$$

Should the surface of the isophase layer be closed, then from this coincidence, on the basis of the theorem

of the uniqueness of the relation of the wave function to the boundary conditions, it would have been possible to conclude that the wave function of the radiation reflected by the isophase layer coincides with the wave function ψ_0 of the radiation scattered by the object with accuracy up to the multiplier χ. Solution of the problem for a non-closed surface is substantially simplified when the dimensions of the isophase layer are much greater than the wavelength. In this case the well-known hypothesis of Kirchhoff diffraction theory—involving the fact that in calculating the perturbation behind a screen with apertures, one may take the boundary conditions on the aperture surface as the boundary conditions corresponding to free propagation of light, and the boundary conditions on the surface adjacent to the screen as equal to zero—becomes completely accurate.[4] Taking the inverse of this assumption we conclude that the wave function of the radiation reflected by the isophase layer $d\psi_s(r)$ which satisfies the boundary condition (13) coincides with the wave function of the radiation which, being reflected from the object, passed through the surface of the isophase layer as if it were passing through an opening in an opaque screen. We denote such a function as $d\psi_0'(r)$ and we write

$$d\psi_f(r) = d\psi_0'(r) \tag{15}$$

The wave function $d\psi_0'$ coincides with the wave function ψ_0 only in the sector of space bounded by the cone connecting the object and the edge of the isophase layer, i.e., in this case

$$d\psi_0'(r) = \chi\psi_0(r). \tag{16}$$

In the remaining portion of space, this function, with accuracy up to the diffraction limit is equal to zero, i.e.,

$$d\psi_0'(r) = 0. \tag{17}$$

In accordance with what has been said above, the observer h (Fig. 2a), registering the radiation reflected by the isophase layer, sees the virtual space image of the object O′, situated at the same place which this object occupied when the photograph was made. Thereby the surface layer will seem to him a window set in a space of objects.

We consider the mechanisms of reflection of the radiation from the isophase layer from the point of view of geometrical optics. Having taken the gradient of the left side of (5) and taking into account that $\nabla L = 1$ one may obtain the following relation:

$$\mathbf{n} = \frac{\mathbf{l}_s - \mathbf{l}_0}{|\mathbf{l}_s - \mathbf{l}_0|}, \tag{18}$$

where n is the normal to the isophase layer, l_s is the ray vector of the incident radiation and l_0 is the ray vector of the radiation scattered by the object. On the other hand, the law of reflection of radiation from the interface between two media may be written in this form:

$$\mathbf{n} = \frac{\mathbf{l}_s - \mathbf{l}_f}{|\mathbf{l}_s - \mathbf{l}_f|}, \tag{19}$$

where l_f is the ray vector of the radiation reflected by the boundary. Equating (18) to (19), we get $l_0 = l_f$, i.e., the direction of the rays reflected by the isophase layer coincides with the direction of the rays reflected by the object. Since the amplitude of the rays reflected by the isophase layer also coincides with the amplitude of the rays reflected by the object (11), then the observer sees a virtual image of the object O′. The corresponding path of the rays is shown in Fig. 2a.

A wave photograph may form not only a virtual image of the object, but a real one as well. Such an image is obtained when the photograph during observation is illuminated by radiation which converges into the real image of the source. To show this, it is necessary to vary the sign of the eikonal of the wave function of the incident radiation and to carry out the transformation analogous to (12) and (13). The corresponding case is shown in Fig. 2b.

We proceed to consideration of the interaction of the radiation with the wave photograph in its entirety. To do this, we generalize the theory to the case when the wave photograph, during observation, is illuminated by a source with a complex spectrum, i.e., we assume that

$$\psi_s = \int_0^\infty a_s(k')\, e^{ik'L_s(r)}\, dk'. \tag{20}$$

Substituting for ψ_s in (12) and using Eqs. (5) and (11), we find the value which belongs in the given case to the wave function of the radiation reflected by the isophase layer at the surface of the layer itself

$$d\psi_f(\rho) = \zeta a_0(\rho) \sin kp\, dp \int_0^\infty a_s(k')\, e^{ik'L_0(\rho)} e^{ik'p}\, dk'. \tag{21}$$

It is not difficult to note that (21) is the sum of functions the eikonal of which is the same as the eikonal of the radiation scattered by the object. Accordingly we may find the value assumed at the point h by the wave function of the radiation reflected by the isophase layer by replacing the radius vector of the points of the isophase surface ρ by the radius vector of the observation point r of (13), (15), (16) just as in the previous case. The wave function of the radiation reflected by the entire wave photograph is found by summing the wave functions of the radiation reflected by the separate isophase layers. In this, one need take into account only the layers for which the cone connecting the edge of the layer and the object includes the point of observation; see (16) and (17). In the case shown in Fig. 2a, such an isophase layer is included between the layers p_1 and p_2, passing through the points in which the straight line connecting the object and the point of observation cuts the surface of the volume of the wave photograph. Substituting r for ρ in (21) integrating this expression from p_1 to p_2, signifying by ψ_g the integral with respect to the boundary of the volume where ε_f undergoes a discontinuity and d does not satisfy (11), and representing sinkp in exponential form, we obtain the wave function of the radiation reflected by the entire wave photograph,

$$\psi_f(r) = \psi_g + \zeta a_0(r) \int_{p_1}^{p_2} dp\, \frac{e^{ikp} - e^{-ikp}}{2i} \int_0^\infty a_s(k')\, e^{ik'L_0(r)} e^{ik'p}\, dk'. \tag{22}$$

The first term of this expression is the wave function of the radiation reflected by the boundary of the photograph volume. We consider the second term more carefully, designating it ψ_0''. Changing the order of the integration with respect to p and k′ we get

$$\psi_0'' = -\frac{i}{2}\zeta a_0(r) \int_0^\infty dk' a_s(k')\, e^{ik'L_0(r)} \int_{p_1}^{p_2} \left[e^{i(k+k')p} - e^{i(k'-k)p}\right] dp.$$

Carrying out the integration with respect to p we find

$$\psi_0'' = -\frac{i}{2}\zeta a_0(r)\int_0^\infty a_s(k')\,e^{ik'L_0(r)}\,[\delta_1(k+k')-\delta_1(k'-k)]\,dk', \quad (23)$$

where

$$\delta_1(k'-k) = 2e^{\frac{i(p_2+p_1)}{2}(k'-k)}\sin\frac{(p_2-p_1)(k'-k)}{2}\cdot\frac{1}{(k'-k)}.$$

The functions $\delta_1(k + k')$ and $\delta_1(k' - k)$ have the properties of Dirac delta functions. The function $\delta_1(k' - k)$ has a maximum for $k' = k$, where it assumes the value $p_2 - p_1$. Analogously, $\delta_1(k + k')$ has a maximum for $k' = -k$. The width of these maxima is determined by the dependence

$$\Delta k' = \frac{2\pi}{p_2 - p_1}. \quad (24)$$

Inasmuch as in our case the dimensions of the volume of the wave photograph are much greater than a wavelength, i.e., $p_2 - p_1 \gg 1/k$ when $\Delta k' \ll k$ and the delta functions may be replaced by rectangular pulses of width Δk and height $p_2 - p_1$. Substituting this function into (23) and transforming with the use of the derived expression (22), we find

$$\psi_f(r) = \psi_g + \frac{i}{2}\zeta(p_2-p_1)\,a_0(r)\int_{k'=k-\frac{\Delta k}{2}}^{k'=k+\frac{\Delta k}{2}} a_s(k')\,e^{ik'L(r)}dk'. \quad (25)$$

Thus, the wave function of the radiation reflected from the wave photograph is made up from the wave function of the radiation reflected by the boundary of its volume, and the packet of wave functions of which the wavelength differs little from the wavelength of the radiation which exposed the photograph; its eikonal agrees with the eikonal of the radiation scattered by the object; its amplitude is proportional to the amplitude of the radiation scattered by the object, and the path $(p_2 - p_1)$, which this radiation traversed in the volume of the wave photograph. All these signs give the right to identify such radiation as that which, being scattered by the object, passed through the volume of the wave photograph, as through a medium with a slightly negative absorption. The observer detecting such radiation sees a virtual spatial light image of the object; moreover, the features of the object the rays from which traveled through the volume over a long distance will seem clearer than the features the rays from which intersect the volume where its spatial extension is small.

Changing the limit of integration in (20) with respect to k' to $-\infty$ and making all the subsequent transformations, one may show that the wave photograph also forms a real image of the object.

It must be noted that the more complete theory gives for ψ_f an expression differing from (25) by the presence of a term which corresponds to the radiation being propagated in the region of the geometric shadow of the object. The reason for the absence of this term in the present case is sufficiently clear: in the region of the geometric shadow of the object, the isophase surfaces degenerate into lines, and the mathematical apparatus based on them no longer has any meaning.

To confirm the theory, a series of experiments was set up. Below we present the results for a special case when a spherical mirror was used as an object. Being the optical equivalent of the object, the wave photographs of this mirror must according to the theory, reproduce the optical strength and resolving power of the original for the same wavelength as that for which the exposure was carried out.

The scheme of the wave photograph obtained with the spherical mirror is shown in Fig. 3a. Above the convex aluminized mirror Z a photo-plate a is situated. The normal to the surface of the photoplate makes an angle α with the optic axis of the collimator, which is located above the system. The plane monochromatic wave which emerges from the collimator, on passing through the photo-plate is reflected from the mirror. As a result of the superposition of the incident and reflected radiation, above the mirror a system of standing waves is formed, which is recorded by the emulsion layer e.

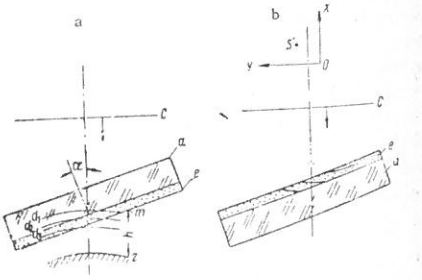

Fig. 3. (a) Diagram of the production of wave photograph of convex mirror. c—Wave surface of incident radiation, a—photo-plate, e—emulsion layer of photo-plate, d_1, d_2, d_3—antinode surfaces of the standing waves, Z—convex mirror with outer aluminizing. (b) Diagram of measurement of optical characteristics of wave photograph of convex mirror. S'—image of monochromator slit or hatched globe, formed by wave photograph. XOY is the coordinate system in which the position of the image is measured.

The photography is carried out on a special Lippmann photo-plate which had been hypersensitized.[5] Chemical processing of the exposed photo-plate is achieved by two methods. In the first of these the exposed plate, after development in a metol-hydroquinone developer and and fixing, was bleached with mercuric chloride. As a result, in the volume of the photograph, clear dielectric in an amount approximately proportional to the intensity of the standing wave was formed. See (7), (8). In development by the second method the exposed plate is developed in a pyrogallic developer. As a result metallic silver with a high coefficient of reflection was formed at the standing wave antinodes.

The fact that the optical properties of the photographs thus obtained duplicate the optical properties of their originals, could easily be seen even during a simple visual observation. Thus, if the radiation of an incandescent lamp is incident on the photograph from the side of the emulsion layer, then after reflection it is collected in a real image of the filament of this lamp; if the same radiation were to fall from the other side, then the image of the filament would be virtual (Figs. 2a and 2b). The chromaticity of the images of the filament coincided with that of the radiation which exposed the photo-plate.

In Fig. 4 we present curves showing the dependence of the reflection coefficients of certain photographs on the wavelength. The setup for these measurements was

that of Fig. 3b. Incident on the photograph from the side of the emulsion layer was radiation emanating from a monochromator slit which was situated in the focal plane of the collimator objective. The radiation reflected by the photograph converged in a real image of the slit S'. This image was projected on a photomultiplier which registered the value of the current of the reflected radiation. After this, in the position of the wave photograph an arc shaped mirror was set, equal in dimension and radius of curvature to the convex original mirror, and the current of the radiation scattered by this mirror was found. As may be seen from Fig. 4, the reflection coefficient of the wave photograph is small but has a clearly expressed maximum in the region approximately corresponding to the wavelength of the radiation which exposed the photograph. A certain shifting of the maximum in the region of short wavelengths is explained by the shrinkage of the layer, which occurs during the chemical processing.

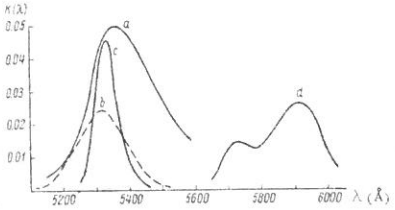

Fig. 4. Dependence of the reflection coefficient of wave photographs of convex mirrors on the wavelength.

Curve	Wavelength of the radiation which exposed the photograph (Å)	Thickness of emulsion layer (μ)	Type of chemical processing
a	5460	4	pyrogallol
b	5460	4	bleaching
c	5460	10	bleaching
d	5890	4	bleaching

We measured, in addition, the resolving power of the wave photographs obtained for $\alpha = 0°$. The general setup of this measurement was similar to the one shown in Fig. 3b with the sole difference that in the focal plane of the collimator objective in the given case a hatched globe was placed, which was illuminated by radiation from a mercury lamp ($\lambda = 5460$ Å). Investigation of the image of the globe S' showed that the resolving power of the wave photographs differed little from the resolving power of their originals. Thus, if at field of view angles from 0° to 5.4° the resolving power of the mirror of radius 2058 mm both for sagittal and for meridional rays was 53 lines/mm, then the resolving power of the wave photograph in the same conditions was 48 lines/mm. Similarly, for a radius of curvature of the original of 1000 mm and resolving power of 110 lines/mm, the resolving power of the wave photograph was 80 lines/mm.

The study of the wave photographs of convex mirrors was completed by measuring the dependence of their focal lengths on the wavelength. The device setup in this case was similar to the one for the measuring of the spectral curves of the reflection coefficient (Fig. 3b). We judged the focal distances of the wave photograph according to the position of the image of the monochromator slit S' in the coordinate system XOY. Here, as the origin of the coordinate system, the point was chosen which the image of the slit would pass through when in place of the wave photograph, a curved mirror with a radius of curvature equal to the radius of curvature of the mirror original is put.

In Fig. 5 is shown the result of the measurement of the focal length of the wave photographs of mirrors of different radii of curvature. The photographs were made for $\alpha = 0$ and $\lambda = 5460$ Å. Wavelength is given along the ordinate axis of the figure, and the point $\lambda = 5460$ Å was taken as the ordinate origin. Along the abscissa the displacement of the images of the slits along the axis OX of the chosen coordinate system (Fig. 3b) is given; the image displacement along the axis OY is absent in this case.

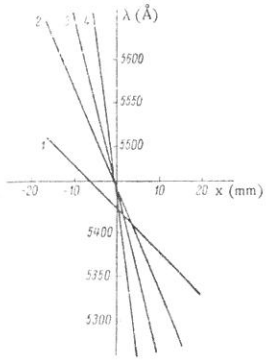

Fig. 5. Dependence of the focal lengths of the wave photographs on the wavelength for different radii of curvature of the original mirror. The surface of the photoplate was normal to the incident radiation, and $\lambda = 5460$ Å. 1—R = 2058 mm, 2—R = 1000 mm, 3—R = 600 mm, 4—R = 300 mm.

Figure 6 shows the results of measurements of the position of the image of the slit when it was inclined with respect to the incident radiation ($\alpha \neq 0$, Fig. 3a) during exposure of the photoplate. The coordinate axes of the graph correspond to the axes represented in Fig. 3b, and the experimental curves are the trajectories which describe in this system of coordinates the image of the slit upon variation of the wavelength of the radiation which forms it. On the curves the point at which the image of the slit is found for $\lambda = 5460$ Å is sharply separated.

It is easy to see, that thanks to the special choice of the coordinate system XOY, in which the position of the slit is taken into account, and of the coordinate systems of the graphs, the experimental curves shown in Fig. 5 pass through the origin of coordinates only when the wave photographs corresponding to them accurately reproduce the focal length of the original mirror for the monochromatic radiation with wavelength equal to the wavelength of the radiation incident on the photograph during the making of the photograph. In Fig. 6, the coincidence of the point $\lambda = 5460$ Å with the origin of coordinates corresponds to such a case. As is seen from these graphs, the wave photographs we obtained reproduce the focal length of the original to an accuracy of not less than 0.6%.

We treat some questions related to the practical application of the photographs we made. As is seen from Fig. 5, the wave photographs exposed to the radiation incident normal to the surface of the photoplate have an extraordinarily strong longitudinal chromatic

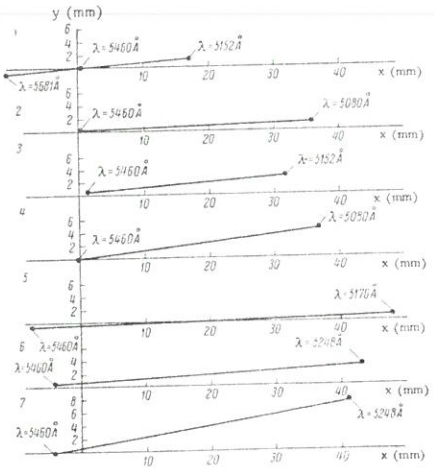

Fig. 6. Spectral disposition of the wave photographs of the convex mirrors obtained for different angles of inclination of the photoplate during exposure; λ = 5460 Å. 1—R = 600 mm; α = 1°47'; 2—R = 1000 mm, α = 58'; 3—R = 1000 mm, α = 2°35'; 4—R = 1000 mm, α = 3°35'; 5—R = 2058 mm, α = 58'; 6—R = 2058 mm, α = 1°47'; 7—R = 2058 mm, α = 5°11'.

aberration with sign opposite to the sign of the aberration of an ordinary lens. The fact that elements with such properties may find application in optical device design should not be overlooked.

For the wave photographs exposed with inclined positions of the photoplate, there is added to the longitudinal chromatic aberration a transverse aberration which increases with angle of inclination of the plate. It is not difficult to show that the magnitude of this aberration is determined by the same laws as hold for diffraction gratings. Actually, using the known relations for the first-order spectra of the usual diffraction grating, one may find t_1, the grating constant for the grating, the dispersion of which is equal to the dispersion of the given photograph. On the other hand, knowing the inclination of the photoplate and the distance between the antinodes of the standing wave, one may determine the period t_2 of the surface structure of the wave photograph directly. The table gives the values of t_1 and t_2 calculated by this means for each of the photographs represented in Fig. 6. The fact that these values come out in good agreement shows that the mechanism of the interaction of the radiation with the wave photograph is analogous to the mechanism of interaction of the radiation with a diffraction grating. Of course, there are differences too. They find their expression in the fact, for example, that the spectrum in the given case does not lie on the Rowland circle.

Radius of curvature of the original mirror (mm)	Angle α	Photographic constant t_1, calculated with respect to the dispersion (μ)	Number of striations per millimeter corresponding to t_1	Photographic constant t_2 calculated from the standing wave geometry (μ)	Number of striations per millimeter, corresponding to t_2
600	1°47'	7.1	140	8.7	115
1000	58'	17.2	58	16.1	62
1000	2°36'	6.4	156	6.0	166
1000	3°35'	4.1	244	4.3	230
2058	58'	21.0	48	16.1	62
2058	1°47'	8.1	123	8.7	115
2058	5°11'	2.8	356	3.0	330

It should be noted that the parameters of the diffraction gratings we obtained are not limited. By increasing the angle of inclination of the plates, one could have prepared grating lattices with still greater dispersion. The fundamental difficulty which is encountered in this method consists of the absence of sufficiently bright sources of monochromatic radiation. Actually in producing the given photographs the maximum permissible dimensions of the source and the degree of its monochromaticity were determined according to the formulas

$$\Delta S = \frac{\lambda R f}{2hd} \tag{26}$$

and

$$\Delta\lambda = \frac{\lambda^2}{4h}. \tag{27}$$

Here ΔS is the dimension of the radiation source, f is the focal distance of the collimator, h is the depth of the standing wave pattern, R is the radius of curvature of the original mirror, d is the diameter of the original mirror, and Δλ is the permissible width of the spectrum of the source radiation. From these relations it follows that the increase in the depth of the standing wave pattern (Fig. 3a) connected with the increase in the angle of inclination, is attained on account of the diminution of the dimensions of the source and the rise in its monochromaticity. However, the intensity of the standing wave pattern is decreased by this, and the exposure time grows beyond reasonable limits. Substantial progress in this direction should result from the use of quantum generators, which provide high-intensity radiation and are highly monochromatic. The practical application of wave photographs as diffraction gratings may also be precluded by the smallness of their reflection coefficients. It is easy to see, however, that if in the surface layer of the wave photograph the unexposed emulsion is removed, then a relief is formed, which is typical of a grating with a concentration of intensity in the given part of the spectrum. Metalizing such a relief plate, one may obtain a diffraction grating with a high reflection coefficient.

In conclusion I consider it my pleasant duty to express my deep gratitude to P. L. Kapitsa, V. P. Linnik, and I. V. Obreimov for their attention and support.

REFERENCES

1. D. Gabor, Proc. Roy. Soc. (London) A197, 454 (1949).
2. G. Lippman, J. Phys. 3, 97 (1894).
3. Yu. N. Denisyuk, Dokl. Akad. Nauk SSSR 144, 1275 (1962), Soviet Phys.—Dokl. 7, 543 (1962).
4. M. Born, "Optik". Springer, Berlin, 1933. State Publishers of Science and Technology, Khar'kov-Kiev 1937.
5. Yu. N. Denisyuk and I. P. Protas, Opt. i Spektroskopiya 14, 721 (1963), Opt. Spectry. 14, 381 (1963).

JOURNAL OF THE OPTICAL SOCIETY OF AMERICA VOLUME 53, NUMBER 12 DECEMBER 1963

Wavefront Reconstruction with Continuous-Tone Objects*

EMMETT N. LEITH AND JURIS UPATNIEKS
The Institute of Science and Technology, The University of Michigan, Ann Arbor, Michigan
(Received 24 April 1963)

Holograms and high-quality reconstructions have been made by using a two-beam interferometric technique. The extraneous twin image and other interfering terms have been eliminated. Two types of objects have been used which are not suitable for the conventional wavefront reconstruction technique: objects which do not transmit a strong background wave (e.g., transparent lettering against a dark background) and continuous-tone objects.

1. INTRODUCTION

A TWO-STEP imaging process developed by Gabor[1] consists of photographing the Fresnel diffraction pattern of an object and using this recorded pattern to construct an image of the original object. The recorded diffraction pattern, called a hologram, bears little resemblance to the original object, but contains most of the information needed to reconstruct the object. When the hologram is illuminated with monochromatic light derived from a point source, the interaction of the hologram transparency with the incident light generates diffracted wavelets, a component of which is identical to the wavelets which were used to produce the hologram. This component can be used to reconstruct an image of the original object.

A primary difficulty with the process is that the phase of the incident beam is lost in the recording process. This, in general, makes a reconstruction impossible, except for the special class of object in which the major portion of the incident beam is transmitted without scattering. The scattered light combines vectorially with the direct beam to produce a resultant whose phase differs only slightly from that of the direct beam alone. Here the loss of phase is of relatively less importance and does not prohibit a recognizable reconstruction. Even in this case, however, the loss of phase exacts its toll, in that not more than half of the light transmitted by the hologram contributes to the reconstructed image. A second component, with energy equal to that of the desired component, forms an extraneous image whose Fresnel diffraction pattern is superimposed on the desired image, causing its degradation. Another component, which represents intermodulation distortion, contributes further to the degradation.

The conventional Gabor technique is thus limited to relatively simple objects which transmit a large proportion of the light without scattering. For example, transparencies which contain dark lettering against a transparent background are well suited to the process and to the authors' knowledge, are the only kind which have appeared in the published literature. The reverse of this, an object with a dark background, is wholly unsuited to the process. Continuous-tone objects also are unsuitable because the extraneous terms generated in the process are sufficiently large as to completely obscure the reconstructed image.

In the 15 years since Gabor's announcement of the process, various published papers have described means for eliminating the extraneous twin image. In particular, a technique described by the present authors[2] removes not only the extraneous image term, but also the intermodulation distortion term and, in addition, tends to reduce other distortion terms such as may arise from nonlinearities in the film transmittance–exposure characteristic. The process, in theory, permits perfect reconstructions for any type of object transparency. Initial experimental results, as shown in the authors' previous paper, demonstrated the correctness of the ideas presented, but the reconstructions obtained were lacking in sharpness and were generally of low quality, owing to a lack of equipment. This condition has been corrected and the potentialities of the process have now been realized.

2. MAKING THE HOLOGRAM

The technique was described briefly in the previous paper[2] and is reviewed here with emphasis on a descriptive approach. A two-beam interferometric process is used in producing the hologram, as shown in Fig. 1. The object, located at plane P_1, is illuminated with collimated monochromatic light, and a Fresnel diffraction pattern of the object is formed at plane P_2. Adjacent to the object is a prism. The portion of the incident beam

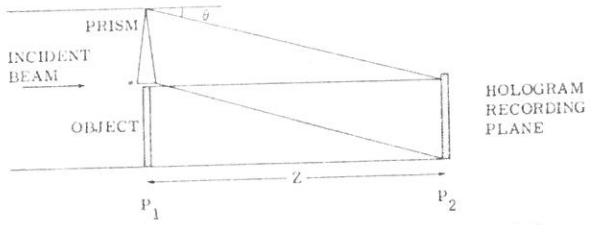

FIG. 1. Wedge technique for producing a two-beam hologram. The object is placed in the lower part of plane P_1; the hologram is recorded at plane P_2.

* This research was sponsored by the A. F. Office of Scientific Research of the Office of Aerospace Research, as part of the Advance Research Projects Agency's Vela Uniform Program. It was presented at the March 1963, Jacksonville meeting of the Optical Society of America [J. Opt. Soc. Am. 53, 522 (1963)].

[1] D. Gabor, Nature **161**, 777 (1948); Proc. Roy. Soc. (London) A197, 454 (1949).

[2] E. Leith and J. Upatnieks, J. Opt. Soc. Am. 52, 1123 (1962).

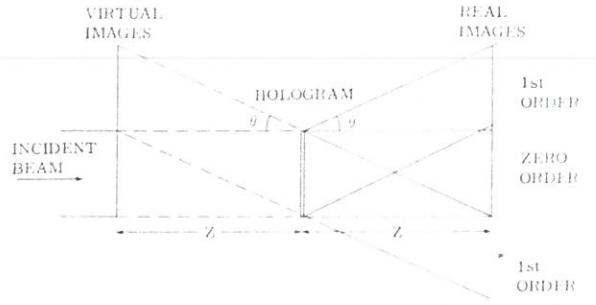

FIG. 2. The reconstruction process. Low-quality conventional reconstructions occur on hologram axis. High-quality reconstructions occur in the first-order diffracted waves.

which impinges on the prism is deviated through an angle θ and thereby becomes superimposed on the lower portion of the beam. The superposition of the two beams results in a fringe pattern which is superimposed on the Fresnel diffraction pattern of the object. A photographic plate at P_2 records the resultant pattern, thereby producing the hologram.

In the absence of the upper beam, the photographic plate at P_2 produces a conventional Gabor hologram. Let the amplitude of the light at P_2 be given by

$$U(x,y)=A(x,y)e^{i\phi(x,y)}, \tag{1}$$

where A is the amplitude modulus and ϕ is the phase of the impinging light. The photographic plate records only the magnitude factor A; the phase portion $e^{i\phi}$ is discarded. The conventional hologram is thus an incomplete record.

The interference pattern produced when the second beam, which we call the reference beam, is present results in a hologram in which the phase portion ϕ of the Fresnel diffraction is also recorded. Let the reference beam have an amplitude modulus A_0. This beam produces at P_2 a wave of amplitude $A_0e^{i\xi_c x}$, where the phase term $e^{i\xi_c x}$ results from the beam impinging on P_2 at an angle. A beam impinging on a plane at an angle θ produces (for small values of θ) a progressive phase retardation $\exp i2\pi\theta x/\lambda$ across this plane. Hence we have the relation $\xi_c=2\pi\theta/\lambda$.

When the reference beam is present, the light amplitude distribution at the hologram recording plane is $A_0e^{i\xi_c x}+Ae^{i\phi}$. Let us assume that the plate which records this distribution has a response which is linear with intensity, that is, suppose the amplitude transmittance of the plate after development to be given by

$$T=T_0-kI, \tag{2}$$

where I is the intensity distribution at plane P_2,

$$I=|A_0e^{i\xi_c x}+Ae^{i\phi}|^2, \tag{3}$$

d k are constants determined by the trans-
posure characteristic of the plate. Equation
eral, a reasonable approximation to the
ristic over a transmittance between
measured relative to the base trans-

mittance. The resultant tra[illegible]ttance of the recording plate is, therefore,

$$\begin{aligned}T&=T_0-k|A_0e^{i\xi_c x}+Ae^{i\phi}|^2\\&=T_0-kA_0^2-kA^2-2kA_0A\cos(\xi_c x-\phi).\end{aligned} \tag{4}$$

The plate thus behaves like a square-law modulating device, producing a term $2kA_0A\cos(\xi_c x-\phi)$ which is the real part of the original Fresnel diffraction pattern, modulated onto a carrier ξ_c. In the absence of the diffracting object this term represents a uniform fringe pattern produced by the interference between the two beams. When the diffracting object is present, its Fresnel diffraction pattern modulates this fringe pattern. The amplitude modulus of the diffraction pattern produces an amplitude modulation of the fringes, and the phase portion ϕ produces a phase modulation (or spacing modulation) of the fringes.

It appears, then, that this process has permitted the photographic plate to record both the amplitude modu-

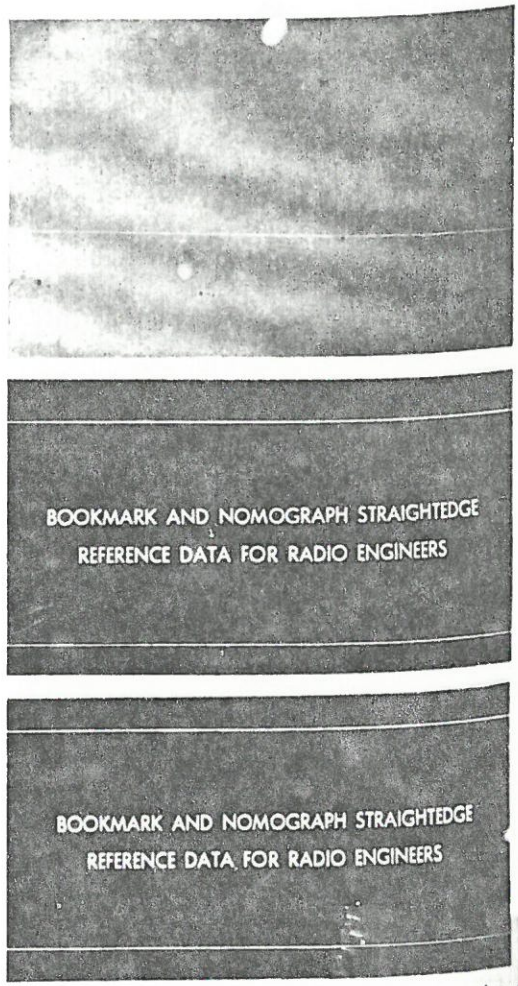

FIG. 3. Hologram and reconstruction of transparent lettering on dark background. (a) Hologram; (b) reconstruction; (c) original object. The original object was about 1.5 cm in length; the distance between objects and hologram planes was about 2 ft. The hologram was made with Kodak Spectroscopic Plates, Type 649-F.

FIG. 5. Hologram and reconstruction of a portrait. The object was about 1.5 cm square and the distance between object and hologram was about 2.5 ft. The hologram was made with Kodak Spectroscopic Plate, Type 649-F.

image a distance z from the hologram. The factor $e^{i\xi_c x}$ alters this view only in that it results in the virtual image being displaced laterally a distance proportional to ξ_c. The conjugate term $\frac{1}{2}kA_0A e^{-i(\xi_c x-\phi)}$ produces the real image, which likewise is displaced from the axis, as implied by the factor $e^{-i\xi_c x}$.

DISCUSSION OF THE TECHNIQUE

ding results are based on the square-law of the recording plate, as given by Eq. ion is only approximately obtained, there er distortion terms present on the hologram. These will, for the most part, give rise to second and higher-order diffracted waves, which in the reconstruction process will form additional images at greater off-axis positions, and will therefore be separated from the first-order images. Hence, while we have assumed a specific and only approximately realized film characteristic, the actual characteristic is not at all critical to the process, and in no case was it necessary, or apparently even desirable, to consider controlling this characteristic.

By controlling the relative amplitude of the object-bearing beam and the reference beam, for example, by the use of attenuating filters placed in one of the beams, the contrast of the fringe pattern can be controlled. If this contrast were made sufficiently small by attenuating the object-bearing beam, then Eq. (2) could certainly be made to hold to great accuracy, if this were desired. However, if the fringe contrast is too low, the reconstructed image will tend to be grainy. Good reconstructions are in practice possible over a wide range of fringe contrasts.

The reconstructed image that results has the same contrast as the original object, irrespective of the gamma of the recording plate, or of the manner in which the plate is developed. The reason for this is that all spatial frequency components of the object, including the dc or bias term, are preserved on the hologram in their proper proportion, except for whatever minor effects are produced by the modulation transfer function of the hologram plate. Such is not the case for the conventional hologram, in which the reconstruction includes an ambient background or dc term which tends to reduce the contrast of the reconstructed image, and whose magnitude is a function of the recording process.

Another feature of interest is that the reconstructed image is a positive, that is, it has the same polarity as the original object. If the hologram is contact printed so as to produce a negative of the original hologram, then this negative hologram also produces a positive reconstruction. This situation is different from the conventional wavefront reconstruction process, in which the hologram produces a negative reconstruction, and the contact-printed copy of the hologram produces a positive image.

5. EXPERIMENTAL RESULTS

The effectiveness of the process is shown by Figs. 3-5. Figure 3 shows a hologram and reconstruction of transparent lettering against a dark background. Such an object is not suitable for the conventional type of hologram, since no strong background wave is produced. However, the object is quite suitable for the two-beam process. The reconstruction is very nearly equal in quality to the original, which is shown for comparison.

Figures 4 and 5 show holograms and reconstructions of continuous-tone transparencies. This type of object is fully an order of magnitude more difficult to reconstruct than simple objects like lettering. Figure 4 shows a

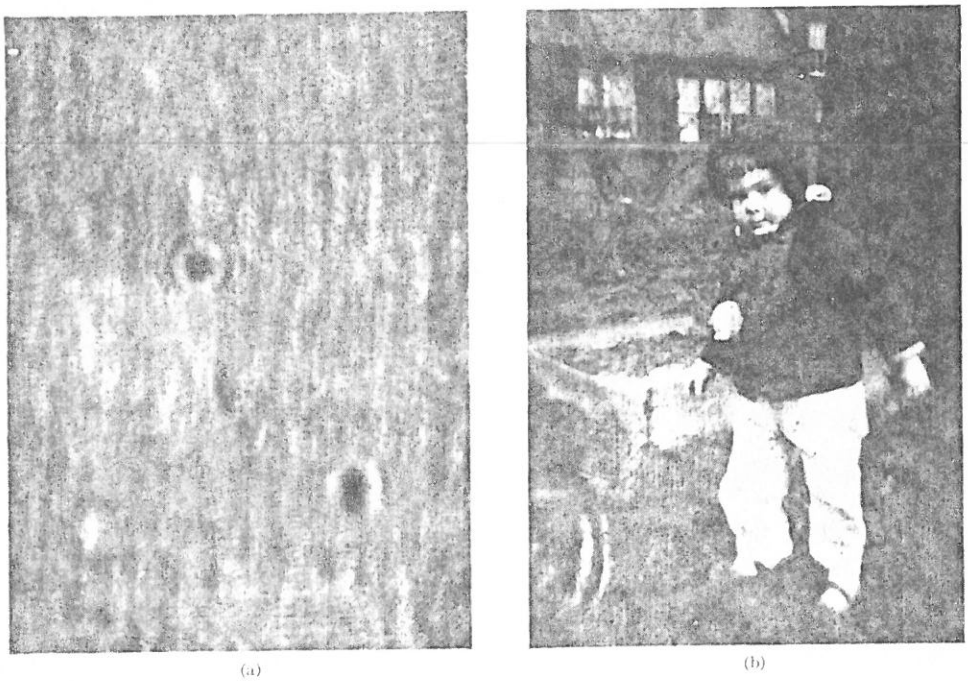

(a) (b)

FIG. 4. Hologram and reconstruction of a scene. The object was about 1.5 cm in height, and the distance between object and hologram was about 4 ft. The hologram was made with Kodak High Contrast Copy.

tus and the phase of the Fresnel diffraction pattern. However, the complete demonstration of this requires that the final term of Eq. (4) be separable from the remaining terms. Also, for our purpose there is the additional problem of how this term can be used to reconstruct the original object.

3. RECONSTRUCTION

The various terms of Eq. (4) can indeed be separated and a reconstruction achieved. There are two different, although somewhat similar, methods for doing this. The more general one, described in Ref. 2, requires forming the Fraunhofer diffraction pattern, or spatial frequency spectrum, of the hologram by the use of a lens, and then carrying out a spatial filtering procedure. The other method is more simple in that it does not require such spatial filtering, but requires a larger value of the spatial carrier frequency, ξ_c.

The second method of reconstruction is used here. The reconstruction is made in much the same way as with conventional holograms. The hologram is placed in a collimated beam of monochromatic light, as shown in Fig. 2. The bias term $T_0-k.1_0^2$ and the term $k.1^2$ combine to form a reconstruction that is essentially the reconstruction produced by the conventional hologram, in which a real image forms at a distance z on one side of the hologram, and a virtual image forms at an equal distance on the other side of the hologram. The distance z, of course, is just the distance that existed between the object and the recording plate when the hologram was produced, assuming light of the same wavelength is used throughout. Both the real and virtual images form about the optical system axis and for this reason the two images are inseparable, i.e., each image must be viewed with the other as a background. In this region there occur also the extraneous intermodulation terms described previously[2] and prevent reconstructions of good fidelity from all but simple objects.

The fine-line structure of the hologram, embodied in the term $k.1_0.1\cos(\xi_c x-\phi)$, causes the hologram to act like a diffraction grating, producing a pair of first-order diffracted waves, as shown in Fig. 2. One of these produces a real image, occurring in the same plane as the conventional real image, but displaced to an off-axis position. Similarly, the other diffracted wave produces a virtual image, situated in the plane of the conventional virtual image, but displaced. As seen from Fig. 2, the light components comprising these two off-axis images are nonoverlapping, and both components are removed from the region where the conventional reconstructions occur. These images are of high quality, and are free from the effect of any of the extraneous terms which the reconstruction produces. Either the real or virtual image can be photographed, but it is more convenient to use the real image, since this can be recorded by placing a plate at the image position, thus avoiding the need for a lens. Hence, the entire process is carried out without lenses.

A comprehensive analysis supporting the above contentions about the reconstructions was given previously[2] and is not repeated here. However, we show the plausibility of the contentions. If the term $k.1_0.1\cos(\xi_c x-\phi)$ of Eq. (4) is rewritten in its exponential form, $\frac{1}{2}k.1_0.1e^{i(\xi_c x-\phi)}+\frac{1}{2}k.1_0.1e^{-i(\xi_c x-\phi)}$, it is seen that the first exponential term is, to within a constant multiplier and an exponential term $e^{i\xi_c z}$, exactly the complex function that describes the Fresnel diffraction pattern produced at plane P_2 by the object. This term can therefore be considered as having been produced by a virtual

scene containing a number of objects which are quite recognizable in the reconstruction, although the hologram is unintelligible.

Figure 5 shows the hologram and the reconstruction of a portrait; this is the most difficult type of object for wavefront reconstruction. There is considerable resolution present in the picture (which, of course, is not entirely preserved in the publication process). However, the difficult part of the reconstruction is not in the fine detail, but in the broad, uniform areas, which constitute a considerable part of Fig. 5. These will appear mottled in the reconstruction unless considerable care is taken; the hologram must be extremely clean, free from defects (scratches, etc.) and if made on film instead of plate, must be placed in a liquid gate containing a fluid which closely matches the index of refraction of the film. The need for the liquid gate arises from the thickness variations of the hologram film. The effect of film-thickness variations in this type of work is discussed by Ingalls.[3]

The holograms shown in Figs. 3–5 warrant some discussion. First, it should be pointed out that, in addition to what is reproduced in the figures, there is a fine-line fringe structure which is completely lost in the publication process. Most of the visible structure is noiselike and is unrelated to the useful data contained on the hologram. This feature is characteristic of two-beam holograms. The hologram of Figs. 3 and 5 show prominent coarse fringes. These result from interference between the incident beam and reflected light from the back surface of the recording plate. Their presence has no relevance to the recorded data, but neither do they noticeably degrade the reconstructed image.

The holograms and reconstructions were made using a helium–neon gas laser operating at 6328 Å. The light produced by the laser is highly monochromatic and can be imaged to a fine point; these features make the laser an excellent light for this application.

Holograms and high-quality reconstructions have also been made using a conventional mercury arc lamp in combination with a Mach–Zehnder interferometer (as also suggested in Ref. 2). This technique appears to work as well as the method used here, but is more difficult to carry out experimentally.

[3] A. Ingalls, Phot. Sci. Eng. 4, 135 (1960).

6. COMMENTS AND FUTURE POSSIBILITIES

The results shown here should encourage development of practical applications of the wavefront reconstruction process. In addition, there are many other directions in which investigation can proceed. One possibility is the production of the generalized hologram described previously.[2] Presently the authors are working on a color process of wavefront reconstruction. Another interesting facet is the superposition of several holograms on a single plate by means of multiple exposures. The various reconstructed images will be separated if the fringe pattern of each hologram has a different orientation, since the reconstructed images will then be displaced in different directions. This process has been demonstrated with three overlapping holograms, without noticeable deterioration of the reconstructed images. Another possibility is to make the hologram and the subsequent reconstruction in highly divergent light beams. This will produce a reconstruction which is a magnified image of the original object. This process constitutes a lensless microscope which should be highly corrected and work over a large field. Moderate magnifications (about 10) have been demonstrated, and magnifications far greater than this seem attainable.

ACKNOWLEDGMENT

The authors wish to acknowledge the assistance of B. A. Vander Lugt, who, in performing work of a related nature, showed the authors the value of a gas laser for a light source. While the laser is not essential to the process, its considerable brilliance, spatial coherence, and monochromaticity immensely facilitated the work.

Journal of the
OPTICAL SOCIETY
of AMERICA

VOLUME 54, NUMBER 11 NOVEMBER 1964

Wavefront Reconstruction with Diffused Illumination and Three-Dimensional Objects*

EMMETT N. LEITH AND JURIS UPATNIEKS
Institute of Science and Technology, The University of Michigan, Ann Arbor, Michigan 48107
(Received 12 June 1964)

Holograms of transparencies have been produced in diffused light. The reconstructions are free from flaws and are of a quality comparable to pictures produced by conventional photography with incoherent light. Holograms of three-dimensional scenes have been produced by reflected light. Such holograms produce three-dimensional reconstructions having all the visual properties of the original scene: parallax between near and distant objects, a requirement to refocus the eyes when viewing objects in different parts of the scene, and a stereo effect equal to that of ordinary stereo photography.

1. INTRODUCTION

IN the wavefront reconstruction process of Gabor,[1] the Fresnel diffraction pattern of an object is recorded and subsequently used to produce an image of the original object. Such a record is called a hologram. In the recording process, the phase of the incident illumination is lost. However, it was shown by Gabor that when the diffracted waves from the object are attended by a strong coherent background, the loss of phase is of less importance and a fairly good image of the original object can be recovered from the intensity record alone.

In a paper by the authors,[2] it was shown that a two-beam interferometric process, whereby the object transparency is placed in one beam and the two beams are brought together to produce a Young's fringe pattern, yields a hologram from which a reconstruction of high quality can be obtained.

The present paper discusses a number of subsequent developments, the major ones being the diffused-illumination hologram and the hologram of three-dimensional scenes.

A hologram made from a diffusely illuminated object can yield a reconstruction which is entirely free from the flaws that normally occur in reconstructions. Such flaws result from dust particles, etc., in the optical system.

The two-beam technique, when adapted to the photography of three-dimensional solid objects instead of transparencies, produces reconstructions which resemble to a high degree the original objects, e.g., they are three-dimensional and exhibit a parallax between near and more distant objects.

2. THE BASIC PROCEDURE

Since the fundamentals of the two-beam process were described at length in a previous paper,[2] they will be given here in the most summary manner.

A conceptually simple way to produce a two-beam hologram is shown in Fig. 1(a). An object transparency, located at plane P_1, is illuminated with monochromatic, spatially coherent light, and a Fresnel diffraction pattern of the object is formed at plane P_2. Adjacent to the object is a prism, which intercepts a portion of the incident beam and deviates it through an angle θ, so that it becomes superimposed, at plane P_2, on the object-bearing portion of the beam. The superposition of the two beams creates a fringe pattern which is superimposed on the Fresnel diffraction pattern of the object. The illumination at P_2 is recorded by a photographic plate; this process produces a square-law modulation, in which the amplitude portion of the Fresnel diffraction pattern amplitude-modulates the fringes, and the phase portion phase-modulates the fringes. The fringe pattern thus becomes a modulated

*This work was presented in part at the April 1964, Washington, D. C., Meeting of the Optical Society of America [J. Opt. Soc. Am. 54, 579 (1964)].

[1] D. Gabor, Nature **161**, 777 (1948); Proc. Roy. Soc. (London) **197**, 454 (1949).

[2] E. Leith and J. Upatnieks, J. Opt. Soc. Am. **53**, 1377 (1963).

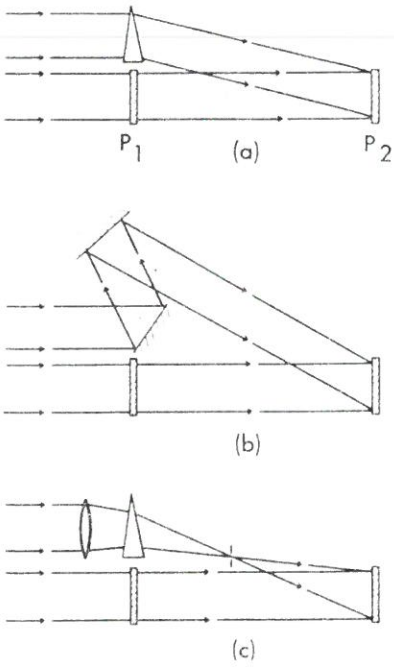

FIG. 1. Methods of introducing the reference beam. In (a), a prism is used; in (b), a pair of mirrors are used; in (c), a lens, prism, and pinhole in combination are used.

carrier, analogous to the *temporal* carrier wave used in communication systems.

Alternatively, the hologram can be thought of as a diffraction grating, and this viewpoint is a convenient one for describing the reconstruction process. When illuminated with monochromatic, spatially coherent light, the hologram produces a zero-order spectrum and a pair of first-order spectra. One of the first-order spectra forms a real image, and the other a virtual image. Whereas a conventional diffraction grating has only inadvertently introduced irregularities, which give rise to undesired ghost lines, the hologram diffraction grating has deliberately introduced irregularities, which give rise to complete, well-defined images.

While the prism method of producing the interference fringes is tutorially attractive, it is not the optimum way to achieve experimental results because a prism introduces astigmatism unless the incident light is accurately collimated. Any aberrations in the non-object-bearing beam (to which we have given the designation *reference beam*) are incorporated onto the hologram and degrade the reconstructed images, just as if the aberrating elements were in the object-bearing beam. Mirrors are preferable for deviating the reference beam, and results of the highest quality have been obtained in this way. A single mirror, in the conventional Lloyd's mirror arrangement, has produced good results. An even better arrangement is to use a two-mirror system, as shown in Fig. 1(b), which permits the light to be incident on the mirrors at nearly normal incidence instead of at nearly grazing incidence as in the Lloyd's mirror arrangement. This method also permits the mirrors to be of a size comparable to the hologram-recording plate, whereas the Lloyd's mirror must, in general, be much larger than the area over which the fringes are generated.

Another arrangement which is highly satisfactory is shown in Fig. 1(c). A prism is used in combination with a lens. This lens can be of extremely poor quality without affecting the image quality. The lens causes the reference beam to be brought to a focus at some position between planes P_1 and P_2. This focused spot is the spread function for the lens-prism combination and will be degraded by the aberrations of these optical elements. However, if a pinhole, with a diameter equal to the resolution of the ideal or aberration-free spread function of the system, is placed at the position of the point image, the aberration will be removed. The pinhole removes the aberrations by removing those light rays whose position of intersection with the focal plane has been altered by the aberrations. The resulting hologram and its reconstructions are free from the aberrations of both the lens and the prism. However, the lens still exerts the effect of its focal power on the reconstructed images, but it now acts like a perfect lens. The pinhole attenuates the reference beam by whatever proportion of the light misses the pinhole, but this loss is a small price to pay for what is achieved.

3. DIFFUSE ILLUMINATION

Suppose that, in the optical system shown in Fig. 1, a diffusing element such as opal glass is placed between the source and the object, thus causing the object to be illuminated with diffused coherent light. The hologram made in this manner thereby acquires several interesting and useful properties.

An objection which the reader may raise is that the diffuser destroys the coherence of the light, thereby making a reconstruction impossible. Indeed, the light thus diffused behaves in some ways as if it were incoherent, but it retains those properties which are essential to the wavefront reconstruction process. The light impinging on the object is no longer a well-defined wavefront, but instead has a phase and amplitude which vary randomly from point to point. These phase and amplitude relations, however, are time invariant, in contradistinction to the case of incoherent illumination.

The two-beam hologram made in this manner reconstructs, as before, to produce a real and a virtual image in the first-order diffracted waves. The reconstructed images have acquired an interesting property: they can now be observed visually without an eyepiece or other optical aids. The virtual image can be seen by looking through the hologram as if it were a window, and the real image can be seen suspended in front of the hologram. If the diffuser had not been used in making the hologram, the reconstructions could not be thus observed. To explain why this is so, let us consider what happens when one observes a transparency which is illuminated from behind with a point source. Except for some scattering, the observer receives light only

from that part of the transparency which lies on the line between the point source and the pupil of the eye; this is usually a negligible portion of the transparency. However, if a diffuser is placed between the source and the transparency, then light from all points of the transparency reaches the eye and the transparency is seen in its entirety.

This argument readily applies to the hologram case case if one thinks of the hologram as reconstructing not only the transparency, but also the diffusing plate. Thus, the observer sees the reconstructed image as if it were illuminated by a diffuse source.

Another consequence of the diffusing plate is that the hologram acquires a different appearance. In the conventional, single-beam hologram, each object is converted into a Fresnel diffraction pattern with definite structure; for example, the letter *o* becomes a series of concentric circles. Also, coarse structure in the object tends to persist rather than lose its identity. Similar effects occur in the two-beam holograms described previously,[2] except that the diffraction pattern of the object is largely submerged by other effects produced by the reference beam. However, in the diffuse type of hologram, no recognizable Fresnel diffraction patterns or surviving coarse structures are discernible. The light from the object, when it impinges on the hologram plate, has a uniform, fine grain-like structure like the grain of photographic film. This pattern is completely homogeneous and always has the same appearance, irrespective of the object. The observable structures seen in the hologram of Fig. 2 are diffraction patterns produced by dust particles, etc. in the reference beam. They neither contribute to nor degrade the reconstructed images in any apparent way.

Another interesting property of the diffuse-illumination hologram is that, since each point on the object illuminates the entire hologram recording plate, the plate can be broken into small fragments, and each piece will reconstruct the entire object. As the fragments become small, resolution is, of course, lost, since the hologram constitutes the limiting aperture of the wavefront-reconstruction imaging process.

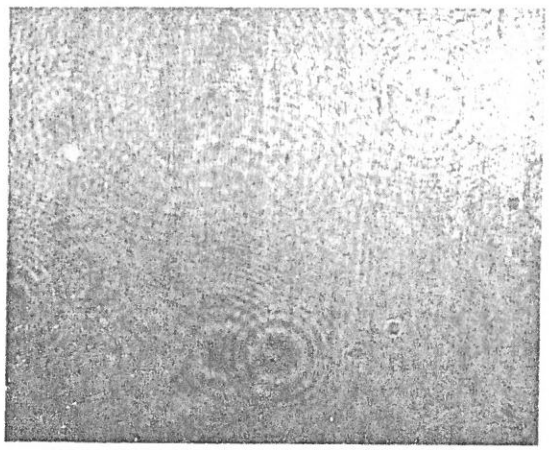

FIG. 2. Hologram of two transparencies which were illuminated with diffused coherent light. The transparencies were placed 14 and 24 in. from the hologram recording plate, in such positions that neither obscured the other when viewed from the position where the hologram was recorded.

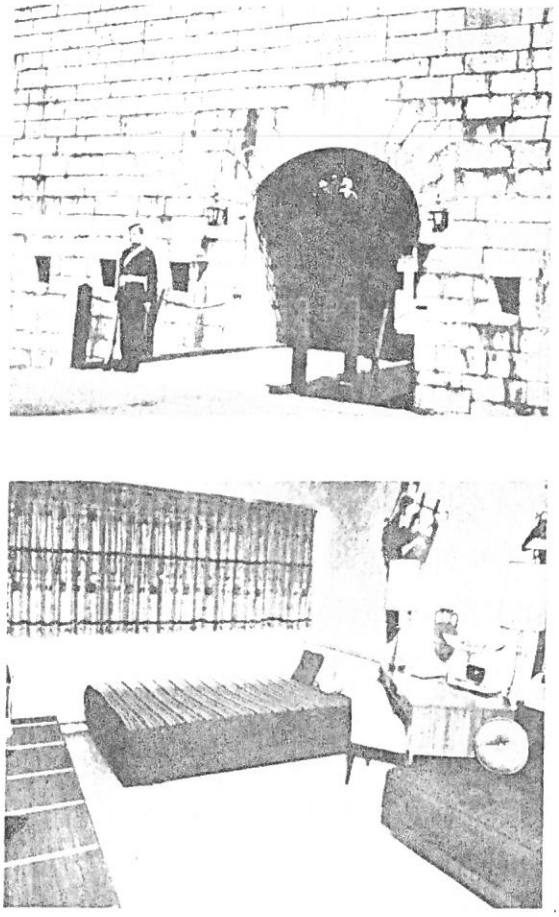

FIG. 3. Reconstructions of two transparencies which were recorded in the hologram shown in Fig. 2.

Possibly the most significant property of the diffused illumination hologram is that local imperfections in the optical elements no longer observably degrade the process. It is well known to experimenters in this field that any scratches, dust, pits, etc., on the hologram recording plate or on other elements of the optical system, cause annoying diffraction patterns that appear in the reconstructed image. These can be minimized by careful technique, but, in practice, never completely eliminated.[3] They can be observed, for example, in the reconstructions in our previous paper.[2] They are not products of the wavefront reconstruction process *per se* but arise from the use of coherent illumination. In the diffused illumination holograms, such imperfections are, to all appearances, completely removed from the reconstructed image. Thus, not only is extremely careful

[3] A technique used by Kirkpatrick and El-Sum goes far toward minimizing these flaws by rotating in a continuous manner some of the optical elements about the optical system axis; J. Opt. Soc. Am. **46**, 825 (1956).

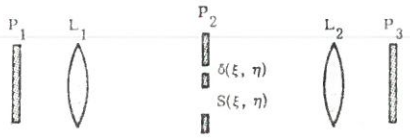

FIG. 4. Fraunhofer diffraction method. Semi-diffusing ground glass at P_1 causes, at P_2, a bright spot on axis, surrounded by diffused light. An opaque mask at P_2 has two openings: a pinhole on axis which passes the focused spot of nondiffused light, and an off-axis aperture in which the object transparency $S(\xi,\eta)$ is placed. The hologram is made at plane P_3.

technique no longer necessary, but the holograms can be scratched, handled so as to receive fingerprints, and otherwise abused without noticeable deterioration of image quality. The reconstructions shown in Fig. 3, for example, are entirely free of such imperfections.

The diffused-illumination hologram is, in fact, more immune to defects of the recording plate than is a picture recorded by conventional photography. A scratch, loss of a piece of the emulsion, etc., in the hologram case does not entail a loss of a part of the picture, since each point on the object spreads its effect over the entire hologram plate. Gross portions of the hologram record can be damaged or removed, yet no portion of the reconstructed image suffers noticeable deterioration.

A further advantage of this type of hologram (and this advantage applies also, to a lesser extent, to the nondiffused-illumination holograms) is that the dynamic range of the photographic process is greatly increased. Small, very bright areas in the object have their energy spread over the entire recording place, and in reconstruction are restored to their proper level. Intensity ratios of 10^4–10^5 between the brightest regions and the smallest distinguishable intensity steps have been observed in the image; this represents a dynamic range of 40 to 50 dB. Even greater ranges seem achievable experimentally.

Some of the properties thus described can be more fully understood by recognizing that the hologram represents an encoding of the original object transparency, or signal. There are, in fact, two distinct encoding processes manifested in this hologram technique. The first is a simple dispersion, in which each resolution element of the object is encoded into a function which occupies the entire hologram plate. Such dispersion-encoding is manifested by, and indeed is fundamental to, all wavefront reconstruction techniques. With diffused illumination, the dispersion is much greater than is usual in previously described methods. The second encoding process embodied in the diffused-illumination technique involves increasing the signal bandwidth by convolving the spatial-frequency spectrum of the object with that of the diffused illumination, which can be thought of as a noise-like signal with a broad, uniform, spatial-frequency spectrum. When the object transparency is illuminated with diffused coherent light and transformed into a hologram, the spatial-frequency spectrum of the hologram thus tends to be much greater than that of the object transparency. Such encoding introduces a redundancy into the hologram in that more bandwidth is recorded than is required for the information content of the signal. This, philosophically, is the basis for the insensitivity of the method to the above-mentioned imperfections, which may be designated noise.

A theoretical analysis of the diffused illumination technique is necessary for any complete treatment, but is outside the scope of the present paper.

An interesting possibility is to superimpose the diffraction patterns of two different transparencies onto a single hologram.[4] This is demonstrated in Fig. 2. In Fig. 3, both pictures have been recovered without any trace of cross-modulation effects. Each picture is without flaws.

The superposition can be achieved in various ways. The object transparencies can expose the hologram simultaneously, using a single reference beam. The two object transparencies would be located at different positions in space and the reconstructed images would similarly be separated. This method we call coherent superposition, since the light from one transparency is coherent with that from the other.

Other methods of superposition include that of multiple exposure, with one object at a time exposing the plate. To provide a basis for separating the reconstructed images of the two object transparencies, the transparencies can occupy different, nonoverlapping positions in space; alternatively, the reference beam can be differently directed for each exposure. These methods may be designated incoherent superpositions. Both the coherent and the incoherent methods have been satisfactorily demonstrated.

4. FRAUNHOFER DIFFRACTION HOLOGRAMS

Another type of diffused-illumination hologram is produced by recording the Fraunhofer, rather than the Fresnel, diffraction pattern. An interesting way to produce such a hologram is shown in Fig. 4. A plate of partially diffusing ground glass is illuminated by a collimated beam of monochromatic spatially coherent light. The plate diffuses only a portion of the transmitted light. A lens L_1 brings the nondiffused portion to a point focus on axis at plane P_2. The diffused light surrounds the point image. An object transparency is placed at P_2 in the diffused light, to one side of the point image. An opaque mask at P_2 then blocks the remainder of the diffused light, but contains a pinhole that allows the point image to be transmitted. A second lens reimages the ground glass at plane P_3 and at the same time collimates the nondiffused light, which then is used as the reference beam. A hologram is made by photographically recording the illumination at plane P_3.

As in other diffused-illumination holograms, the reconstruction can be made visually by looking through the hologram when it is placed in a coherent, mono-

[4] This idea is similar to the theta-modulation concept, as described by A. Lohmann, J. Opt. Soc. Am. 53, 1351 (1963).

chromatic beam of light. As before, two images are reconstructed, but they can no longer be designated as the real and virtual images, since both form at infinity. They are symmetrically positioned about the zero-order spectrum. A reconstruction from such a hologram is shown in Fig. 5.

Since the mathematical description of two-beam holograms given previously[1] is not entirely applicable to this configuration, a separate analysis is presented here. The semidiffusing plate has the amplitude transmittance

$$t(x,y)=a_0+n(x,y), \tag{1}$$

where a_0 and $n(x,y)$ give rise to the nonscattered and scattered components of transmitted light, respectively; $n(x,y)$ can be thought of as a random or noise-like quantity. The lens L_1 produces the Fourier transform of Eq. (1), producing at P_2 a distribution of light whose vector amplitude represents the function.

$$T(\xi,\eta)=a_0\delta(\xi,\eta)+N(\xi,\eta), \tag{2}$$

where $\delta(\xi,\eta)$ is the Dirac delta function, $N(\xi,\eta)$ is the Fourier transform of $n(x,y)$, and ξ, η are spatial-frequency variables, arising from the Fourier transformation.

Since the object transparency is introduced at the plane P_2, which we have designated the Fourier transform or spatial-frequency plane, the transparency will be designated as $S(\xi,\eta)$. This function is multiplied with $N(\xi,\eta)$, and the lens L_2 takes a second Fourier transformation, producing

$$\chi(x,y)=a_0+n(x,y)*s(x,y), \tag{3}$$

where $s(x,y)$ is the Fourier transform of the object transparency $S(\xi,\eta)$, and the $*$ indicates a convolution.

The recording process produces a square-law detection, resulting in

$$|\chi(x,y)|^2=|a_0|^2+|s_0(x,y)|^2 +a_0s_0(x,y)+a_0s_0^*(x,y), \tag{4}$$

where $s_0(x,y)=n(x,y)*s(x,y)$.

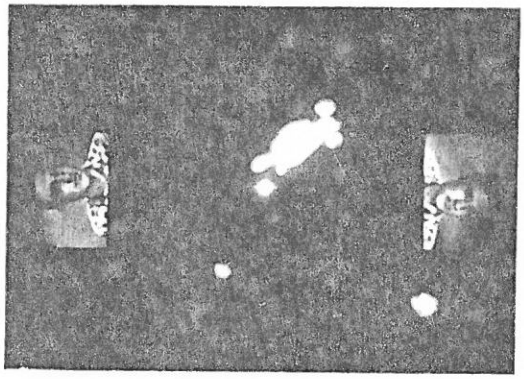

FIG. 5. Reconstruction of a Fraunhofer diffraction hologram. The real and virtual images form at infinity and are thus located in the same plane, but in axially symmetric positions.

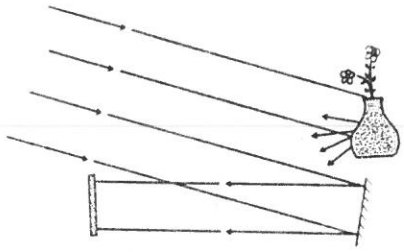

FIG. 6. System for making a hologram in reflected light. The hologram recording plate receives light reflected from the object and from the mirror.

The reconstruction is then accomplished by placing the hologram in a beam of coherent light and using a lens to take the Fourier transform of the hologram, producing the result shown in Fig. 5. This lens can be that of the eye, if the observer looks through the coherently illuminated hologram. In the Fourier transform plane, the term a_0^2 is just the attenuated image of the Dirac delta function that produced the reference beam. The term $|s_0|^2$ produces the noise-like distribution of light around the source, and can readily be discerned in Fig. 5.

The two remaining terms have, respectively, the Fourier transforms $a_0N(\xi,\eta)S_0(\xi,\eta)$ and $a_0N^*(-\xi,-\eta)\times S_0^*(-\xi,-\eta)$. The first is an image reconstructed just as the original object appeared in the diffused illumination. The second is a similar image, but each point on this image is reflected about the origin with respect to the corresponding point in the first image. This is the image that is generated by the square-law process and corresponds to the real image in the case of the Fresnel diffraction hologram.

5. THREE-DIMENSIONAL PHOTOGRAPHY

The basic concepts of wavefront reconstruction imply that three-dimensional objects should reconstruct as three-dimensional images, a fact recognized by Gabor.[1] The two-beam method has proved effective with three-dimensional objects. Holograms made from diffusely reflecting objects have, by virtue of this diffuse reflection, all the properties of the diffused-illumination hologram described in Sec. 3.

To photograph a solid, three-dimensional object by the wavefront reconstruction method, an arrangement like that shown in Fig. 6 is used; this is a fairly obvious adaptation of the techniques shown in Fig. 1. A monochromatic, spatially coherent source illuminates the object to be photographed. Reflected light from the object exposes the photographic plate, which is placed at some convenient and noncritical distance from the object. A high-quality mirror, located adjacent to the object, intercepts a portion of the coherent illumination and reflects it onto the plate. This provides the reference beam against which the phase of the object is compared. The mathematical description of the process is identical with that given previously[2] for making holograms from transparencies.

Reconstruction occurs when the hologram is placed in a monochromatic coherent light beam. Either the real or the virtual reconstructed image may be observed

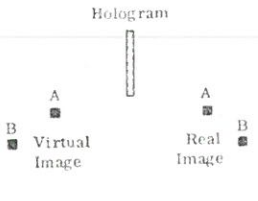

FIG. 7. Diagram showing geometry of objects in the real and virtual images. This diagram is presented as an aid to the text in describing a curious property of the real image.

visually. The virtual image is readily viewed by looking into the hologram as if it were a window. This image has all the appearance of the original object. A three-dimensional effect exists which is equal to that produced by ordinary stereo photography, but here the effect is obtained without the need for a stereo pair of photographs. The reconstruction has some additional properties not produced by ordinary stereo photography. For example, if the observer moves his head while viewing the reconstructed image of the scene, he will observe a change in perspective in the image. There is a parallax between near and far objects which is exactly that which occurs when viewing the original scene. If the observer finds, at one viewing position, that an object in the foreground lies in front of and obscures the viewing of another object, then he can by changing position actually look around the obstructing object and see what lies behind it, just as he could do if viewing the original scene. The observer must refocus his eyes when shifting his observation from near to far objects in the reconstructed scene. Similarly, if the reconstruction is photographed with a camera, the effects of finite focal depth are evident; it is necessary to stop the camera lens if a reasonable depth of field is to be achieved.

The real image forms in front of the plate and can be readily photographed by placing a photographic plate at some suitably chosen position, which, of necessity, is a compromise position, since the image is three-dimensional and thus cannot be imaged on a plane. For visual observation, however, the virtual image is preferred. The real image can be observed visually, but the observer may have some initial difficulty in coordinating his eyes when so doing, for reasons possibly having their origin in physiological optics. If this difficulty is overcome, the results are rewarding, for then one can see the entire reconstructed image suspended in space between himself and the hologram plate.

The real and virtual images are for the most part identical; however, the real image has a curious property not possessed by the virtual image. This is described with reference to Fig. 7. When one observes the virtual image, he will see object A in front of object B, and when the two objects are in line, object A will obscure object B, as indeed it should. To observe the real image, the eye is placed at the position indicated in Fig. 7, in which object B is closer to the eye than is object A. As the observer moves his head, the parallax between A and B is in accord with their positioning. The curious feature is that when the objects A and B are brought into alignment, it is the object B rather than A which is obscured. The near object disappears and one sees the far object through the hole created by the disappearance of the near object.

In making a hologram of a scene in reflected light, two conditions must be met which do not arise when the object is a transparency. First, the coherence length of the source must be greater than the maximum difference in light path between the reference beam and the object beam. Thus, the depth of the scene cannot be greater than the coherence length of the light source. When a laser is used as the source, it should be carefully adjusted so as to eliminate nonaxial modes, otherwise the coherence length is reduced to only a few inches. An electronic spectrum analyzer has been useful both as an aid in tuning the laser and as a laser monitoring device during the exposure.[5]

Second, the reflecting object must remain stationary to less than about $\frac{1}{8}$ the wavelength of the illuminating light for the duration of the exposure. This restriction is not severe for a pulsed laser. For example, if the pulse duration of a laser operating at 6238 Å is 3×10^{-8} sec (30 nsec), an object moving at 2 m/sec will move only $\frac{1}{10}$ the wavelength of the light during this exposure, and a good hologram can be made.

Examples of three-dimensional reconstructions are shown in Figs. 8 and 9. Figure 8 shows a reconstruction of an HO-gauge model railroad engine and various other objects. A hexagonal wrench was placed in the foreground so as to introduce parallax effects. The published print was made from the real image by placing a photographic plate at the position of best focus. To obtain sufficient depth of focus so as to bring the greater portion of the scene into focus, it was necessary to restrict the illumination to only a small portion (about 1.2%) of the entire hologram, i.e., the hologram was stopped just as if it were a lens. The average focal

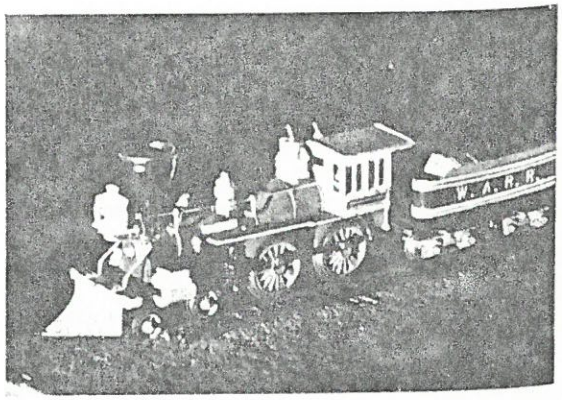

FIG. 8. Photograph of a three-dimensional reconstruction of a model train engine. This photograph was made from the real image after stopping the hologram from its full $f/4$ aperture down to about $f/48$. Note that even at this aperture the foreground is unsharp.

[5] The use of this technique as an aid to producing holograms was suggested and demonstrated to the authors by F. B. Rotz.

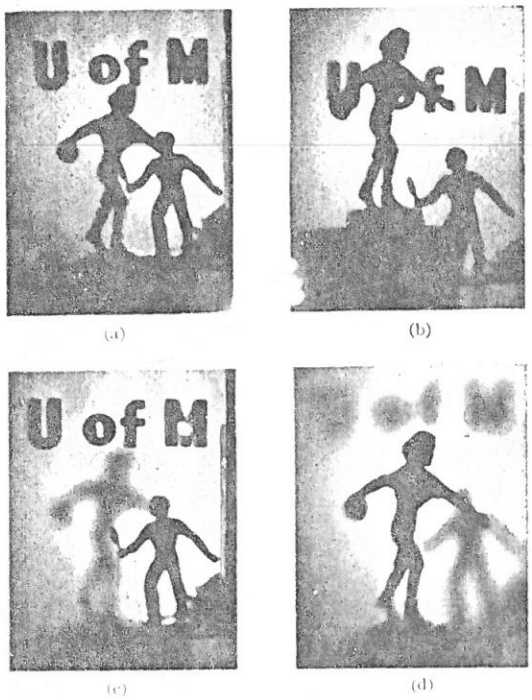

(a) (b) (c) (d)

FIG. 9. Reconstruction of a three-dimensional silhouetted scene, consisting of plastic letters about 1.5 in. high and two metal statues about 4 in. high. The virtual image was photographed using a camera with the lens stop at $f/8$ for (a) and (b); these two photographs were made with the camera at different positions in order to show the parallax between near and far objects. Photographs (c) and (d) were taken with the camera lens at $f/2.3$, which decreased the focal depth. The camera was focused on different planes in (c) and (d). Note that in (c), only the word *of* is in sharp focus, and in (d), only the head and one arm are in sharp focus.

length of this hologram is about 18 in. and its dimensions are 4×6 in. Thus, the hologram is about f 4, and was stopped to about f 48. Even with this setting, the foreground of the scene is unsharp. Further, it was necessary to tilt the recording film plane so as to orient its position with that of the train. It is apparent that the reconstructed scene, for the hologram at full aperture, extends through many hundreds of focal depths. The quality of the image is good despite the severe restriction of the hologram aperture.

Figure 9 shows the reconstruction of a silhouette, made by placing various objects in front of a sheet of opal glass, which was then illuminated from behind. The letters U of M are attached to the surface of the glass, and the two metal statues are located 3 and 20 in. from the glass. The reference beam was introduced by diverting a portion of the coherent illumination around the scene by means of a Lloyd's mirror arrangement.

To demonstrate the three-dimensional properties of the reconstruction, appropriate combinations of photographs are shown in Figs. 9(a) to 9(d). These were made by photographing the virtual image with a conventional camera, which was placed at different positions and set at various f-stops. Figures 9(a) and 9(b) show the virtual image from two different positions; the parallax is evident. The camera lens was set at $f/8$ in order to provide an adequate depth of focus to encompass the entire scene. Figures 9(c) and 9(d) show the same scene with the camera lens set at $f/2.3$. Here, the depth of focus is small, so that when the camera is focused on one part of the scene, other parts are quite unsharp.

6. MULTICOLOR WAVEFRONT RECONSTRUCTION

Using the superposition techniques described at the end of Sec. 3, it is possible to produce reconstructions in full color. We could, for example, illuminate a scene with coherent light in each of the three primary colors, and the hologram would receive reflected light of each color.[6] Three mirrors could be placed at different locations about the periphery of the scene. Each mirror would receive light of only one color; thus, three reference beams, one for each color, would impinge on the plate and produce the required interference effects with light of the same color reflected from the scene. The resulting hologram would comprise three incoherently superimposed holograms.

To reconstruct, we can place the hologram in the same position that it occupied during the exposure, and illuminate it with the three reference beams. Each beam would interact with each of the three hologram components, producing a total of nine virtual images (as well as nine real images). Three of these images would exactly coincide and produce, at the position originally occupied by the object, a reconstructed virtual image of the object in full color. The remaining images, which are, for example, the red-light reconstruction from the blue-light component of the hologram, etc., would form in other angularly displaced positions and would thus cause no problem. Hence, a three-dimensional image, in full color, can be obtained from a black and white hologram record. This process is related to the Lippman color process,[7] except that the process described here does not require that the emulsion be sufficiently thick as to constitute a three-dimensional storage medium.

ACKNOWLEDGMENTS

The authors wish to acknolwedge the assistance of many members of the staff of the Radar Laboratory of the Institute of Science and Technology, The University of Michigan. Special thanks is given to Dr. F. B. Llewellyn and other Institute officials for their assistance in providing support for this work, and to the former for his valuable technical suggestions.

[6] It has been pointed out, by an anonymous reviewer, that an object illuminated by monochromatic light in three primary colors may not produce the same color rendition as would the object if illuminated by ordinary white light. This could happen if the wavelength variation of object transmittance or reflectance were not a smooth, slowly varying function of wavelength.

[7] G. Lippman, J. Phys. 3, 97 (1894).

JOURNAL OF THE OPTICAL SOCIETY OF AMERICA VOLUME 55, NUMBER 8 AUGUST 1965

Microscopy by Wavefront Reconstruction*

EMMETT N. LEITH, JURIS UPATNIEKS, AND KENNETH A. HAINES
Institute of Science and Technology, The University of Michigan, Ann Arbor, Michigan 48107
(Received 3 March 1965)

Magnification by the wavefront-reconstruction imaging method is discussed. An analysis is given of the aberrations which arise in this type of imagery. Conditions are derived which lead to aberration-free reconstructions.

1. INTRODUCTION

IN the wavefront-reconstruction process of Gabor,[1] imagery is accomplished in a two-step process. The first step produces an intermediate record, called a hologram, from which the final image is later constructed.

The two steps of the process are carried out using monochromatic, spatially coherent light; radiation produced by lasers is excellently suited to this purpose. The hologram is essentially a photographic record of the waves which have emanated from the object. When illuminated with a beam of coherent light, the hologram modulates the light incident on it in such a manner as to produce replicas of the waves which were initially recorded on the hologram. These waves then form an image, thereby completing the process.

The major difficulty in producing high-quality imagery by the wavefront-reconstruction method is in achieving adequate preservation of the phase component of the light waves incident in the hologram. Incomplete recording of the phase causes in the reconstruction a pair of images that focus in different planes but which are inseparable in that one must be viewed with the other as a defocused background.

Many methods of eliminating the twin image have been proposed. A two-beam method used by the authors has produced holograms from which high-quality reconstructions are obtained.[2] In this method, part of the coherent light passes around the object and combines, at the hologram recording plane, with the light transmitted through the object. This method has the aim of modulating a spatial carrier frequency with the diffraction pattern of the object. Thus, the two beams impinge on the recording plate at some angle to each other, so as to produce a Young's fringe pattern. This pattern constitutes the spatial carrier, which becomes modulated by the diffraction pattern of the object: the amplitude portion of the diffraction pattern amplitude-modulates the fringes, and the phase portion phase-modulates the fringes. Thus, the entire diffraction pattern is recorded on a single hologram.

Gabor[3] and El-Sum[4] proposed the use of a two-beam process to produce "in phase" and "quadrature" pairs of holograms. Here, the bypassing beam is made parallel to the beam containing the object. After producing the first hologram, the phase of the nonobject-bearing beam is shifted by $\pi/2$, and a second hologram is made. The reconstruction is made in a two-beam device, with each beam containing a hologram. This method, like the carrier-frequency method, accomplishes the removal of the twin image, and has both advantages and disadvantages relative to the carrier-frequency method.

An advantage, described by Gabor,[5] of passing a portion of the beam around the object is that the level of radiation needed for illumination of the object is reduced. The secondary beam, when combined with the object beam, produces a heterodyning gain, which permits the object to be observed with a lower level of the radiation than would otherwise be the case. Such a method is valuable in cases where the object would be damaged by relatively high levels of illumination.

The wavefront-reconstruction method of imagery has, since its origin, been closely related to microscopy.[1,4,6,7] The present paper is concerned with the application of the two-beam carrier-frequency method of wavefront reconstruction to microscopy. Magnifications of $\times 60$ to $\times 120$ using this method have been demonstrated by the authors.[8]

2. THE MODIFIED GABOR MICROSCOPE

A two-beam wavefront-reconstruction microscope is shown in Fig. 1. Two microscope-objective lenses produce two divergent beams which overlap at the plane where the hologram is recorded. The specimen to be magnified is placed so as to be illuminated by only one of the two beams. The divergence of the beams results in a hologram in which the recorded diffraction pattern is magnified, similar to the manner in which a shadow-

* Presented in part at Dallas Meeting of Optical Society [J. Opt. Soc. Am. 55, 595A (1965), abstract WB 13].

[1] D. Gabor, Proc. Roy. Soc. (London) **A197**, 454 (1949); Proc. Phys. Soc. (London) **B64**, 449 (1951).

[2] E. Leith and J. Upatnieks, J. Opt. Soc. Am. **54**, 1295 (1964).

[3] Paper presented at Washington Conference on Electron Microscopy, National Bureau of Standards, November 1951.

[4] H. M. A. El-Sum, "Reconstructed Wavefront Microscopy," Ph.D. thesis, Stanford University (November 1952).

[5] D. Gabor, "Light and Information", in *Progress in Optics. Vol. 1*, E. Wolf, ed. (North Holland Publishing Co., Amsterdam, 1961).

[6] M. E. Haine and T. Mulvey, J. Opt. Soc. Am. **42**, 763 (1952).

[7] A. V. Baez, J. Opt. Soc. Am. **42**, 756 (1952).

[8] E. Leith and J. Upatnieks, J. Opt. Soc. Am. **55**, 569 (1965).

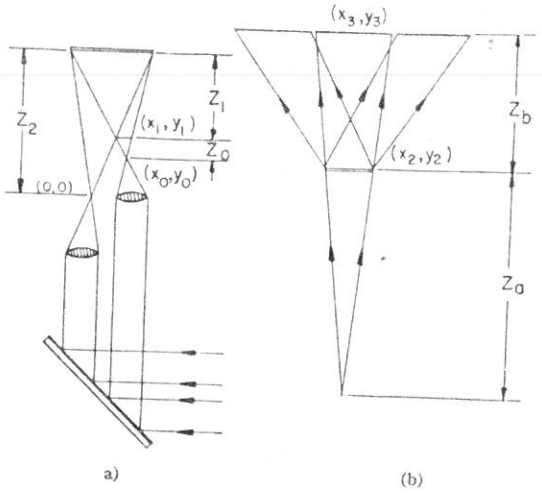

FIG. 1. Two-beam Gabor microscope.

gram image made in diverging light is enlarged in accordance with the rules of geometrical optics.

When illuminated with a beam of monochromatic, spatially coherent light, the hologram behaves like a diffraction grating, producing a pair of first-order spectra. One of these spectra gives rise to a real image and the other to a virtual image. This illuminating beam is also divergent. The divergence of the various beams results in the reconstructions being highly magnified. Magnification in wavefront-reconstruction imagery by the use of diverging beams has previously been demonstrated by El-Sum[4] and Baez.[7]

Let the object specimen (Fig. 1) have amplitude transmittance $s(x_1,y_1)$. The incident light is assumed to be linearly polarized, and the object is assumed to transmit this light without change in polarization; hence scalar theory applies. Or, stated more generally, $s(x_1,y_1)$ is that fraction of incident light which, upon emerging from the specimen, has the same polarization as the incident light. The other polarized component cannot produce interference with the reference beam, hence is essentially ignored by the hologram-producing process.

Let the radiation impinging on the specimen be $\exp(-ik_1r_0)$, where $k_1=2\pi/\lambda_1$, λ_1 is the wavelength of the incident radiation, r_0 is the distance from the point (x_0,y_0) of origin of the beam to the point (x_1,y_1) in the specimen, and the impinging wave is assumed to have unity amplitude. As is customary, the time-varying component of the signal has been suppressed.

The light emerging from the specimen is thus $s\exp(-ik_1r_0)$, and the light impinging on the hologram plate is, from the Fresnel–Kirchhoff diffraction formula,

$$U(x_2,y_2)=i/(\lambda_1z_1)\int\int s(x_1,y_1)\exp[-ik_1r_0(x_1,y_1) -ik_1r_1(x_2-x_1,y_2-y_1)]dx_1dy_1, \quad (1)$$

where r_1 is the distance from the point x_1,y_1 on object to the point x_2,y_2 on the recording plate.

The reference beam produces, at the hologram recording plane, a spherical wavefront

$$U_0=a_0e^{-k_1r_2(x_2,y_2)},$$

where a_0 is the amplitude of the wave and r_2 is the distance from the origin of the wavefront to the point x_2,y_2 on the recording plate.

The photographic plate, after exposure and suitable development, has an amplitude transmittance which is a function of $|U_0+U|$; for simplicity, assume that the film transmittance becomes

$$T=|U_0+U|^2=|U_0|^2+|U|^2+2\,\mathrm{Re}(U_0U^*). \quad (3)$$

When the hologram is illuminated by a divergent beam having the form $e^{-ik_1r_a}$ [where r_a is the distance from the point (x_2,y_2) on the hologram to the center of curvature of the incident wave], several diffracted waves are produced. The zero-order wave is produced by the terms $|U_0|^2$ and $|U|^2$, and is of no interest.

The term $2\,\mathrm{Re}U_0U^*=U_0U^*+U_0^*U$ represents the two first-order images; U_0^*U represents the virtual image and U_0U^* the real image. In expanded form, these are written as

$$\left\{\begin{matrix}U_0U^*\\U_0^*U\end{matrix}\right\}=i/(\lambda_1z_1)ae^{\mp ik_1r_2}\int\int se^{\pm ik_1(r_0+r_1)}dx_1dy_1, \quad (4)$$

where the upper set of signs and symbols refers to the real-image term and the lower to the virtual; the z's are defined in Fig. 1. The transmittance function s is assumed to be real, and thus s^* is equal to s.

In the reconstruction process, the hologram is assumed to be illuminated with a coherent monochromatic wave $e^{-ik_2r_a}$, where $k_2=2\pi/\lambda_2$, and λ_2 is the wavelength of the radiation used on the reconstruction. Let the reconstructed image be focused at a plane a distance Z_b from the hologram; Z_b is positive for a real image and negative for a virtual image. Similarly, if the hologram is illuminated with convergent illumination, Z_a (Fig. 1) is negative. The reconstructed image has, therefore, the form

$$U_r=C\int\int e^{\mp ik_1r_2}\left[\int\int se^{\pm ik_1(r_0+r_1)}dx_1dy_1\right] \times e^{-ik_2(r_a+r_b)}dx_2'y_2, \quad (5)$$

where all the constants have been absorbed onto C; the upper signs on the exponentials refer to the real image, the lower to the virtual; r_b is the distance from the point x_2,y_2 on the hologram to the point x_3,y_3 on the reconstructed image. This cumbersome but general equation is the basis for the analysis which follows.

Let Eq. (5) be written as

$$U_r = C\int\int\int\int s(x_1,y_1) f_1 f_2 dx_1 dy_1 dx_2 dy_2, \quad (6)$$

where

$$f_1 = \exp[\mp i(k_1 r_2 - k_1 r_0 - k_1 r_1 \pm k_2 r_a)], \quad (7a)$$

$$f_2 = e^{-ik_2 r_b}. \quad (7b)$$

If f_1 can be written in the form

$$f_1 = \exp[ik_2 r_b (x_2 - x_1 M,\ y_2 - y_1 M) + ih(x_1,y_1)], \quad (8)$$

then the reconstructed image is perfect and has magnification M. This can be verified by making the substitution $Mx_1 = x'$, $My_1 = y'$ in Eq. (6). Then

$$\int\int s(x'/M, y'/M) f_1 dx' dy'$$

represents the Fresnel diffraction pattern of an object $s(x'/M, y'/M)$ a distance r_b from the hologram. To find such solutions, we equate Eqs. (7a) and (8).

Obviously, the case $r_2 = r_a = \infty$, $\lambda_1 = \lambda_2$, yields

$$f_1 = \exp[ik_2 r_1 (x_2 - x_1,\ y_2 - y_1)] \exp[ih(x_1,y_1)], \quad (9)$$

which equals Eq. (8) with magnification $M = 1$ and $r_b = r_1$ for the real image and $r_b = -r_1$ for the virtual. This is the well-analyzed case of producing and reconstructing the hologram in collimated light.[9]

Two more general perfect-reconstruction solutions exist, as the appropriate algebraic manipulations show. One of these applies to the virtual image, and is obtained when $\lambda_1 = \lambda_2$, $r_a = r_2$, which result in $r_b = -r_1$, and $M = 1$. The other solution applies to the real image, and is obtained when $\lambda_1 = \lambda_2$, $r_a = -r_2$, giving $r_b = r_1$ and $M = 1$. The former solution states that the reconstructing source is placed at the same position, relative to the hologram, that the reference source occupied. The second solution calls for the reconstructing source to be in mirror-image position to the reference source.

We have also found four other solutions, which are perfect only for a single point of the reconstructed image: viz., $\lambda_1 = \frac{1}{2}\lambda_2$, $r_a = \pm r_1$, and $r_2 = \infty$, producing $r_b = \pm r_1$ and $M = 2$, $\lambda_1 = \lambda_2$, and $r_a = \pm r_1$, producing $r_b = \pm r_2$.

Two generalizations are evident. First, no magnification is possible without introducing aberrations, and second, aberrations occur unless the reconstruction is made using the same wavelength of radiation for both stages of the process.

If we allow the additional degree of freedom of scaling the hologram, for example, by copying with enlargement p, then the above conditions for exact reconstruction become $r_a = \mp r_2 p_1$ and $\lambda_2 = p\lambda_1$. This results in $M = p$ and $r_b = \pm r_1 p_1$.

Other schemes may alleviate the aberration problem. For example, the aberrations may be corrected by means of compensating lens elements in the reconstruction process.

3. FIRST-ORDER ANALYSIS

By using first-order analysis, some useful relations are readily derived which are analogous to those derived by Gabor[1] and El-Sum[4] for their respective configurations. Let the approximation

$$r_0 = [Z_0^2 + (x_1 - x_0)^2 + (y_1 - y_0)^2]^{\frac{1}{2}} = Z_0 + \tfrac{1}{2}(x_1 - x_0)^2/Z_0 + \tfrac{1}{2}(y_1 - y_0)^2/Z_0 \quad (10)$$

be made, with similar approximations for r_1, $r_2 r_a$ and r_b, and where the Z's are defined in Fig. 1. Substituting these relations into Eqs. (7) and (8), we obtain

$$f_2 = \exp\frac{-i}{2}[k_2(x_3 - x_2)^2/Z_b], \quad (11a)$$

$$f_1 = \exp\frac{i}{2}\left[\mp k_1 \frac{x_2^2}{Z_2} \pm k_1 \frac{(x_1 - x_0)^2}{Z_0} \pm k_1 \frac{(x_2 - x_1)^2}{Z_1} - k_2 \frac{x_2^2}{Z_a}\right], \quad (11b)$$

$$f_1 = \exp\frac{i}{2}\left[k_2 \frac{(x_2 - x_1 M)^2}{Z_b} + ih(x_1,y_1)\right]. \quad (12)$$

In these equations, the constant-phase terms $ik_1 Z_0$, etc., have been ignored, since they contribute only constant-phase delays. Also, the quadratic terms involving the y variables have been left out, since their presence does not contribute to the analysis, i.e., no generality is lost by considering points only along a radius $y = 0$.

We equate Eqs. (11b) and (12), analogously to what was done with Eqs. (7) and (8), producing

$$Z_b = \frac{\pm Z_1 Z_a Z_2}{Z_a Z_2 (\lambda_2/\lambda_1) \mp Z_1 Z_2 - Z_1 Z_a (\lambda_2/\lambda_1)} \quad (13)$$

as the location of the reconstructed image, and a magnification

$$M = Z_b = \left(1 \mp \frac{Z_1}{Z_a}\frac{\lambda_1}{\lambda_2} - \frac{Z_1}{Z_2}\right)^{-1}. \quad (14)$$

In these equations, the upper set of signs refers to the real image, and, the lower to the virtual. These relations are similar to those of El-Sum.[4]

Several interesting observations can be made from Eq. (14). First, if $Z_a = Z_2 = \infty$ (i.e., if reference beam

[9] As one of the r's becomes infinite, the phase delay associated with it likewise becomes infinite. However, we ignore a constant phase delay, and consider only relative phase delays of different parts of the incident wavefront.

and reconstructing beam are both collimated), no magnification is produced, regardless of λ_2/λ_1. Second, if $Z_a=\infty$, then $M=Z_2/(Z_2-Z_1)$, and magnification is independent of λ_2/λ_1, as well as of Z_0.

Since we are describing a two-step imaging process, it is appealing to think of each step as contributing a portion of the magnification, in which case we would have $M=M_1M_2$, where M_1 and M_2 are the magnifications attributable to the first and second steps, respectively. If we think of the reconstruction step as being a shadowgram process, then, for $Z_a\rightarrow\infty$, collimated light impinges on the hologram, and the magnification of the reconstruction step is unity. The overall magnification $M=Z_2/(Z_2-Z_1)$ must then be attributed to the first step. This is a satisfying conclusion for the reason that if the object were placed in the reference beam and a shadowgram image formed, the geometrical magnification would likewise be $Z_2/(Z_2-Z_1)$.

In the case of the single-beam hologram, in which the coherent reference beam passes through the subject, this expression for M_1 is realistic and meaningful. However, for the two-beam process, the division of the magnification into two parts, each associated with one of the two steps of the imaging process, is artificial, and other criteria for such division lead to different conclusions. For example, we can associate first-step magnification with the reduction in spatial-frequency content that occurs between object and hologram. Such a reduction bears no simple relation to the parameters Z_0, Z_1, and Z_2, but qualitatively, it can be stated that large values of $Z_2/(Z_2-Z_1)$ do significantly reduce the spatial-frequency content, and analysis shows that the most favorable case is $Z_2=Z_1$.

4. ABERRATIONS OF THE WAVEFRONT-RECONSTRUCTION PROCESS

The wavefront-reconstruction process, as observed previously, gives rise to aberrations in the reconstructed image whenever the conditions of reconstruction do not accurately duplicate or complement those of the hologram-producing process. These aberrations could be studied by including higher-order terms in the expansion of Eq. (10).

Rather than do this, we take advantage of an analysis available in the literature. Kamiya[10] has made an analysis of the third-order aberrations present in the Fresnel zone plate. Since the hologram of a point image is a Fresnel zone plate,[11] it is apparent that such an analysis is applicable to the wavefront-reconstruction process. We give here a discussion of the results. Some details are given in the Appendix.

Kamiya's analysis requires modification, since the zone plate used in his analysis has, in our notation, the form

$$U_k=b_0+b_1\cos b_2x^2, \tag{15}$$

where b_0, b_1, and b_2 are constants. The hologram to be analyzed is given by Eqs. (3) and (4). A point x_1,y_1 on the object produces the recorded zone-plate-like function

$$\begin{aligned}U_m&=c_0+c_1\cos k_1(r_1-r_2)\\&=c_0+c_1\cos k_1\{[Z_1^2+(x_2-x_1)^2+(y_2-y_1)^2]^{\frac{1}{2}}\\&\qquad-[Z_2^2+x_2^2+y_2^2]^{\frac{1}{2}}\}.\end{aligned} \tag{16}$$

We have modified Kamiya's analysis by using our Eq. (16) as the zone-plate expression, and have expanded this expression in a manner paralleling Kamiya's expressions.

The results of the analysis indicate the presence of the following third-order aberrations: curvature of field, spherical aberration, coma, and astigmatism. While our analysis does not show the presence of distortion, this aberration is also present, as shown in Meier's analysis.[12] The results, given in the Appendix, agree with the observations made in Sec. 2 that in certain special cases aberrations are absent.

One additional observation of significance is that, for large magnifications, the spherical-aberration term can be made quite small. This can be seen from Eq. (24) of the Appendix. If we impose the condition

$$Z_a\approx\pm(\lambda_1/\lambda_2)^{\frac{1}{2}}Z_1,$$

then the spherical aberration $\Delta\rho$ (defined in the Appendix) becomes

$$\Delta\rho=\tfrac{1}{2}r_b\sigma^3[Z_b^{-3}\mp(\lambda_2/\lambda_1)Z_2^{-3}]. \tag{17}$$

But for large magnification, Z_b is large, hence $Z_b^{-3}\rightarrow 0$. If Z_2 is large, then $\Delta\rho\rightarrow 0$. Another large-magnification arrangement that is free from spherical aberration is obtained from $Z_1\simeq Z_2$ and $Z_a=\infty$; this case is readily verified by inspection of Eq. (24), and noting that Z_b is large, thus making $1/Z_b^3$ small.

To the extent that it is meaningful to associate a portion of the magnification with each of the two steps of the process, then it can be said that the first of these minimal-aberration arrangements places most of the magnification in the reconstruction step, while the second places it in the hologram-making step. Certainly, other arrangements that minimize spherical aberration exist, but are not obtained readily by inspection.

The other aberrations, however, cannot all be eliminated by proper choice of parameters, except for the perfect reconstruction cases described in Sec. 2.

5. UNDISTORTED THREE-DIMENSIONAL IMAGERY

Here we analyze the conditions under which a three-dimensional image can be reconstructed without producing the distortion which generally occurs when a three-dimensional object undergoes magnification; namely,

[10] K. Kamiya, Sci. Light 12, 35 (1963).

[11] The hologram was first analyzed as a Fresnel zone plate by G. L. Rogers, Proc. Roy. Soc. (Edinburgh) A63, 193 (1952).

[12] R. Meier, J. Opt. Soc. Am. 55, 987 (1965).

that the longitudinal or axial magnification is equal to the square of the lateral magnification.[13] In addition, the lateral magnification of a three-dimensional object generally varies with the axial coordinate, except when the optical imagery system is of the affine or telescopic type.[14]

In general, the distortion that a three-dimensional object undergoes when highly magnified results in a complete loss of recognizability of the shape of the object. For example, a lateral magnification of 10^3 is accompanied by a longitudinal magnification of 10^6, and the object shape is distorted by a relative elongation of 10^3.

This problem can be solved in principle and within limitations, through the use of the wavefront-reconstruction method. The magnification M, which we now specify as the lateral magnification, and redefine as M_x, is

$$M_x=\frac{pZ_2Z_a(\lambda_2/\lambda_1)}{Z_2Z_a(\lambda_2/\lambda_1)-Z_1Z_a(\lambda_2/\lambda_1)\mp p^2Z_1Z_2}, \quad (18)$$

where p is the factor mentioned earlier, indicating a change in scale of the hologram, as would occur if the hologram were enlarged, for example, by photographic or electronic means. The longitudinal magnification is

$$M_Z=dZ_b/dZ_1=(\lambda_1/\lambda_2)M_x^2. \quad (19)$$

It is apparent that making the lateral magnification equal to the ratio of the wavelengths λ_2/λ_1 produces a reconstructed image in which $M_x=M_Z$.

Another condition which must be satisfied for undistorted magnification is that M_x should be independent of Z_1, i.e., all parts of the object should be magnified by the same amount. It is readily verified that the condition

$$Z_2/Z_a=\mp(\lambda_2/\lambda_1)p^{-2} \quad (20)$$

when applied to Eq. (18) produces

$$M_x=p, \quad (21)$$

which is independent of Z_1. This is precisely the condition which must be satisfied to eliminate aberrations, as indicated in Sec. 2.

Thus, to achieve uniform magnification in all three dimensions, it is necessary to scale the hologram in the same ratio as the wavelength change, and use magnification M_x equal to this wavelength change. The scaling could, of course, be carried out by imaging the hologram through a telescopic system in the process of making the reconstruction; it is not necessary to actually produce a new hologram transparency.

Satisfaction of the above condition produces a three-dimensional virtual image that is identical in appearance to the original object. The real image, however, poses special problems to the observer. Were the observer to view the image from the hologram side the appearance would be normal. Of necessity, however, he views it from the side away from the hologram, which causes the perspective of the reconstructed object to be wrong. All protrusions on the object become intrusions, objects in front of others now appear behind, etc. This gives the real image an unnatural and confusing appearance. The real image is thus described as pseudoscopic.[15]

6. USES OF THE GABOR MICROSCOPE

A workable arrangement of a Gabor microscope can be constructed essentially in accordance with the arrangement shown in Fig. 1. Pinholes could be placed at the positions where the lens brings the incident beam to a focus. Such pinholes act as dc spatial filters, removing from the system any light scattered by the lenses, or misdirected because of lens aberrations. Alternative ways to produce two coherent point sources include prisms, mirrors, beamsplitters, and diffraction gratings.

It would be most convenient to record the hologram on a medium which does not have to be removed and developed chemically. Self-developing films which might be used for the hologram can be divided into two classes: Those which return to the original, unexposed state when, or shortly after, the exposing illumination is removed, and those which do not. Implementations using either method can readily be conceived.

7. X-RAY AND FAR-ULTRAVIOLET HOLOGRAMS

It is not apparent that a Gabor wavefront-reconstruction microscope operating in the visible region can be competitive with conventional microscopes. It would appear, however, that the Gabor microscope would be valuable in spectral regions where microscopy is less perfectly developed than in the visible. The x-ray and far-ultraviolet are regions where wavefront-reconstruction methods have potential, and indeed, such methods have been demonstrated in these regions.[16] Technical difficulties have obstructed progress, but the problems do not appear insurmountable. In particular, should laser technology be extended into the far-ultraviolet and x-ray regions, wavefront reconstruction microscopy in these regions would become highly feasible.

At present, one of the standard methods of x-ray microscopy is to illuminate the specimen with a diverging beam of x rays derived from a small source. A shadowgraph image is then recorded at some appropriate distance from the specimen. Because of the divergence of the beam, this image is greatly magnified.

[13] This problem is touched upon briefly by Gabor, Ref. 1, p. 483.

[14] For a discussion of this type of optical system, see, for example, M. Born and E. Wolf, *Principles of Optics* (Pergamon Press, Inc., New York, 1959), pp. 144–159.

[15] The use of the term pseudoscopic to describe these properties was pointed out to the authors by F. W. Brock and R. Innes.

[16] H. M. A. El-Sum and A. V. Baez, Phys. Rev. **99**, 624 (1955).

It is however, an unfocused image, and its sharpness is degraded. The resolutions reportedly obtainable by this method are about 1000 Å, using radiation of 1 Å.[17]

In the two-beam wavefront-reconstruction microscope, this magnified image would be recorded as a hologram, with a similarly diverging x-ray beam being brought around the object, by means, for example, of an x-ray mirror. Since x rays are specularly reflected from a surface only at near-grazing incidence, the mirror would be operated as a Lloyd's mirror. The hologram would be reconstructed with visible light, and a sharply focused image would be obtainable.

As described in Sec. 3, both steps of the wavefront reconstruction process can, in general, be regarded as contributing to the magnification. In the x-ray or far-ultraviolet case, placing much of the magnification in the first step is desirable, since this reduces the spatial frequency of the recorded fringes. This reduction is advantageous for two reasons. First, at these short wavelengths, the resolution limit of the recording film is an important factor in setting the resolution limits of the over-all process. Second, even if the film records resolution finer than, say, 5000 Å, such resolution would be lost in the reconstruction process, since the reconstructing light cannot resolve such fine structure. Magnification in the first step overcomes both of these difficulties.[18]

8. SUMMARY

We have analyzed the magnification produced in the two-beam wavefront-reconstruction process when divergent beams are used, both for making and reconstructing the hologram, and when the reconstruction is made with radiation of a wavelength different from that which produced the hologram. In general, unless lenses are used, magnification can be achieved only at the expense of introducing aberrations in the reconstructed image.

The third-order aberrations have been analyzed and found to consist of spherical aberration, astigmatism, curvature of field, and coma. By using collimated radiation for either the reference beam or the reconstructing beam, large magnifications result without spherical aberration.

APPENDIX

In this appendix, we present the results of our zone-plate analysis, which is essentially Kamiya's[10] analysis adapted to our case. Our analysis, while paralleling Kamiya, is more lengthy and tedious because of the more complicated form of the zone plate.

In the following equations, x_3, y_3 are the coordinates of the Gaussian image point, and Δx_3, Δy_3 are the deviations of the aberrated rays from this image point.

Spherical Aberration

Spherical aberration is given by the expression

$$\Delta\rho=\tfrac{1}{2}r_b\sigma^3[Z_a^{-3}+Z_b^{-3}\mp(\lambda_2/p^4\lambda_1)(Z_1^{-3}-Z_2^{-3})], \quad (24)$$

where the upper sign refers to the real image, and the lower to the virtual; σ is the radius of a circular annulus in the hologram; the annulus is centered about $x_2=y_2=0$; $\Delta\rho$ is the radius of a circular annulus about the Gaussian image point. Thus, rays passing through a cylindrical ring of radius σ on the hologram, fall on a cylindrical ring of radius $\Delta\rho$ in the Gaussian image plane.

Coma

The coma is calculated for an object point $(x_1=0, y_1)$; obviously, no loss of generality occurs. The coma is then given by

$$\left[\frac{\Delta y_3}{r_b}-\sigma^2\left(\frac{y_a}{Z_a^3}+\frac{y_3}{Z_b^3}\mp\frac{\lambda_2}{p^3\lambda_1}\frac{y_1}{Z_1^3}\right)\right]^2+\left[\frac{\Delta x_3}{r_b}\right]^2=\left[\frac{\sigma^2}{2}\left(\frac{y_3}{Z_a^3}+\frac{y_a}{Z_b^3}\mp\frac{\lambda_2}{p^3\lambda_1}\frac{y_1}{Z_1^3}\right)\right]^2. \quad (25)$$

Astigmatism and Field Curvature

These are likewise calculated for an object point $(x_1=0, y_1)$, and are defined by the expression

$$\left(\Delta y_3\Big/\left\{\frac{3}{2}\sigma r_b\left[\frac{y_a^2}{Z_a^3}+\frac{y_3^2}{Z_b^3}\mp\frac{\lambda_2}{p^2\lambda_1}\frac{y_1^2}{Z_1^3}\right]\right\}\right)^2+\left(\Delta x_3\Big/\left\{\frac{1}{2}\sigma r_b\left[\frac{y_a^2}{Z_a^3}+\frac{y_3^2}{Z_b^3}\mp\frac{\lambda_2}{p^2\lambda_1}\frac{y_1^2}{Z_1^3}\right]\right\}\right)^2=1, \quad (26)$$

which is the equation of an ellipse.

Equations (25) and (26) are less general than those of Meier,[12] since we have taken the reference source to lie on the axis of the system.

ACKNOWLEDGMENT

Since the submission of this paper, we have become acquainted with Meier's work, from which we have corrected an error in ours, viz., a statement that distortion is not present in wavefront-reconstruction imagery.

[17] *Encyclopedia of Microscopy*, G. L. Clark, ed. (Reinhold Publishing Corp., New York, 1961).

[18] These problems were first called to our attention by C. R. Worthington of the University of Michigan, Physics Department, in private conversation in 1963. J. T. Winthrop and C. R. Worthington [Phys. Letters **15**, 124 (1965)] have proposed Fourier-transform holograms as a method of solving these problems.

WHITE-LIGHT RECONSTRUCTION OF HOLOGRAPHIC IMAGES USING THE LIPPMANN-BRAGG DIFFRACTION EFFECT*

G. W. STROKE and A. E. LABEYRIE
The University of Michigan, Ann Arbor Michigan

Received 27 January 1966

An extension of the 1962 Denisyuk method to record reflection holograms in Lippmann emulsions has permitted us to reconstruct monochromatic images with white light (e.g. sun) and demonstrate possibilities of simulating three-dimensional gratings for crystallographic studies.

Fig. 1a shows an arrangement which we have used for recording holograms of two- or three-dimensional objects in such a way that illumination of the hologram with ordinary sun-light (or other white light, e.g. from a flash light), as in fig. 1b will produce a 'single-color' image of the object by wavefront reconstruction. An example of a reconstruction of the image of a grasshopper which we have obtained with sun-light illumination of such a hologram is shown in fig. 2. The original object in this case was a 24×36 mm^2 Kodachrome transparency placed at about 1 inch from the photographic plate (along the z-direction), so as to produce a reflection version of a 'projection' hologram [1], by recording in 6328Å laser light. Reconstructions with three-dimensional objects, both diffusing and speculary reflecting have been equally successful.

The physical principles of holographic imaging with the method illustrated in fig. 1 may be readily given in simple terms. Basically the 'single-color' selection in the reconstruction with white light may be attributed to a multilayer interference effect, resulting from the stratifications of the emulsion caused in the recording fig. 1a by the interference between the reference field and the field scattered by the object, very much like in the original Lippmann color photography method [2], first described in 1894. The spacing of the stratifications (along the z-direction) in the recording is $\frac{1}{2}\lambda$ in case where both fields are plane waves incident normally on the plate. In the case of scattering by an arbitrary object (fig. 1a), the multilayer stratification maxima are locally displaced along z, according to the local values

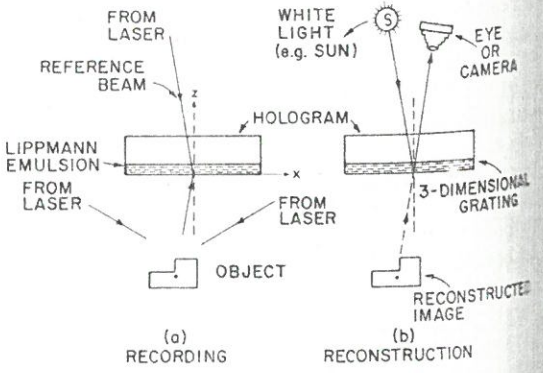

Fig. 1a. Recording (in laser light) of crystal (grating)-like hologram capable of b. reconstructing single-color images upon white-light illumination, using a Lippmann-Bragg diffraction effect.

of the phase of the resultant scattered electric-field vector (as measured with respect to the reference field). In addition, the resultant local intensity modulation of the processed photographic emulsion (in depth, say along z, for a given x-coordinate in the plane of the hologram) is determined by the resultant magnitude of the scattered field vector.

In the resconstruction (fig. 1b) white-light illumination of the hologram from the reference beam side produces, just like from a diffracting crystal, one spectrally selected single-color 'reconstructed wave', capable of forming an image by wavefront reconstruction, according to the principles first described by Gabor in 1948 [3]. In the 'reconstructed wave', (1) the local phase modulations are determined by the local displacements of the reflecting multiplayer stratifications, (2) the local amplitude modulation is determined by the local intensity modulation of the hologram, and (3) the color selection is obtained by Bragg diffraction from the grating-

* Parts of this work were first publicly presented by G. W. Stroke on 5 January 1966 in the board room at the National Science Foundation, Washington, D.C., by special invitation from Dr. John M. Ide, NSF Division Director for Engineering.

like stratifications. (The spacing of the stratifications may be suitably varied by omitting photographic fixing and other techniques [6, 7].

A basic theory of this type of reflection hologram recording was first given by Yu. N. Denisyuk in 1962 [4], for the case when the object was actually illuminated *through* the hologram, rather than with a separated beam (split before the incidence on the hologram, as in fig. 1a). An experiment with mirrors used as objects and recording with mercury light was also described by Denisyuk, but no photographic results were shown, presumably because of the well known difficulties of recording good holograms before the advent of lasers [3]. The readily obtained very good result which we show here was obtained with sun-light reconstruction from a hologram recorded in 6328Å laser light. (Equally good and readily observable images are obtained with very sufficient brightness with the light from a small pocket flash light.)(It may be of interest to note that an arrangement similar to that which we use for the recording of Lippmann-Bragg reflection holograms has been described in ref. 5. for the purpose of demonstrating the possibility of using "inverted reference beam" illumination in the recording of 'monochromatic transmission holograms', such as those in general use heretofore, and *not* for the purpose of recording the 'white-light reflection holograms' which we describe here. The inverted reference-beam illumination in the recording of transmission holograms has the important advantage, pointed out in ref. 5., of permitting one to place the reference mirror close to the laser source, rather than next to the distant object, when a sufficient coherence length [1] in the laser is available. Reflection images from conventional 'transmission' holograms upon illumination with monochromatic laser light have also been widely observed. In a general way all methods of holography are based on the original work by Gabor [3].)

The theoretical description of the white-light reflection holography process which we describe here may be readily given in the form of a 'modulated Lippmann-Bragg reflection-grating' formulation. Details will be given in a more extensive publication [6]. For the case of a scattered field describable by $A(x)\exp i\varphi(x)$ on the hologram surface(x-plane), say upon normal incidence along the z-direction, and with the reference field also incident along the z-direction, the intensity recorded in the hologram emulsion may be written as $I(x,z) \propto 1 + A(x)\cos\{2kz + \varphi(x)\}$, where $k = 2\pi/\lambda$ and λ is the recording wavelength. Illumination with a 'plane' white-light wave reconstructs the field $A(x)\exp i\varphi(x)$ in a single wavelength by a holographic Lippmann-Bragg diffraction process from the three-dimensional grating described by the equation.

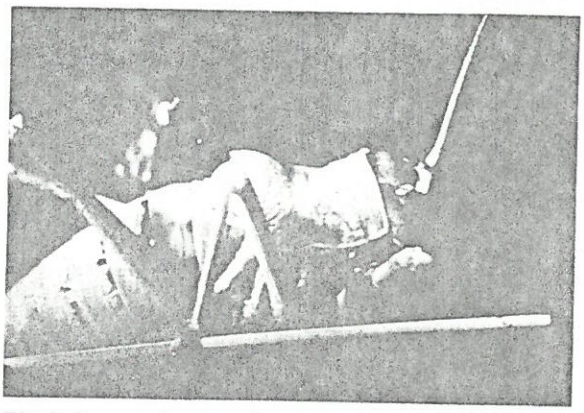

Fig. 2. Image of a grasshopper reconstructed with sunlight illumination of a hologram according to fig. 1b. (The original 'object' in this case was a 24×36 mm^2 Kodachrome transparency, placed at about 25mm in front of the hologram which was recorded in 6328Å laser light, see text.) Very bright, sharp images were obtained by reconstruction from the same hologram upon illumination with only the light from an ordinary pocket flash light.

(It may be of interest to note that particularly brilliant reconstructions are obtained in this manner by recording the hologram in an arrangement where the scattered field is brought to focus, say with a lens, at some distance behind the hologram, on the reference-beam side, after the illuminating beam has been scattered by the object, e.g. the transparency used in the recording of the hologram for fig. 2. Among many other experimental refinements which we have investigated, we have also found most useful the techniques of treating Lippmann emulsions described by Ives [7] in 1908, especially in controlling the spacing of the elementary stratifications.)

In our ref. 6. we shall also further discuss extensions of our method of 'reflection holography' to the generation of three-dimensional crystal-like gratings in photographic emulsions, which may be of a particular interest for the purpose of simulating crystallographic lattices for diffraction studies in the visible-light domain, and possibly for simplifying or aiding some aspects of X-ray image synthesis, e.g. in crystallography and protein structure investigations. Applications to interferometry, spectroscopy as well as to color holography, among others, have also appeared to be possible.

We wish to especially acknowledge most fruitful conversations with Gilbert B. Devey which were at the origin of generating our interest in investigating possibilities of 'white-light holography', such as that described here. We also wish to acknowledge the interest and fruitful conversations with several colleagues, notably

with R.C. Restrick. We are most grateful for a most generous grant from the National Science Foundation in support of major parts of our research.

References

1. G.W. Stroke, An introduction to coherent optics and holography (Academic Press Inc., New York and London, 1966), 270 pages (including reprints of the three original wavefront-reconstruction papers by D. Gabor).
2. G. Lippmann, J. de Physique 3 (1894) 97.
3. D. Gabor, Nature, 161 (1948) 777.
4. Yu.N. Denisyuk, Soviet Physics-Doklady, 7 (1962) 543.
5. A.S. Hoffman, J.G. Doidge and D.G. Mooney, J. Opt. Soc. Am. 55 (1965) 1559.
6. A.E. Labeyrie and G.W. Stroke, Optica Acta (to be published)
7. H.E. Ives, Astrophys. J. 27 (1908) 325.

* * * * *

OBSERVATION OF SOUND WAVES IN AFTERGLOW PLASMAS* BY MEANS OF TONKS-DATTNER RESONANCES

K. J. NYGAARD
Sperry Rand Research Center, Sudbury, Massachusetts

Received 22 January 1966

The electrical breakdown of a gas by a high voltage pulse will excite various sound waves. The propagation of an axial shock wave and a radial standing sound wave in afterglow plasmas has been studied by means of Tonks-Dattner resonances.

Recently, we have been using the electroacoustic Tonks-Dattner resonances to measure electron densities [1] and electron temperature transients [2] in noble-gas afterglow plasmas. During these investigations, we also observed perturbations on the Tonks-Dattner resonance curves due to sound waves in the neutral gas.

Other investigators [3] have reported on a standing sound wave, or a shock with Mach number very close to unity, following the breakdown of the gas in a discharge tube with a rectangular cross section. They detected the sound wave in the partially ionized gas by means of the changes that were produced in the transmission of a microwave signal and in the intensity of the recombination light. By means of the new Tonks-Dattner resonance technique, we have discovered a radial sound wave following the electrical breakdown of the gas enclosed in a cylindrical discharge tube. The breakdown pulse also produced a shock wave that traveled parallel to the tube axis.

A schematic drawing of the hot filament discharge tube is shown in fig. 2. For simplicity, we have excluded all electronic equipment. A microwave signal was applied to the strip line, which could slide along the tube. The dipolar electric field between the arms of the strip line will excite local electroacoustic resonances at certain electron densities. The excitation and detection of these resonances is well known from the literature [4]. The microwave signal that is reflected from the plasma carries with it information pertaining to the Tonks-Dattner resonances as seen in fig. 1. This is an enlarged picture showing only the first resonance. Of particular interest here is the modulation of the resonance curve. Higher order resonances exhibit a similar modulation. The amplitude of this modulation was found to increase with the electrical energy dissipated in the tube. Therefore, in the following measurements, we used maximum available breakdown energies, which were of the order of 0.1 joule. The period τ_0 of the modulation was found to be independent of neutral gas pressures from 1-10 Torr and independent of exciting frequencies between 500 and 1800 Mhz. We also found that the period did not depend on the position of the strip line along the tube. Furthermore, microwave heating of the electrons did not change τ_0. Finally, the modulation was very weakly damped, since it could be observed as late as 2.5 msec after breakdown.

*This work was supported in part by the Air Force Cambridge Research Laboratory, Office of Aerospace Research, under Contract No. AF19(628)-4183.

Wavefront Reconstruction Photography

New interest has arisen in the wavefront reconstruction process of Gabor. With the aid of the laser, photographic images have been produced in which the image is, to all appearances, a three-dimensional reconstruction of the original, complete with parallax and other visual effects.

By Emmett Leith and Juris Upatnieks

Wavefront reconstruction, or holography, is a fascinating photographic process which is a major departure from conventional photography. In this process, discovered in 1947 by D. Gabor of Imperial College, London, the photosensitive device does not directly record an image of the subject; instead, the electromagnetic waves reflected or scattered from the subject are recorded as a standing wave pattern. The resulting photographic record is called a hologram (from the Greek word holos, meaning whole), a name given by Professor Gabor to indicate that the whole, or entirety, of the wave pattern is recorded.

The photographic record thus produced is quite unintelligible, consisting of numerous whorls, swirls, and other irrelevant patterns. However, beneath this occluding veil is an image with many fascinating and remarkable properties. When the image is uncovered, it appears projected in space in full three-dimensional form, complete with all the visual properties of the original subject, including change of perspective with shift in the observer's viewing position, and parallax between near and more distant parts. The image, in short, is an accurate re-creation of the original subject.

Since its origin by Gabor, holography has been explored by many researchers throughout the world. Recently, there has been a resurgence of interest in this area, due in part to efforts by the present authors at the University of Michigan, as well as to others elsewhere, and in part to the development of the laser, which, through the highly coherent light it produces, enables the potential inherent in holography to be realized to a degree that heretofore has simply not been possible.

Theory of holography

The fundamentals of holography have been described in many ways. The most complete treatment is contained in the various papers of Gabor.[1] Rogers[2] has described the process in a physically attractive way on the basis that each point on the subject produces on the hologram a Fresnel-zone plate. Kirkpatrick and El-Sum[3] have given a pleasing heuristic description.

The authors are members of the staff of the University of Michigan's Institute of Science and Technology. Emmett Leith is head of the optics group in the Radar Laboratory at Michigan. Juris Upatnieks is a graduate research assistant.

We prefer to describe the process from a communication-theory-oriented viewpoint; Gabor briefly discussed the process from this viewpoint and Lohmann[4] carried its development further.

In Fig. 1, monochromatic, spatially coherent light illuminates the subject, which then reflects or scatters, a portion of this light. At some plane P, the light waves can be written in the general form

$$u = a\,(x,y)\,\cos\,[2\pi ft + \phi\,(x,y)].$$

This expression represents a carrier wave that is simultaneously amplitude- and phase-modulated. f is the frequency of the light. The quantities a and ϕ are related to the reflecting surface of the subject through the Kirchhoff diffraction integral. We have assumed that scalar theory applies here, and that polarization effects can be ignored. The data a and ϕ, although functions of spatial variables, are contained on a temporal carrier wave. In holography, the objective is to transform the data from the temporal to a spatial carrier. This is done by introducing a second beam of light, which bypasses the object but impinges also on the plane P. This beam we can write as

$$u_o = a_o\,(\cos\,2\pi ft + 2\pi f_c x_o).$$

The second term of the argument indicates a linear phase shift across the plane, and the wave thus impinges on the plane at some oblique angle.

At plane P, we place a photosensitive device, for example, a photographic plate; such a device responds to the time-averaged value of the intensity of the incident light, thus acting as a square-law device. As a result, the function

$$<(u_o + u)^2> = a^2{}_o/2 + a^2/2 + a_o a\,\cos\,(2\pi f_c x -$$

is recorded on the plate, where the $<\ >$ indicate

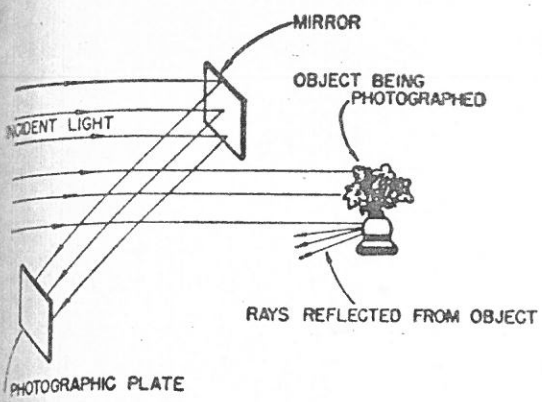

Fig. 1. Optical system for making a hologram

a time average. The auxiliary beam has functioned as a local oscillator signal, and the photographic plate, in addition to its role as a storage device, has functioned as a mixer, producing the difference frequency term $a_o a \cos(2\pi f_c x - \phi)$. The signal carried by the light beam has been modulated onto a spatial carrier wave $\cos 2\pi f_c x$, in such a way that the information is preserved in its entirety without degradation.

The reconstruction

The reconstruction process is essentially the inverse of the hologram producing process: the interaction of a coherent light beam with the hologram record causes the modulation present on the spatial carrier of the hologram to be transferred to the light beam, in the following manner. Let $u_1 = a_1 \cos(2\pi f' t + 2\pi f_c x)$ represent the light impinging on the hologram; the light impinges obliquely, just as did the reference beam used in making the hologram. Note that the frequency f' of the light used in the reconstruction is not necessarily that of the light used in making the hologram. The light emerging from the surface of the hologram is thus

$$[a_1 \cos(2\pi f' t + 2\pi f_c x)]\left[\frac{a_o^2}{2} + \frac{a^2}{2} + a_o a \cos(2\pi f_c x - \phi)\right]$$

$$= \frac{a_1}{2}(a_o^2 + a^2)\cos(2\pi f' t + 2\pi f_c x)$$

$$+ \frac{a_1 a_o a}{2}\cos(2\pi f' t + 4\pi f_c x - \phi) + \frac{a_1 a_o a}{2}\cos(2\pi f' t + \phi).$$

The emerging light is seen to consist of three terms; the first of these is of no interest, since it carries no phase modulation. The other two are the usual sum and difference frequencies produced by a mixing process. The difference frequency is identical in form to the original signal-bearing wave recorded on the hologram. This term represents a reconstruction of the original waves, and, when presented to an observer, appears to emanate from a virtual image located on the source side of the plate. This image has all the visual properties of the original object; if the original object were three-dimensional, then the reconstructed image is likewise; this three-dimensional effect is produced without the need for stereo pairs of holograms and without the need for any viewing devices such as polaroid glasses. In addition, as the viewer moves his head, his perspective of the picture changes. Parallax between near and far objects is observed.

The sum term represents a real image, which forms on the side of the plate away from the source. The observer can view this image also; he finds it suspended in space between himself and the plate. The real image, however, has the property of being pseudoscopic; this is an effect that occurs in stereo viewers when the stereo pair of pictures is interchanged. Anomalous effects occur; hills become valleys, protrusions become indentations, etc. These effects give the real image an unnatural and confusing appearance.

One of the major problems in holography has been the separation of the three terms given above. Pursuing our carrier-wave viewpoint, it is apparent that a spatial filtering technique can achieve this separation, providing the spatial carrier term f_c is sufficiently great that the spatial-frequency spectra of the three terms do not overlap. This separation could be effected on the basis of ideas developed by Duffieux,[5] who pointed out that, in an imaging process carried out with coherent illumination, the Fourier spectrum of the object is displayed at the back focal plane of the imaging lens. Stops and slits placed here act like stop-band and pass-band filters. When the hologram is thus imaged through an optical system, a slit can select either the real- or the virtual-image term while rejecting the others.

The three terms can be separated on a more simple basis, which is readily explained by thinking of the hologram as a diffraction grating. The three waves emerging from the hologram can be identified with the zero order and the two first orders of the grating. The waves associated with these orders propagate in different directions and at some distance from the hologram are separated, as shown in Fig. 2. The two first-order diffractions correspond to the real and virtual image terms.

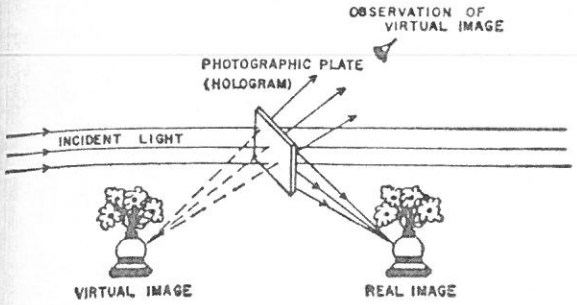

Fig. 2. The reconstruction process

Holograms have become familiar to many as patterns of lines, specks, blobs, and whorls; this is an association which, if not wrong, is misleading. Such manifestations arise from dust particles on the reference-beam mirror and other such anomalies; they can be eliminated with good experimental technique, as the pictured hologram, Fig. 3 (a), shows. The recorded signal appears as an isotropic random granular pattern, like that shown in the magnified view, Fig. 3 (b).

In Fig. 4 we have attempted to show the three-dimensional properties by means of several reconstructions of the real image, taken at different positions of the recording plate, and at different *f*-numbers (the *f*-number of the recording system can be varied by stopping the hologram itself—i.e., by restricting its aperture, just as one stops a lens). In Fig. 4 (*a*) and (*b*) the hologram was stopped considerably by illuminating only a small area (a circular area approximately 3 mm in diameter). The parallax differences between (*a*) and (*b*) were produced by using different portions of the hologram for the two pictures. A similar effect would be produced by moving one's head while viewing the reconstruction. In (*a*) we are looking up at the tank; in (*b*) we are looking from above the tank. The parallax differences are most prominent in the way the gun barrel is seen against the rest of the tank. Pictures (*c*) and (*d*)

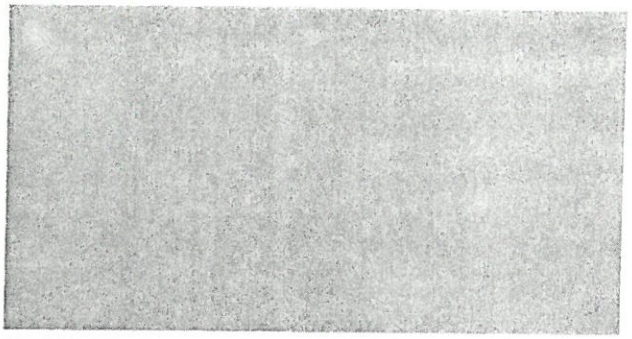

(a)

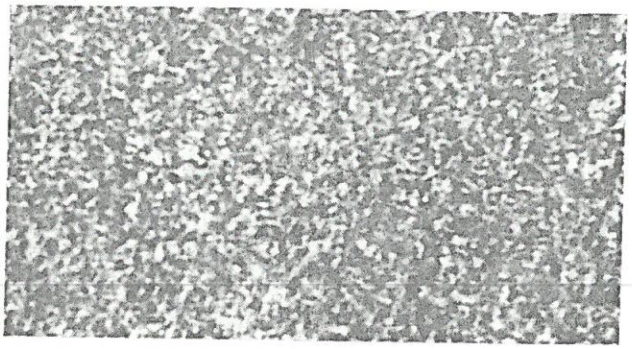

(b)

Fig. 3. Example of a hologram; b shows a highly magnified portion of a hologram.

were produced by broadening the illumin beam to about 40 mm; the depth of focus is s compared to the depth of the tank, and on small piece is in focus at a time.

In the past year, many persons have attem to produce holograms; some have been succe others have encountered difficulty. Good re are readily attained if proper equipment is u otherwise failure is likely. Since the method type of interferometry, stability of the var components is essential. The work is best f formed on a granite block using subjects equipment that will not vibrate during the posure. A helium-neon cw gas laser of 1-m output power is suitable, but a 40-mW laser vastly better, since the exposure times are red from several minutes to several seconds.

The development of holography

Gabor originally conceived of the wavefront construction process as a means for improving imagery of the electron microscope. The prob was to overcome the spherical aberration inher in the electron lenses; the solution was to pro a hologram as the output image from the elec microscope and to make the reconstruction u visible light. The spherical aberration would pear in the reconstructed waves and could be moved by using the well-developed methods visible-light optics. The potential gains are gr since the electron microscope falls far short approaching the theoretical resolution limits. though Haine and others[6,7] continued the velopment, technical difficulties have prevented practical realization of this goal.

El-Sum and Baez[8,9] in the early 1950's inve gated the adaptation of the wavefront reconstr tion technique to x-ray microscopy. The ho gram would be made with x radiation, and t reconstruction would be made with visible li Since x rays cannot be focused except cru and with great difficulty, the resolutions achie with x rays fall short of the theoretical limits several orders of magnitude; the wavefront rec struction technique, however, has the possibil of overcoming this limitation. The reconstruc waves, produced with visible light, could be sh ly focused and an image of high quality co thus be produced.

Baez and El-Sum[10] demonstrated the meth but technical difficulties prevented the realiza of the full potential of wavefront reconstruct methods. The difficulty lay primarily in findi an x-ray source with sufficient spatial coheren and yet with reasonable intensity.

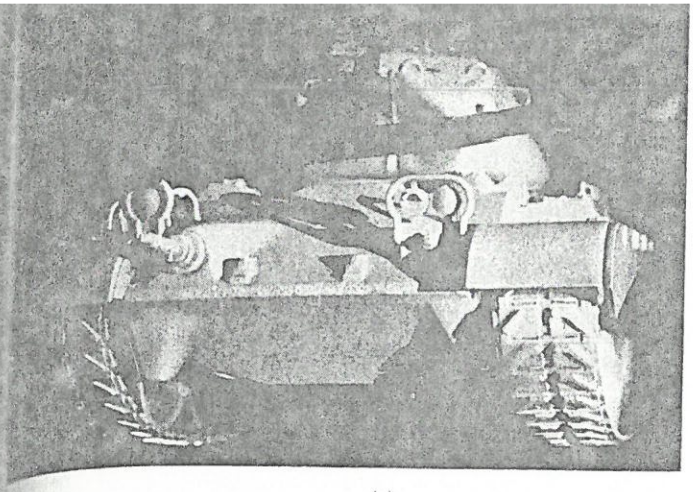

(a)

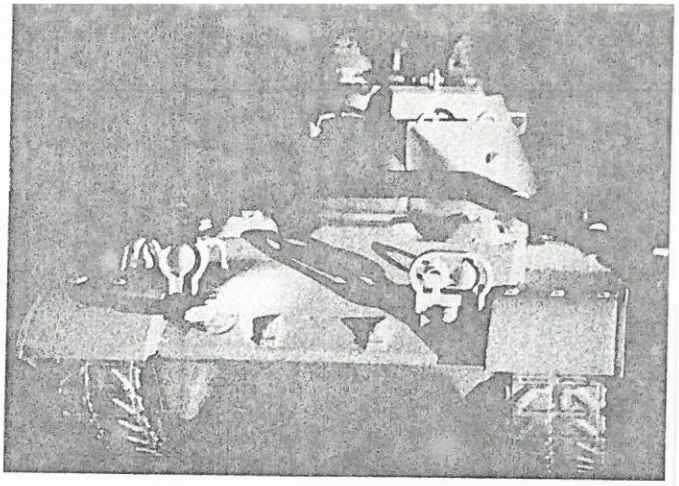

(b)

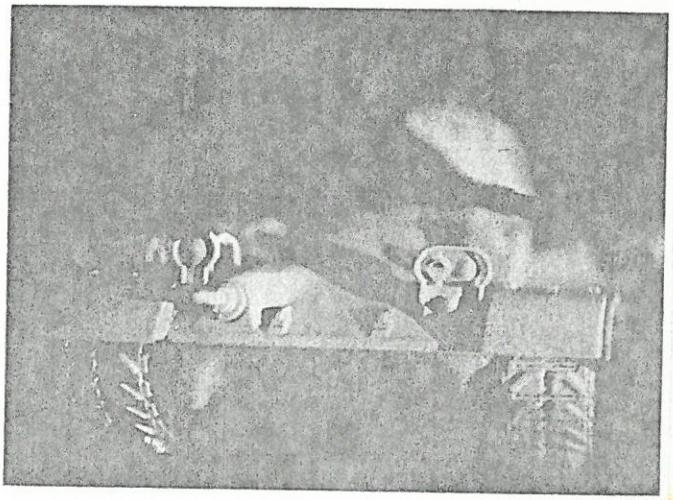

(c)

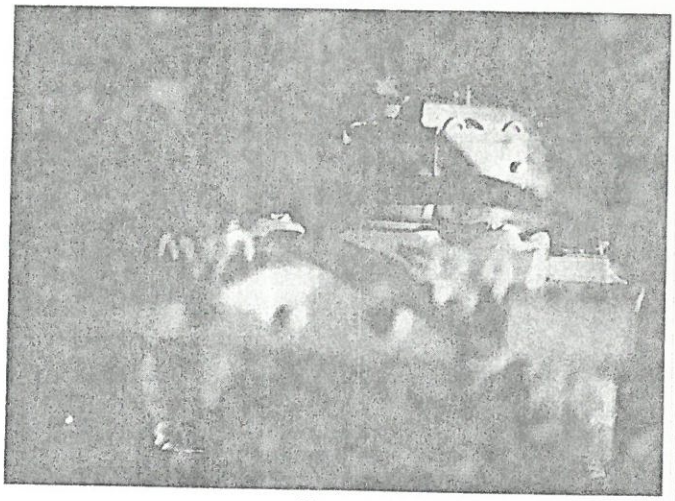

(d)

Fig. 4. Three-dimensional reconstruction of a toy tank; a and b show two views with different parallax. An aperture of 3 mm exists at the hologram. In c and d, the aperture is opened to 40 mm. Note the decrease in depth of field. In each case, only a small portion of the object is in focus. Pictures are further discussed in text.

Holograms made with visible light were produced by Gabor and by many others since. The resolutions achieved have been comparable to those attained by means of more conventional optical systems. However, the overall quality has been deficient, largely because of the inability to separate the three terms previously noted. This has meant generally that whichever image was used, real or virtual, the other image was present as a defocused background. In addition, the remaining term, which has noise-like properties, was also present. Consequently, most examples of wavefront reconstruction have been carried out with high-contrast, relatively simple objects.

It may be wondered why this separation has been a problem, since the separation, as we have seen, automatically occurs in the reconstruction process as we have described it. The difficulty has been that the traditional hologram-producing methods have used a spatial carrier frequency, θ, equal to zero. Under this condition, it is seen that the three terms noted earlier do not separate.

The separation of the real and virtual image has been one of the traditional problems of holography, and many methods have been proposed for doing this. The most simple of these methods involves placing masks of some sort in the light path between source and reconstructed image. These methods gave moderate improvements, but are not among the more effective solutions.

The presence of the twin images results from the incomplete recording of the phase of the incident light. Accordingly, one might consider the production of two holograms which are complementary in the sense that the deficiencies of one are compensated by the other. The reconstruction would be made by using both holograms together. Bragg and Rogers,[11] Gabor,[12] and El-Sum[9] have proposed this kind of technique. Such techniques are sound, but they present technical problems, one of which is that, in the reconstruction process, extremely precise alignment of the two holograms is required. These methods have some advantages over the spatial-carrier method employed by the authors[13]; for example, they require less spatial coherence and monochromaticity in the light source.

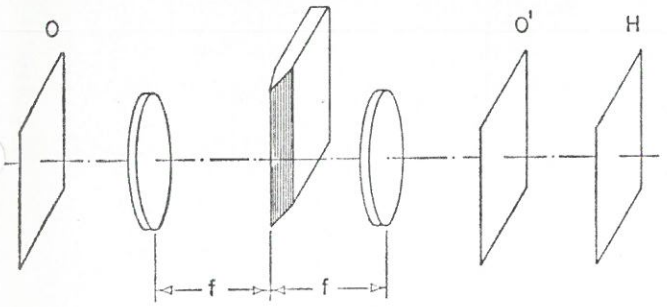

Fig. 5. Lohmann's single-sideband method for removal of the twin image; object is placed at O, image appears at O′, and the hologram is made at H. A half-plane stop is placed midway between the two lenses, each of focal length f and separated by the distance 2f.

Lohmann[4] in 1956 proposed for removal of the twin image, a method which is similar to the spatial-carrier or off-axis–reference-beam method. Lohmann's method is illustrated in Fig. 5. The hologram is made through a lens system containing a stop in the focal plane of the first lens. The object, in this case a transparency, is imaged at plane O′, after removal of half of its spatial frequencies as a consequence of the half-plane spatial filter. The hologram is made at the plane labeled *H*.

In the reconstruction process, the hologram may be placed in its original position and the light sent through the optical system in the opposite direction. The spectrum is displayed, as before, at the focal plane of the lens. The virtual image term appears on one side of the optic axis; the real term on the other; the spectra are thus separated. A half-plane stop removes either the real- or the virtual-image term, and in the reconstruction (which occurs to the left of the lens system) the interfering twin image is absent.

The holograms being produced nowadays have a quality that is considerably higher than had heretofore been published. There are two reasons for this. First is the use of the carrier-frequency or off-axis reference-beam method, which effects the removal of the desired image from its twin image and from other, noise-like terms. Second is the use of the laser, which provides a highly coherent source far more intense than previously used sources. While conventional sources, such as the mercury arc, have yielded good results with photographic transparencies for the subject, the holograms made from diffusely reflecting, three-dimensional objects, which produce the most dramatic results, almost have to be made with a laser source. The chief reason for this is that the source must have a coherence length equal to the depth of the scene. Coherence length is proportional to the monochromaticity of the source, and, if a conventional source is made monochromatic to the required degree for an object several inches in depth, the intensity becomes quite low and the required exposure time becomes quite long. If laser technology were extended into the far ultraviolet or x-ray regions, holography at these short wavelengths would presumably become an important method of x-ray and uv microscopy.

The technique of bringing the reference beam onto the recording plate from an off-axis position is an adaptation of well-known techniques used in electronic engineering, and it was because of our experience in microwave work that the idea occurred to us.

For example, in certain radars of the pulse-compression type, a linearly frequency-modulated waveform is radiated, and the received signal is passed through a network which compresses the pulse, thus providing resolution equal to that which would have been produced had a single pulse with the same bandwidth been radiated. Such a radar system is a close analog of the wavefront reconstruction process. In each case, the signal produced by a point target is a structure resembling a Fresnel-zone plate, and in both cases the final processing consists of converting each zone-plate response into a point spot. In holography, this is done through the focal properties of the zone plates recorded on the hologram; in pulse-compression radars this is done usually by means of electrical networks that carry out an equivalent operation.

Before the radar signal is compressed, it is converted from its rf carrier onto a suitable if carrier. The carrier, however, is selected to be at least equal to the bandwidth of the pulse, so that the sidebands of the pulse spectrum are not folded into each other. The recording of the hologram is analogous to conversion of the radar pulse to if, and clearly, on the basis of the comparison drawn here, the hologram should be on a spatial carrier; the off-axis reference beam accomplishes exactly this. The off-axis reference beam, then, is not the adaptation of a technique from one discipline to another.

Current status of holography

Currently, there appears to be a high level of interest in holography; throughout the country experimenters are producing holograms, and suppliers of the Lippman-type emulsions which are so suitable to this application are reportedly doing a brisk business. At the recent Optical Society meeting in Dallas, a total of eight papers on holography were presented. Areas of application for holography are being extensively explored, including the original ones proposed by Gabor, El-Sum, and others who pioneered in this area.

One of the most promising applications is reported by Thompson and Parrent. These investigators use the technique for examination of small fog-like particles enclosed in a confined volume. A hologram is made of the entire volume, using a pulse laser; this, in effect, freezes the motions of the particles and enables one, in the reconstruction process, to examine at length the particle configuration as it existed at the instant the hologram was made. Thompson and Parrent have thus (as have the authors) made use of the excellent coherence properties of the laser, and of the three-dimensional imagery inherent in holography. Their effort, it should be noted, has paralleled and in no way stems from, the work of the present authors. Thompson and Parrent do not employ an off-axis reference beam, but the subjects they work with do not require such a technique.

Two of the authors' colleagues, Powell and and Stetson,[14] have explored the use of off-axis reference-beam holography for examination of vibratory motions. The method is based on the loss of coherence and its consequent effect on the reconstructed image, of light reflected from a vibrating object. Horman,[15] in a recent paper, has proposed several applications of wavefront reconstruction to interferometry.

The possibility of carrying out holographic techniques with incoherent light was proposed by Mertz.[16] As yet, high-quality imagery by this method has not been attained, although new attention is being directed to this end by Cochran.[17] The need for coherent light is a severe constraint, the elimination of which would be highly desirable.

The successes achieved in the visible region of the spectrum have generated new interest in the old problems of making holograms with x rays and with electrons in an electron microscope. El-Sum has previously demonstrated such holograms, but the technique has not been developed thus far to a practical stage. We hope for new advances in these areas, but the problems remain formidable.

The production of holograms in a three-dimensional storage medium was discussed in a paper by P. Van Heerden.[18] Here, the recorded fringes become surfaces within the medium, and the read-out, or reconstruction, is carried out on the basis of Bragg-angle diffraction, in a manner analogous to diffraction from crystals. The reconstructed image is produced only when the orientation of the hologram relative to the illuminating beam is proper.

A photographic emulsion is generally regarded as a two-dimensional medium, but, when the recorded detail becomes greater than the emulsion thickness, the emulsion must be regarded as a three-dimensional medium. The spectrographic plate on which we have made our holograms has an emulsion thickness of about 6×10^{-3} [illegible] thus, when the recorded fringe pattern exceeds about 200 lm/mm, the emulsion behaves as a three-dimensional medium. Our holograms have been made at spatial frequencies ranging from a few lm/mm up to about 2000 lm/mm, and at the higher range the Bragg diffraction characteristics become prominent. Hence, our holograms certainly demonstrate the ideas of Van Heerden, although this was not our intent.

We were not motivated in our work by practical applications; however, we are quite interested in seeing such applications develop; indeed it seems to us that the dramatic imagery produced by this method must inevitably lead to worthwhile uses in addition to those already proposed or demonstrated.

References

1. D. Gabor, Nature 161, 777 (1948); Proc. Roy. Soc. (London) A 197, 454 (1949); Proc. Phys. Soc. (London) B 64, 449 (1951).
2. G. L. Rogers, Proc. Roy. Soc. (Edinburgh) A 63, 193 and 313 (1952); A 64, 209 (1956).
3. P. Kirkpatrick and H. M. A. El-Sum, J. Opt. Soc. Am. 46, 825 (1956).
4. A. Lohmann, Opt. Acta (Paris) 3, 19 (1956).
5. P. M. Duffieux, *l'Intégrale de Fourier et ses Application à l'Optique*, chez l'Auteur, (Université de Besançon, Franch, 1946).
6. M. E. Haine and J. Dyson, Nature 166, 315 (1950).
7. M. E. Haine and T. Mulvey, J. Opt. Soc. Am. 42 (1952).
8. A. V. Baez, J. Opt. Soc. Am. 42, 756 (1952).
9. H. M. A. El-Sum, "Reconstructed Wavefront Microscopy", PhD Thesis, Stanford University, November (Available from University Microfilm, Inc., Ann Arbor, Michigan).
10. H. M. A. El-Sum and A. V. Baez, Phys. Rev. 99 (1955).
11. W. L. Bragg and G. L. Rogers, Nature 167, 190 (1951).
12. Papers presented at Washington conference on electron microscopy, National Bureau of Standards, Nov. 1951.
13. E. Leith and J. Upatnieks, J. Opt. Soc. Am. 53, (1963); 54, 1295 (1964).
14. R. Powell and K. Stetson, J. Opt. Soc. Am. 5, 612 (1965).
15. M. H. Horman, J. Appl. Opt. 4, 333 (1965).
16. L. Mertz and N. O. Young, Proceedings of the International Commission on Optics Conference on Optical Instruments (London 1961) p. 305.
17. G. Cochran, J. Opt. Soc. Am. 5, 615 (1965).
18. P. Van Heerden, J. Appl. Opt. 2, 393 (1963).

Progress in holography

As this method of imaging becomes better understood, it can offer the best solution for problems in fields as diverse as architecture, medicine and mechanical engineering.

Emmett N. Leith and Juris Upatnieks

With the award of the 1971 Nobel prize in physics to Dennis Gabor, holography has reached a new pinnacle of prestige. Gabor won his prize for the invention of holography, a form of wavefront reconstruction in which a coherent reference wave appears to unlock a three-dimensional replica of an object from a two-dimensional standing-wave pattern.

The science of holography has taken some curious turns in its relatively short 25-year history. The time divides itself naturally into three periods: The first could be considered a precursor stage, when the aim was to record wavefronts diffracted from crystals that had been irradiated with x radiation or electron waves. If reconstruction with visible light were successful, a highly magnified image of the crystal lattice would result. Recording the phase of the radiation was, however, a difficult problem that was soluble only for rather special cases. (For a description of this early work, carried out principally by Sir Lawrence Bragg and Hans Boersch, see reference 1.)

In 1948, Gabor developed a way to introduce a coherent background or reference wave, and the second period began.

Emmett Leith and Juris Upatnieks are both at the University of Michigan, Ann Arbor; Leith is Professor in the Electrical Engineering Department, and Upatnieks is a Research Engineer at the Institute of Science and Technology.

The third stage began in the early 1960's, when high-quality holographic imagery was demonstrated; the beginnings of this stage coincided in time with the development of the first lasers. Our attention here shall center on the latter two stages, particularly on the more recent work, for the history of holography gives us indications of what it can be reasonably expected to do in the future.

Early holography

Gabor's method, simple and elegant, solved in quite a general way the basic problem of recording the phase, as well as the amplitude, of a wave. In three principal papers between 1948 and 1951,[2] he developed the theory in considerable depth and offered convincing experimental results. Gabor's original purpose, to record electron waves and regenerate them at optical wavelengths, thereby compensating with optical techniques for the uncorrectable aberrations of electron lenses, is an historical point that today receives at best a passing notice. However, the holographic process has been revealed to have far more potential than one could, at that time, have imagined.

The excitement that must have attended the first accomplishment of the method is known, perhaps, only to Gabor and his associates. Our own excitement in 1960, when we duplicated for our own curiosity the experiments he described, was considerable, even though the expected results were known beforehand. With an eyepiece, we followed the optical paths of the reconstructed wavefronts downstream to their focal position and observed a sharp, well defined image that had the startling property of having no apparent antecedent; nowhere in the optical system was there an object with which to associate the image (see figure 1). The mathematics, simple and easily understood, fully predicted the results; yet, the physical realization seemed altogether mysterious. The first time must have produced a powerful impact indeed!

Interest in holography continued strong for several years afterward, and produced some notable pioneers. Gordon Rogers explored the new technique in many ways, uncovering new ramifications and new insights; one of his best known contributions[3] is his extensive development of holographic image-forming principles in terms of Fresnel zone-plate theory, by which one can grasp in a highly intuitive way the first-order imaging properties of holograms. M. E. Haine, James Dyson and T. Mulvey applied[4] holography to electron microscopy. In the US, Ralph Kirkpatrick and his two students, Albert Baez and Hussein El-Sum, became interested in holography, particularly in its application to x-ray imagery; El-Sum produced the first doctoral thesis in holography.[5] In Germany, Adolf Lohmann first applied communi-

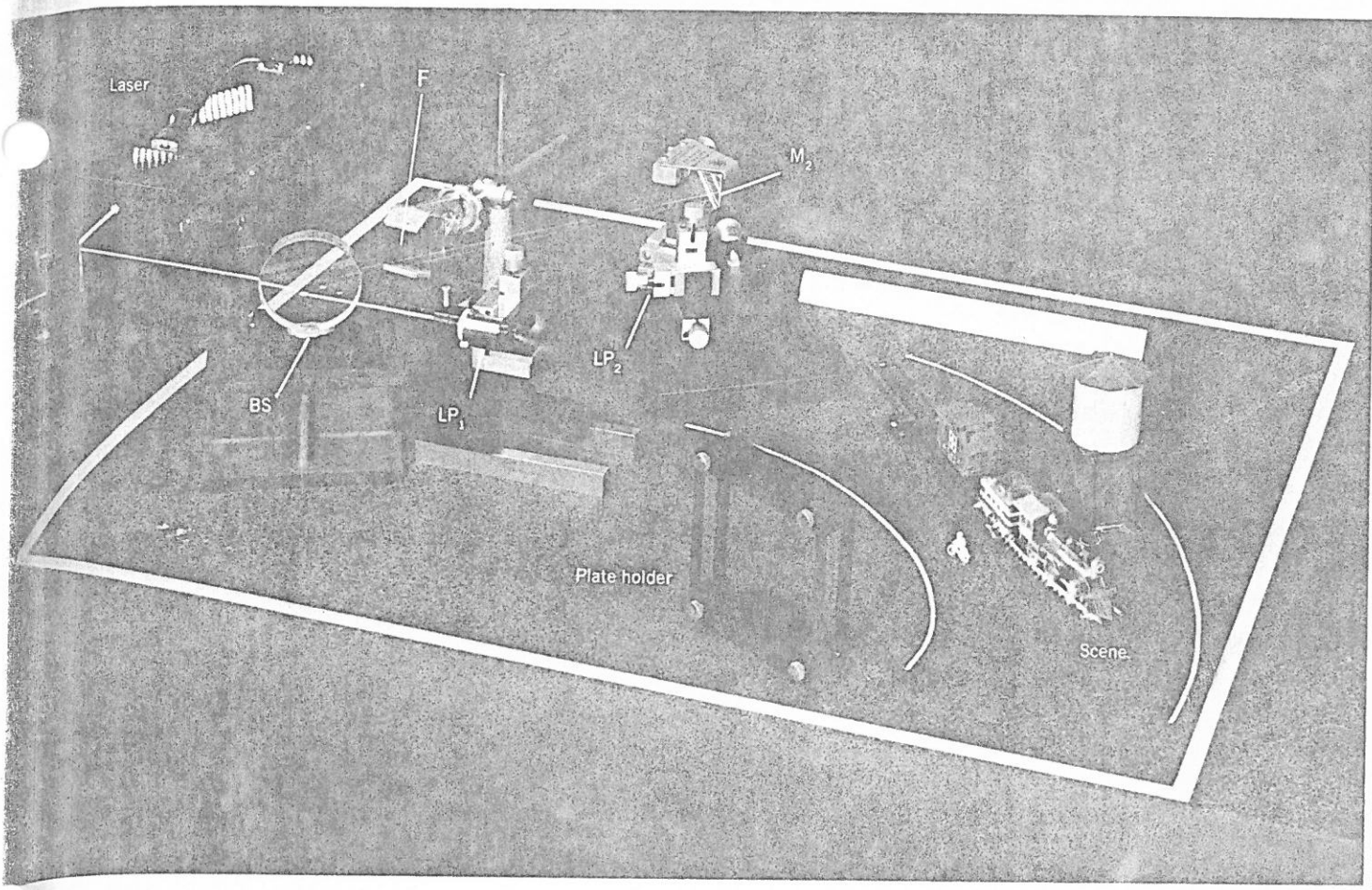

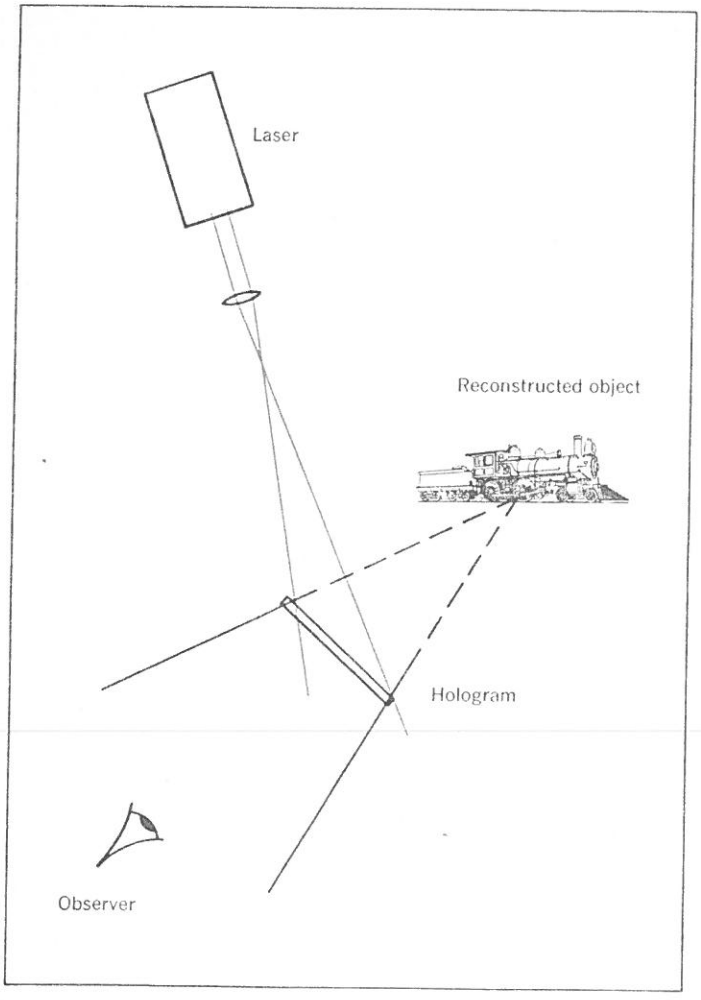

Typical arrangement for holography of a three-dimensional, opaque object (photo, top). The light emerging from the laser is deflected by mirror M_1 to beam splitter BS. The transmitted beam is diverged by lens LP_1, so that it illuminates the scene at right. The reflected beam, after passing through the variable attenuator F, is reflected by mirror M_2 to lens LP_2. The now diverging reflected beam illuminates the plate (held in the plate holder) as the reference beam. When the fringes produced by interference between object and reference beams are recorded on the plate, the result is a hologram. Under illumination by the reference beam alone (diagram, bottom) the developed plate, or hologram, regenerates the object wave, and an observer who looks through the hologram sees what appears to be the original object.
Figure 1

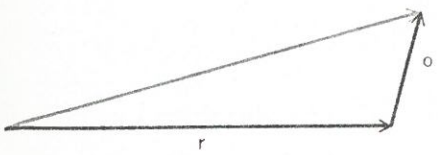

Principle of the coherent background. When the object wave o is attended by a strong coherent background (or reference) wave r, the resultant wave (color) has a phase that varies only slightly from that of the background wave, and the loss of phase of the total field is relatively unimportant. Both the phase and the amplitude of the object wave are preserved to a high degree through its interference with the background wave.
Figure 2

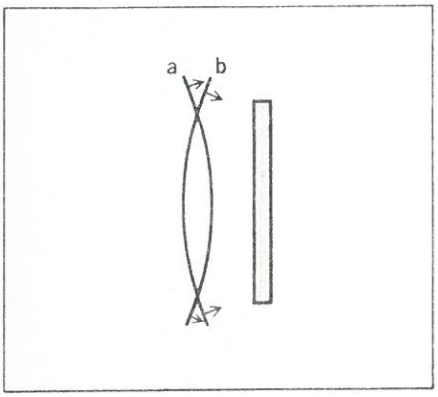

The twin image occurs because the two wavefronts a and b, which have equal but opposite curvature, produce the same fringe pattern when "interfered" with a coherent background wave. On reconstruction, the hologram produces both waves, regardless of which had been present during the recording.
Figure 3

cation-theory techniques to holography and, in consequence, suggested the single-sideband method[6] for removing the "twin image," one of the residual defects of the process. Despite the initial impetus, however, interest in holography waned in the middle 1950's, although activity never completely ceased.

The principal reason for the loss of interest was the relatively poor imagery, due mainly to the previously noted twin image, which occurs because the recording process is sensitive only to the intensity of the incident radiation. As a consequence, the reconstruction process not only recreates the original wave, it also creates a conjugate wave that, under collimated illumination, forms an image in mirror symmetry to the "true" image with respect to the plane of the hologram. Whichever image one elects to use, he must view it against the out-of-focus background of the other, and the result is a noisy image.

The origin of the conjugate image can be described in various ways. Basically, the introduction of the coherent background wave renders the inevitable loss of phase of the total wave (signal plus coherent background) relatively unimportant; the phase of the total wave can vary only slightly from the background wave if the latter is strong (see figure 2), and the phase of the signal is manifested by its interference with the background. Nevertheless, the recording process has a fundamental ambiguity: It cannot distinguish between signals with equal and opposite phase, relative to background (figure 3), because both produce the same intensity. Alternatively, we may say that the surface that records the hologram cannot distinguish an object wave from the left from an object wave in a position of mirror symmetry on the right; the resulting interference pattern is the same. In either view, the reconstruction process resolves the dilemma by generating waves corresponding to both situations.

High-quality imagery

In the early 1960's, several papers appeared that proved to be forerunners of the great explosion of activity that ushered in the next stage of holography. We announced at the October 1961 Optical Society of America meeting a number of new concepts, including the off-axis or spatial-carrier frequency method of holography, which removed the twin-image problem in a simple and practical way.[7] In this method, the reference and object waves are brought together at an angle, to form a rather fine fringe pattern. The resulting hologram, behaving like a diffraction grating, produces several nonoverlapping diffracted orders. The zero-order wave produces the usual inseparable twin images which, in combination with other defects of in-line holography, result in poor imagery; but each first-order diffracted wave produces an image of high quality.

When, however, we extended the process to continuous-tone object transparencies instead of the black and white transparencies used in holography until then, another defect became prominent. The difficulty was the well known "artifact" problem of coherent light—each extraneous scatterer (for example, a dust particle) produces a wake of diffraction patterns that contaminate the resultant image. We surmounted this problem with *diffused* coherent illumination, which properly used, smooths the field produced by these scatterers.

During the course of this work, the laser became available; we used it, as well as the mercury arc source, although it was not at all necessary. Its brightness reduced the exposure time and its great coherence made careful equalization of the object and reference beam paths unnecessary. It offered, however, a thousand times the needed coherence, violating the basic rule that, in a coherent system, one should not be more coherent than necessary. As a consequence, the artifact problem was aggravated. On balance, with transparencies, either the laser or the mercury arc source should do quite well. Indeed, with proper optical system design, the coherence requirements for off-axis holography reduce exactly to those for in-line holography.[8]

Finally, we exploited the great potential of the laser by using three-dimensional, reflecting objects. For such objects, the coherence length should be of the order of the scene depth, a requirement that generally cannot be met with the mercury source. The laser also permits enormous quantitative advances: larger holograms and large objects.

About the same time, Yu. N. Denisyuk of the USSR introduced a new concept into holography, the "volume hologram," which combines holography with the Lippman color process.[9] Object and reference beams are introduced from opposite sides of the recording plate, and the resulting fringes are embedded within the emulsion as surfaces running nearly parallel to the emulsion surface, with half a wavelength spacing between them. Typically, the number of fringes in a cross section is about 50, although for very thick (a few mm) recording materials, there may be thousands. The twin image is eliminated by the thickness effect and, in addition, the holograms, because of their wavelength selectivity, can be viewed in white light derived from a point source. Denisyuk's work is a cornerstone of modern holography. Related work was reported by Pietr J. van Heerden,[10] whose concern was principally with holographic memories. During this same period, Brian Thompson and George Parrent used Gabor's in-line method, in combination with the pulsed laser, for their particle-sizing work, an application ideally suited for this configuration because the objects are extremely simple and a noise-free image was not needed.[11]

The great surge

By late 1964, holography had become probably the most active field of research in optics, engaging hundreds of groups throughout the world. Discovery and invention dominated the next three years; this period produced several techniques of color holography

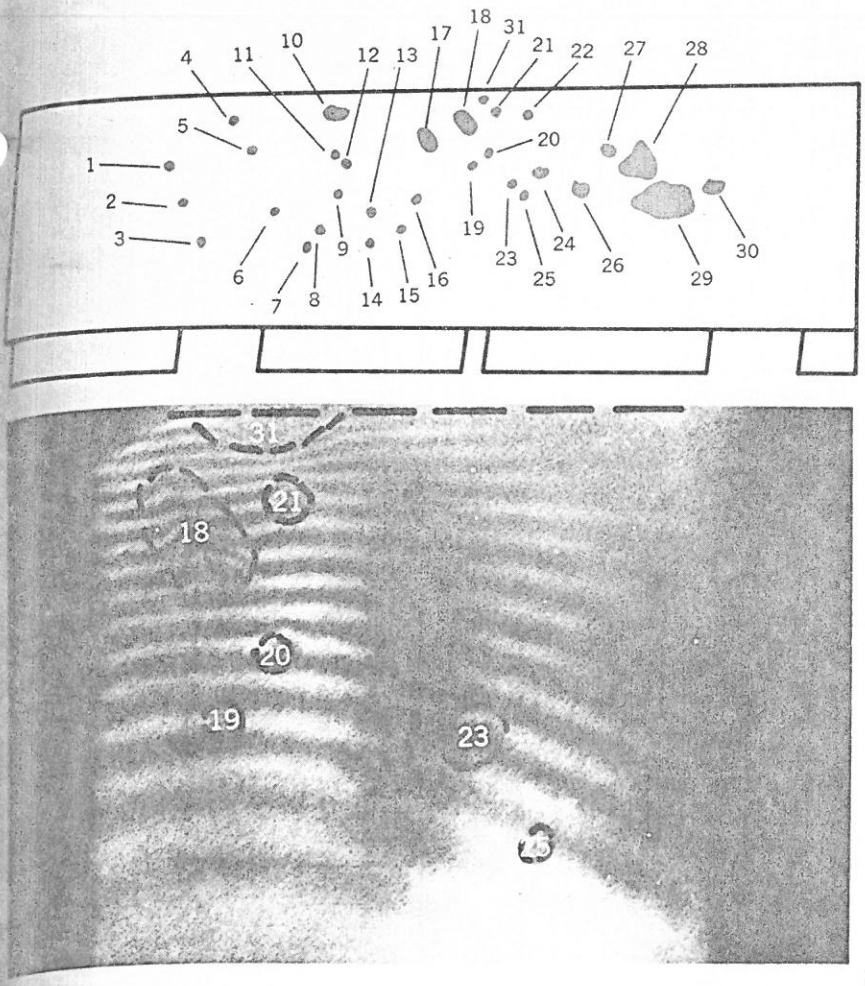

Defects in a section of an airplane trim tab are examined with double-exposure hologram interferometry. The trim tab was holographed a section at a time; each segment was recorded in two exposures, with thermal stress applied for the second exposure. In this way, the various defects were mapped (top). In the holographic image of one section of the wing (bottom), the defects are seen as defects in the fringe patterns that overlay the image. The wing was also examined with conventional, ultrasonic testing methods; the two methods gave substantially similar results. Courtesy C. Vest and D. Sweeney.
Figure 4

ram interferometry in its various techniques for holographic im- through scattering and aberrating ia, and many other basic concepts. vast potential that had been in- in holography now emerged astonishing force.

1967, however, the discoveries to diminish and the inventions on an increasingly restrictive ct, becoming more concerned with design of specific configurations. holographic world appeared to be lidating its gains. Serious analy- the holographic process in its s aspects became more evident, undoubtedly due to pressure by gement and in response to the iling economics (in the US), ap- ions received greater attention. te the shift in emphasis, however, tivity in holography remained at h level.

lography was found capable of an shingly wide variety of tasks that normally done in other ways. graphic methods could be useful tical metrology and offered some sting possibilities for spectroscopy. al memories using holographic niques seemed destined to make ficant inroads into the huge com- -memory field. Optical reading feature-recognition machines that used holography were visualized. Microscopy, at least in the visible wavelength range, seemed promising. With hologram interferometry, a wide variety of nondestructive testing techniques became available, ranging from early detection of fatigue failure, to the detection of "debonds" in multilayered materials such as tires and honeycomb panels (figure 4), to the determination of heat flow in transparent materials, to the study of bending moments and to the dynamic operation of audio speakers and other sound-transducing equipment. A most ingenious and unlikely application of hologram interferometry is the determination of the complex mode structure of a laser.[12] Merely to list the applications of hologram interferometry in reasonable completeness would fill a page. Even in conventional interferometry, it was found that one could apply to the hologram essentially all the techniques—such as schlieren, dark field, and phase contrast—normally done with the actual object.[13]

Holography, we have noted, can be used to detect and examine aerosol particles, such as atmospheric pollutants. Not only was holography unique for visual displays of many kinds, including portraiture, but it could also be used in instrumentation for conventional stereo imagery. Holographically produced optical elements showed promise for improving the performance of optical elements. The versatility of holography seemed limitless. (See figures 5 and 6 for examples.)

Practical uses

Serious efforts to commercialize holography became visible in the late 1960's. Many small companies dedicated to a particular aspect of holography sprang up, and in larger companies, the basic-research programs were reoriented toward product development. Equipment was designed for bringing holographic measuring and testing techniques into the factory, and prototype holographic memories began to develop.

By the end of the 1960's, some defects in the holography bandwagon showed themselves. The hoped-for commercial products either failed to materialize or were not competitive with conventional products. The tremendous versatility of holography proved insufficient to ensure its success; holography would have to be in some way an improvement over the established methods. Often, however, the old ways were better, at least within present state-of-the-art limitations. Thus, holography programs were curtailed or eliminated,

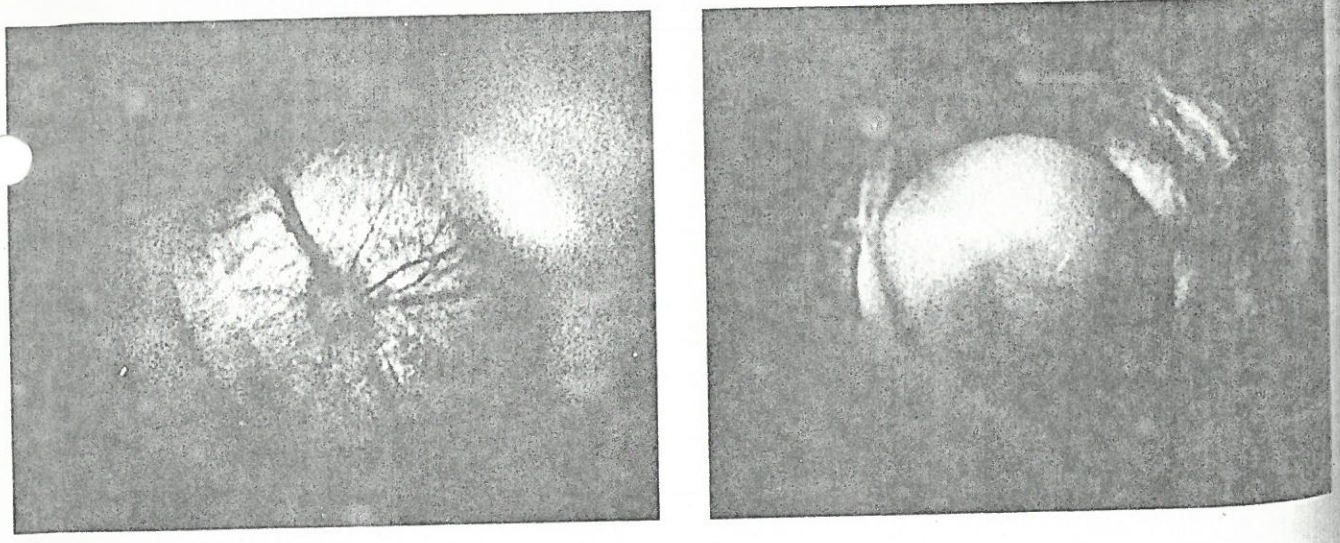

Medical application for holographic three-dimensional imagery. The eye of an anesthetized cat was holographed. From this single hologram it was possible to image any plane throughout the eye: Photo at the left shows the retina, with the blood-vessel structure and optic disk clearly visible, and photo at the right shows the iris. Courtesy J. Caulkins and C. Leonard.
Figure 5

and some small companies disappeared. In many quarters an atmosphere of gloom was observed, but whether or not the level of activity has diminished is problematical: As some groups abandoned holography, others appeared. The number of papers published has decreased slightly but remains high.

In retrospect, this course appears to have been predictable. The attempt to apply holography indiscriminately to all conceivable situations tended to force it into unsuitable molds. In addition, when the game is played for the multi-million dollar markets, the long-shot strategy enters the picture, and to date none of the longshot, large dollar volume areas has paid off.

Increasingly, we find evidences of an alternative approach. As holography has become more widely understood, persons with specific problems and goals have examined it and, occasionally, have discovered that holography appears to offer the best available solution. Additionally, holographers have become more sophisticated in their judgments of holography's capabilities and have searched more deeply for applications. The result is an increase in the number of applications that withstand critical evaluation; such applications are typically those that are highly specific or those in which some fairly simple holographic principle is incorporated harmoniously into a basically nonholographic system. These approaches stand in contrast with the bolder, albeit less successful, ones that pit holography in a broad way against a well developed and well established technology.

A recent example is the work of Ralph Wuerker and Lee O. Heflinger, who used[14] pulsed-laser hologram interferometry to examine the thermally produced deformations in an antenna to be carried on a satellite. The antenna, placed in a space-simulation vacuum chamber, was heated with a solar-radiation simulator. A hologram was made by a double-exposure process, so that the resulting image formed by the hologram was a coherent superposition of the image formed during each exposure. The deformation occurring in the interval between exposures was thus manifested as a fringe pattern overlaying the image; the greater the deformation, the finer the fringe pattern. Here the task is one to which holography is highly suited, and to which other techniques are ill suited.

Anthony Vander Lugt used[15] a holographically produced spatial filter in an optical processing system to analyze cloud motion. The input was a succession of pictures of cloud cover taken by a satellite. Certain frames are converted into Fourier-transform holograms and used as spatial matched filters for the next few successive frames. Portions of the cloud pattern that remain completely unaltered produced a bright cross-correlation spot in the output. Portions that are unaltered except for linear displacement produce displaced cross-correlation peaks. Picture segments can be identified with the corresponding output peaks by covering portions of the input data by an adjustable aperture. If such operations are performed on successive frames, the velocities of the various cloud segments can be found. Rotation of cloud masses can be measured by adjustment of the filter orientation. Alteration of the cloud structure can be determined by measurement of the correlation peaks. As the cloud structure changes with time, later frames can be introduced as spatial filters, so that the filters can be continuously updated. The spatial matched filter thus fits centrally into the system, performing in a simple way precisely the tasks required.

Most promising areas

Presently, the areas of holography that appear most promising are probably hologram interferometry, holographic memories and hologram optical elements.

Shortly after it was announced in 1965, hologram interferometry became the major type of application, a position it retains to the present day and will likely retain at least into the near future. Recently other techniques involving coherent light have developed.[16] For example, interferometers using the well known "speckle" phenomenon of coherent light can do many of the jobs to which holography is suited, such as detection of vibration and measurement of deformations. This method is easier to carry out than hologram interferometry but generally lacks its precision and sensitivity. Thus the method is complementary to, rather than competitive with, holography.

Hologram interferometry has proved quite valuable in certain specific situations. In general situations (such as nondestructive testing techniques for detection of cracks and debonds), it has shown itself to be competitive with such standard techniques as x-ray and ultrasonic analysis (figure 4). However

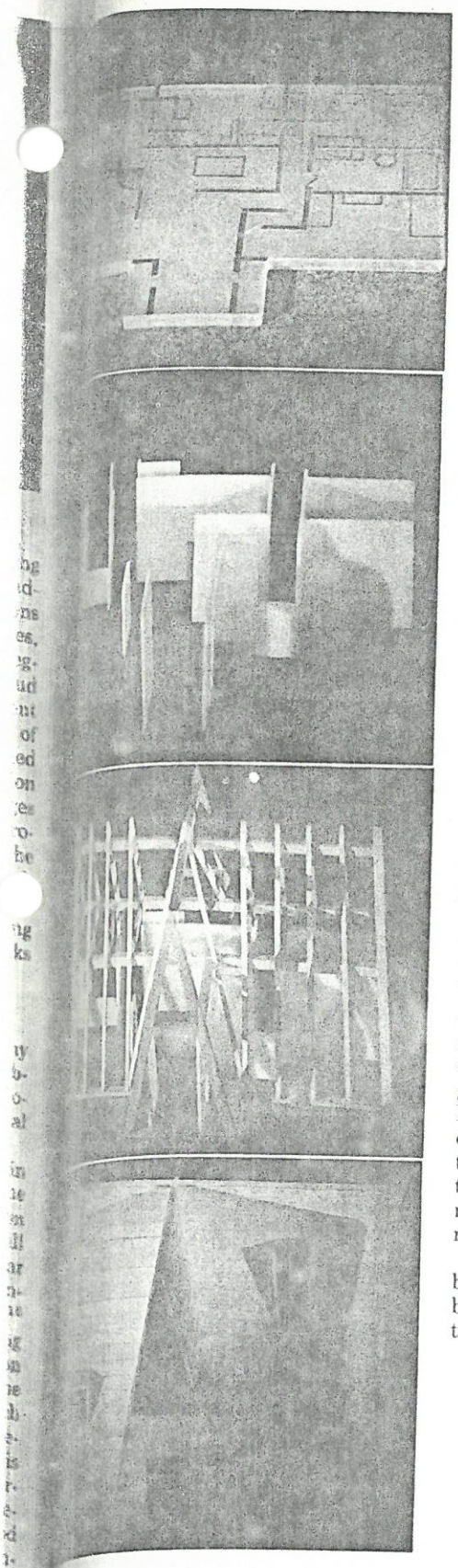

Architectural structures are visualized through holography. A model of a building, in various stages of construction, was formed by multiple storage of images; each image can be read out separately by using the Bragg diffraction effect of thick emulsions. A 5.5-deg rotation of the plate produces the next successive image, and intermediate orientations produce adjacent pairs of images in superposition. As the observer rotates the plate, he can see the structure at any desired stage of completion, and because the images are truly three-dimensional, he can perceive the various structural relations vividly. Courtesy of J. Fader and C. Leonard.
Figure 6

hologram interferometry has as yet made few if any inroads into the standard nondestructive testing methods.

Holographic memories show promise but face an uncertain future. The absence of an erasable, reusable and sufficiently sensitive recording material has generally limited holography to read-only memories, which seem promising when viewed in terms of broad design concepts, such as cost per bit and memory size versus access time. John La Macchia,[17] however, has indicated that serious engineering problems become evident at the prototype stage: variation of diffraction efficiency from one bit to another; inability to achieve satisfactory high diffraction efficiencies and high signal-to-noise ratios simultaneously; detectors that lack uniform sensitivity; expensive and bulky light deflectors; and lasers with inadequate power, insufficient lifetimes and high operating costs.

These are not fundamental problems, but merely problems of engineering design and, quite possibly, they are solvable either by pushing present technology to its limit or by further advances in the appropriate technologies. We can expect that these problems will be surmounted within a time period of five to ten years. Holographic-memory development is apparently being actively pursued by various groups in the US, Germany and Japan.

The outlook for holographic optical elements is presently quite good. There are two basic reasons for this optimism. First, the aberrations of holograms have by now been explored in considerable depth. Second, experimental techniques for producing high-quality, high diffraction-efficiency, low-noise holograms have been developed. John Latta[18] has pioneered in the use of the computer to investigate these aberrations in great detail, and has explored the tandem combination of optical elements in arrangements that greatly reduce the aberrations (figure 7).

Diffraction gratings can be produced by holographic methods.[19] Indeed, because this process involves merely the interference of unmodulated light beams, it should perhaps be viewed as conventional interferometry rather than holography and, in such a context, was explored by James Burch many years ago. The recent advances in holographic recording technology, however, are generally applicable here also.

Major problems to be solved

The intensive research of the past seven years has resolved many difficulties, but severe problems remain that block many of the hoped-for attainments in holography.

The lack of recording materials is one of the foremost problems. At present, high-resolution photographic film is the most commonly used material. Its deficiencies are severe and include lack of optical flatness, variation from plate to plate and among batches of emulsion, nonlinearity, a messy chemical-development process that swells the emulsion and generally leaves some permanent distortions, insensitivity to light in comparison with conventional emulsions, and lack of erasability and reusability. These deficiencies have promoted a search for alternative materials, but the results have generally been disappointing; photographic film remains, in general, the best material.

Bleaching techniques, in which the silver deposits in the developed negative are changed into a transparent material with an index of refraction different from the surrounding emulsion, has led to dramatic increases in diffraction efficiency of holograms. A hologram formed from a diffusely scattering object generally has a diffraction efficiency such that only about 0.5 to 1.0% of the incident light is converted into the reconstructed wave. Bleaching under controlled conditions can raise this conversion to 15 to 20% while preserving good image quality. Even higher diffraction efficiencies can be achieved, but at the expense of increased noise.

Alternative materials include photochromic glasses, which, by virtue of their molecular grain size, offer extremely good resolution and low noise but are several orders of magnitude less sensitive than even the very slowest photographic emulsions. They are erasable but generally have extremely low diffraction efficiency. Holograms of excellent quality have been produced on photopolymers, dichromated gelatin and lithium niobate. Magneto-optic materials, such as MnBi, have produced holograms that can be rapidly formed and erased. But none of these alternative materials is likely to displace photographic film as the most commonly used recording medium.

Another severe problem area is laser speckle, a defect that never escapes the notice of those viewing holograms. Yet, the problem lies not with holography, but with the coherent light that holo-

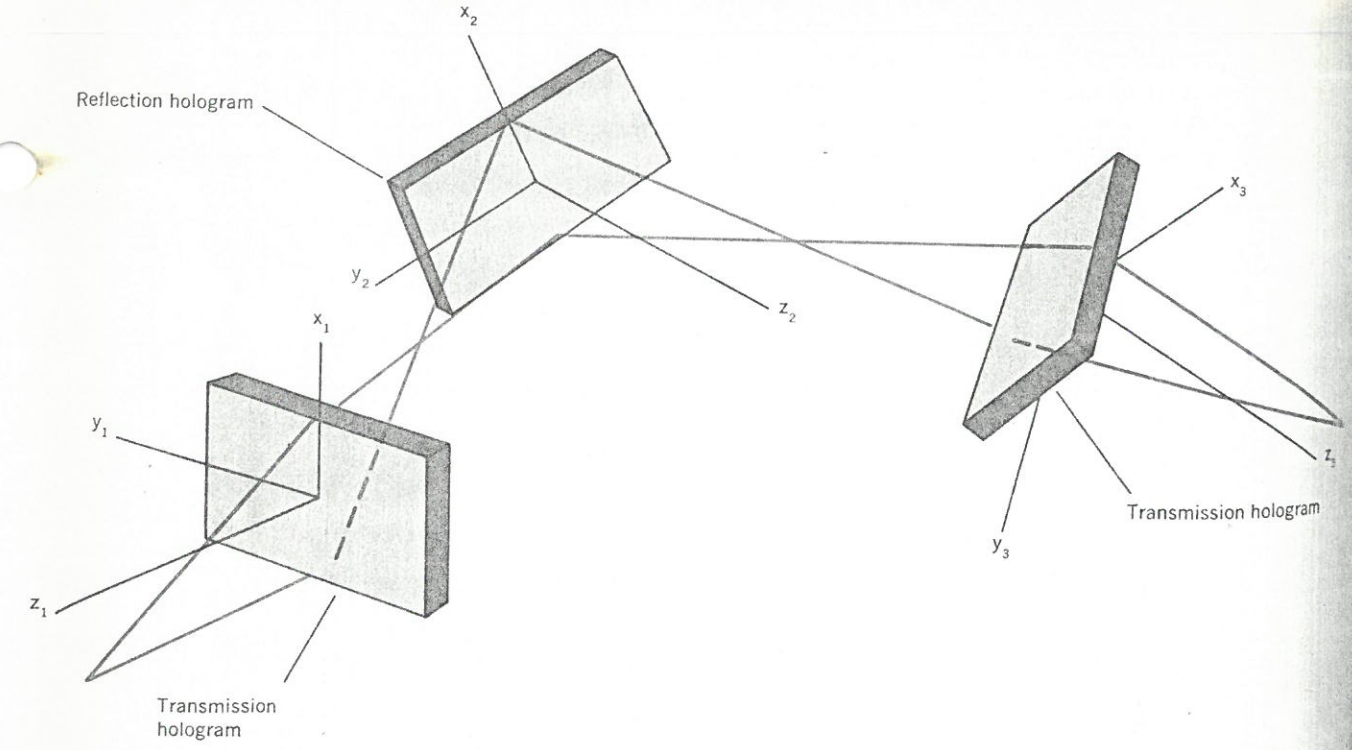

Computer analysis of holographic optical elements in tandem. In this model, developed by John Latta, the geometry is extremely general; it allows for any orientation and spacing of the various elements, as well as for both transmissive and reflective elements. Computer programs that optimize the design of such holographic systems are available. Figure 7

graphy requires. The problem is generally solvable only with the introduction of massive redundancy into the viewing system. For the case where the final image is a recording of the holographically formed image, the redundancy takes the form of a multiplicity of superimposed images (ten or more), each the same except for uncorrelated speckle patterns. Alternatively, the redundancy can take the form of an imaging system with the *f*-number far smaller than necessary for the desired resolution. When the hologram is to be viewed directly, these methods do not apply, except in the awkward case of projecting a multiplicity of pictures at a frame rate higher than the retention time of the eye. In general, the proposed solutions to the speckle problem come with a high price tag and are no panacea.

The light source is a problem that has been yielding to advances in technology. We obtain 1000 times more power, at 1/100 the price per milliwatt, than was available when lasers were first applied to holography. Coherence is better than ever; even pulsed lasers now have coherence properties suitable for holography. Holographic portraiture is one quite dramatic result of pulsed-laser holography. There is, however, need for further improvement in producing powerful, highly coherent, inexpensive and compact lasers.

The future prospects for holography evidently depend on the development of further viable applications, without which holography would become only a laboratory curiosity. Much work remains to be done in the aforementioned problem areas; unfortunately, the reduction of government and industrial research funding for nonmission-oriented and long-term research has adversely affected prospects here. In any event, whatever its usefulness may be, holography will remain a subject of fascination to all who have the opportunity to make holograms and, indeed, even to those who must content themselves merely with viewing them.

References

1. H. Kiemle, D. Roess, *Einführung in die Technique der Holographie*, Akademische Verlagsgesellschaft, Frankfort, 1969 (English translation to be published this year).
2. D. Gabor, Nature **161**, 771 (1948); Proc. Roy. Soc. (London) **A197**, 454 (1949); Proc. Phys. Soc. (London) **B64**, 449 (1951).
3. G. L. Rogers, Nature **166**, 237 (1950); Proc. Roy Soc. (Edinburgh) **A63**, 193 (1950–1951).
4. M. E. Haine, J. Dyson, Nature **166**, 315 (1950); M. E. Haine, T. Mulvey, J. Opt. Soc. Am. **42**, 763 (1952).
5. H. M. A. El-Sum, *Reconstructed Wavefront Microscopy*, PhD thesis, Stanford University (1952).
6. A. Lohmann, Opt. Acta **3**, 97 (1956).
7. E. Leith, J. Upatnieks, J. Opt. Soc. Am. **52**, 1123 (1962); **53**, 1377 (1963); **54**, 1295 (1964).
8. Yu. N. Denisyuk, Sov. Phys.-Dokl. **7**, 543 (1962); Opt. Spectrosc. **15**, 279 (1963).
9. P. J. van Heerden, Appl. Opt. **2**, 393 (1963).
10. E. N. Leith, J. Upatnieks J. Opt. Soc. Am. **57**, 975 (1967).
11. G. B. Parrent, B. J. Thompson, Opt. Acta **11**, 183 (1964).
12. C. Aleksoff, Appl. Opt. **10**, 1329 (1971).
13. M. Horman, Appl. Opt. **4**, 333 (1965).
14. R. F. Wuerker, *Proceedings* of the Society of Photo-optical Instrumentation Engineers Seminar on Developments in Holography, Boston, April 14, 15, 1971; R. F. Wuerker, L. O. Heflinger, Pulsed Laser Holography II, Technical Report No. AFAL-TR-71-323, December 1971.
15. A. Vander Lugt, *Proceedings* of the Society of Photo-optical Instrumentation Engineers Seminar on Developments in Holography, Boston, April 14, 15, 1971.
16. J. M. Burch, *Proceedings* of the Society of Photo-optical Instrumentation Engineers Seminar on Developments in Holography, Boston, April 14, 15, 1971.
17. J. La Macchia, *Proceedings* of the Society of Photo-optical Instrumentation Engineers Seminar on Developments in Holography, Boston, April 14, 15, 1971.
18. J. Latta, Appl. Opt. **10**, 2698 (1971).
19. A. Labeyrie, J. Flamard, Opt. Comm. **1**, 5 (1969).